

# Secular variation in Late Cretaceous carbon isotopes: a new $\delta^{13}\text{C}$ carbonate reference curve for the Cenomanian–Campanian (99.6–70.6 Ma)

IAN JARVIS\*, ANDREW S. GALE†‡§, HUGH C. JENKYN¶ & MARTIN A. PEARCE||

\*School of Earth Sciences & Geography, Centre for Earth and Environmental Science Research,  
Kingston University London, Penrhyn Road, Kingston upon Thames KT1 2EE, UK

†Department of Earth & Environmental Sciences, University of Greenwich, Chatham, Kent ME4 4AW, UK

‡Department of Palaeontology, Natural History Museum, Cromwell Road, London SW7 5BD, UK

¶Department of Earth Sciences, University of Oxford, Parks Road, Oxford OX1 3PR, UK

||Statoil, Forus N-4035, Stavanger, Norway

(Received 27 April 2005; revised version received 26 January 2006; accepted 30 January 2006)

**Abstract** – Carbon stable-isotope variation through the Cenomanian–Santonian stages is characterized using data for 1769 bulk pelagic carbonate samples collected from seven Chalk successions in England. The sections show consistent stratigraphic trends and  $\delta^{13}\text{C}$  values that provide a basis for high-resolution correlation. Positive and negative  $\delta^{13}\text{C}$  excursions and inflection points on the isotope profiles are used to define 72 isotope events. Key markers are provided by positive  $\delta^{13}\text{C}$  excursions of up to +2‰: the Albian/Cenomanian Boundary Event; Mid-Cenomanian Event I; the Cenomanian/Turonian Boundary Event; the Bridgewick, Hitch Wood and Navigation events of Late Turonian age; and the Santonian/Campanian Boundary Event. Isotope events are isochronous within a framework provided by macrofossil datum levels and bentonite horizons. An age-calibrated composite  $\delta^{13}\text{C}$  reference curve and an isotope event stratigraphy are constructed using data from the English Chalk. The isotope stratigraphy is applied to successions in Germany, France, Spain and Italy. Correlation with pelagic sections at Gubbio, central Italy, demonstrates general agreement between biostratigraphic and chemostratigraphic criteria in the Cenomanian–Turonian stages, confirming established relationships between Tethyan planktonic foraminiferal and Boreal macrofossil biozonations. Correlation of the Coniacian–Santonian stages is less clear cut: magnetostratigraphic evidence for placing the base of Chron 33r near the base of the Upper Santonian is in good agreement with the carbon-isotope correlation, but generates significant anomalies regarding the placement of the Santonian and Campanian stage boundaries with respect to Tethyan planktonic foraminiferal and nannofossil zones. Isotope stratigraphy offers a more reliable criterion for detailed correlation of Cenomanian–Santonian strata than biostratigraphy. With the addition of Campanian  $\delta^{13}\text{C}$  data from one of the English sections, a composite Cenomanian–Campanian age-calibrated reference curve is presented that can be utilized in future chemostratigraphic studies.

The Cenomanian–Campanian carbon-isotope curve is remarkably similar in shape to supposedly eustatic sea-level curves: increasing  $\delta^{13}\text{C}$  values accompanying sea-level rise associated with transgression, and falling  $\delta^{13}\text{C}$  values characterizing sea-level fall and regression. The correlation between carbon isotopes and sea-level is explained by variations in epicontinental sea area affecting organic-matter burial fluxes: increasing shallow sea-floor area and increased accommodation space accompanying sea-level rise allowed more efficient burial of marine organic matter, with the preferential removal of  $^{12}\text{C}$  from the marine carbon reservoir. During sea-level fall, reduced seafloor area, marine erosion of previously deposited sediments, and exposure of basin margins led to reduced organic-carbon burial fluxes and oxidation of previously deposited organic matter, causing falling  $\delta^{13}\text{C}$  values. Additionally, drowning of carbonate platforms during periods of rapid sea-level rise may have reduced the global inorganic relative to the organic carbon flux, further enhancing  $\delta^{13}\text{C}$  values, while renewed platform growth during late transgressions and highstands prompted increased carbonate deposition. Variations in nutrient supply, changing rates of oceanic turnover, and the sequestration or liberation of methane from gas hydrates may also have played a role in controlling carbon-isotope ratios.

Keywords: Cretaceous, carbon isotopes, Chalk, chemostratigraphy, sea-level change.

## 1. Introduction

The first detailed carbon and oxygen stable-isotope study of the Upper Cretaceous was published 25 years

ago (Scholle & Arthur, 1980). This pioneering work included summary  $\delta^{13}\text{C}$  profiles based on the analysis of bulk carbonate samples from sections of the English Chalk at Dover–Folkestone, in Norfolk, and on the Isle of Wight which, together with other data from NW Europe, the Italian Apennines and Mexico, were

\*Author for correspondence: i.jarvis@kingston.ac.uk

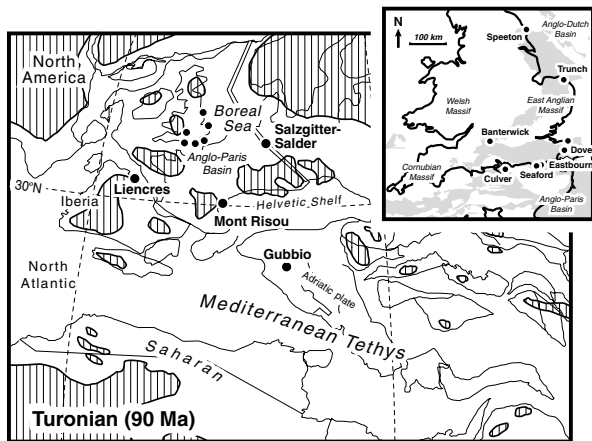


Figure 1. Location of European Upper Cretaceous sections discussed in the text. Turonian (90 Ma) palaeogeographic base map modified from Voigt *et al.* (1999). Thin lines represent the outlines of continental blocks and continents. Land areas indicated by thick lines and vertical hatching. Inset map (top right) shows location of English Chalk study sections; grey areas are outcrop and sub-Pleistocene subcrop of Cretaceous sediments.

used to demonstrate the potential of carbon isotopes for global correlation. Scholle & Arthur's (1980) work was refined by detailed, metre-scale sampling tied to detailed stratigraphic logs by Jenkyns, Gale & Corfield (1994), who confirmed the good correlation between east Kent in England and Gubbio, Italy, and produced  $\delta^{13}\text{C}$  profiles for the two areas which have been used subsequently as international stratigraphic reference curves (e.g. Voigt & Hilbrecht, 1997; Wiese, 1999; Voigt, 2000; Coccioni & Galeotti, 2003; Skelton, 2003).

In this paper, new carbon stable-isotope data are presented for the Cenomanian–Campanian of Culver Cliff, Isle of Wight (Fig. 1; 295 samples) and the Trunch borehole, Norfolk (223 samples), plotted against detailed litho- and biostratigraphic logs. The profiles are correlated with a new compilation of published  $\delta^{13}\text{C}$  data from East Kent (535 samples), Speeton, North Yorkshire (255 samples), Banterwick Barn, Berkshire (106 samples), Seaford Head and Eastbourne, East Sussex (86 and 269 samples, respectively) plotted, in most cases for the first time, against detailed stratigraphic logs. A combination of macrofossil biostratigraphy and a marker-bed lithostratigraphy that includes six key bentonite horizons in the Turonian–Coniacian provides a tight correlation framework for the seven sections that confirms the synchronicity of shifts in the carbon-isotope profiles.

Significant  $\delta^{13}\text{C}$  excursions and inflection points on the correlated English Chalk profiles are used to define an event chemostratigraphy that enables more refined regional correlation. Substantial variations in thickness and facies are demonstrated between the localities, with no single section providing a complete record of the

entire succession. A composite  $\delta^{13}\text{C}$  reference profile is constructed using data from the most complete parts of each section, and this is compared with recently published high-resolution data for coeval successions in Italy and Germany. Excellent agreement between  $\delta^{13}\text{C}$  profiles throughout Europe confirms the synchronicity of changes in the isotope record through the Cenomanian–Santonian, and illustrates the potential of the composite  $\delta^{13}\text{C}$  reference curve as a primary criterion for trans-continental correlation.

## 2. Study sections

### 2.a. Stratigraphic framework

Over the last two decades, a comprehensive named marker-bed stratigraphy has been developed for the English Chalk that enables detailed correlation of sections throughout the region. Some of these marker-bed names were introduced in the nineteenth century, such as the Totternhoe Stone (Whitaker, 1865*b*) and the Cast Bed (Price, 1877) in the Cenomanian, and the Whitaker 3-inch Flint (Whitaker, 1865*a*) in the Santonian. However, more recently, a large number of additional beds have been named independently in northern (Wood & Smith, 1978) and in southern (Mortimore, 1983) England, which have been used for regional correlation. For the southern England sections described in this paper (Fig. 1), the marker-bed terminology of Mortimore (1983) is used in preference to the North Downs lithostratigraphy of Robinson (1986) where marker-bed correlations throughout the area are well established. Marl seams, including geochemically distinct bentonites (Wray & Gale, 1993; Wray *et al.* 1996; Wray & Wood, 1998; Wray, 1999; Wiese, Wood & Wray, 2004), have proven to be particularly reliable for regional correlation. Where appropriate, marker-bed names in general use prior to the work of Mortimore (1983) are retained.

The application of higher order stratigraphic terminology at the member, formation and group levels remains controversial (e.g. Gale, Wood & Bromley, 1987; Gale *et al.* 1999*a*; Robinson, 1987; Mortimore, 1988; Bristow, Mortimore & Wood, 1997; Bristow, 1999; Rawson, Allen & Gale, 2001; Peake, 2002; Woods *et al.* 2002). Here, the traditional member subdivisions of the Cenomanian (Gale *et al.* 1999*a*) are used, whereas the terminology of Gale (1996) is employed for the Turonian, and that of Gale, Wood & Bromley (1987) for the Coniacian–Campanian. This member terminology has been plotted against the lithostratigraphic logs of the Culver section for reference purposes. However, it is recognized that some member boundaries are diachronous, and that the southern England member terminology is not applicable to the lithologically different Trunch and Speeton sections of eastern and northern England (Fig. 1).

Table 1. Key biostratigraphic datum levels used to constrain the carbon-isotope chemostratigraphy

Datum	Description
<b>Campanian</b>	
45	LAD <i>Uintacrinus anglicus</i>
44	FAD <i>U. anglicus</i>
43	LAD <i>Marsupites testudinarius</i> (base Campanian)
<b>Santonian</b>	
42	FAD <i>Marsupites testudinarius</i>
41	FAD <i>Marsupites laevigatus</i>
40	FAD <i>Uintacrinus socialis</i>
39	base <i>Echinocorys</i> aff. <i>elevata</i> bed
38	LAD <i>Cladoceramus</i>
37	base second abundant <i>Cladoceramus</i> bed ( <i>Cladoceramus</i> Bed 2)
36	base first abundant <i>Cladoceramus</i> bed ( <i>Cladoceramus</i> Bed 1) (base Santonian)
<b>Coniacian</b>	
35	FAD <i>Volviceramus involutus</i>
34	acme <i>Volviceramus koeneni</i>
33	FAD <i>Cremnoceramus schloenbachi</i>
32	FAD <i>Cretirhynchia subplicata</i>
31	FAD <i>Cremnoceramus deformis erectus</i> (base Coniacian)
<b>Turonian</b>	
30	FAD <i>Cremnoceramus walterdorfensis hannovrensis</i>
29	FAD <i>Mytiloides scupini</i>
28	base abundant <i>Micraster leskei</i> and <i>Cretirhynchia</i>
27	FADs <i>Micraster leskei</i> and <i>Inoceramus costellatus</i>
26	FAD <i>Inoceramus securiformis</i> , abundant <i>I. lamarcki</i>
25	FAD <i>Inoceramus lamarcki</i>
24	FAD <i>Inoceramus cuvieri</i>
23	base second abundant <i>Roveacrinus</i> bed ( <i>Roveacrinus</i> Bed 2), FAD <i>Mytiloides subhercynicus</i>
22	base <i>Filograna avita</i> bed, abundant <i>Mytiloides mytiloides</i>
21	FAD <i>Mytiloides mytiloides</i>
20	base first abundant <i>Roveacrinus</i> bed ( <i>Roveacrinus</i> Bed 1)
19	FAD <i>Mytiloides puebloensis</i> (base Turonian)
<b>Cenomanian</b>	
18	base abundant <i>Orbirhynchia wiesti</i> (Plenus Marl Bed 7)
17	base <i>Actinocamax plenus</i> – <i>Lyropecten (Aequipecten) arlesiensis</i> – <i>Oxytoma seminudum</i> bed (Plenus Marl Bed 4)
16	base <i>Orbirhynchia multicostata</i> bed (Plenus Marl Bed 2)
15	LAD ‘Cenomanian’ benthonic macrofauna (top Grey Chalk)
14	base abundant <i>Amphidonte</i> bed
13	base abundant <i>Pycnodonte</i> bed (Jukes-Browne Bed 7)
12	FADs <i>Acanthoceras jukesbrownei</i> and <i>Inoceramus atlanticus</i>
11	sharp increase in proportion of planktonic foraminifera (P/B break)
10	base third abundant <i>Orbirhynchia mantelliana</i> beds ( <i>O. mantelliana</i> Bed 3)
9	base <i>Praeactinocamax primus</i> – <i>Oxytoma seminudum</i> bed
8	base <i>Lyropecten (Aequipecten) arlesiensis</i> – <i>Oxytoma seminudum</i> bed
7	base second abundant <i>Orbirhynchia mantelliana</i> beds ( <i>O. mantelliana</i> Bed 2)
6	base first abundant <i>Orbirhynchia mantelliana</i> beds ( <i>O. mantelliana</i> Bed 1)
5	base abundant <i>Inoceramus virgatus</i> ( <i>I. virgatus</i> beds)
4	FAD <i>Inoceramus virgatus</i>
3	base abundant <i>Inoceramus crippsi crippsi</i> ( <i>I. crippsi</i> beds)
2	LAD <i>Aucellina</i>
1	FAD <i>Inoceramus crippsi crippsi</i>

Macrofossil biostratigraphy is used to constrain further the isotopic correlations. The ammonite zonation of the Cenomanian–Turonian (Wright & Kennedy, 1981, 1984; Gale, 1995, 1996) is accompanied by the ‘traditional’ macrofossil subdivisions of the Turonian–Campanian (Rowe, 1899, 1900, 1908; Rawson *et al.* 1978) employing inoceramid bivalves, brachiopods, echinoids and crinoids. The location of zonal boundaries is based on our own observations supplemented by literature information. However, macrofossil zonal biostratigraphy above the Cenomanian provides a relatively coarse stratigraphic resolution with individual zones attaining a thickness greater than 100 m, and zonal boundaries are commonly difficult to place precisely, particularly in boreholes. Additional constraints are provided by the positions of macrofossil datum

levels (Table 1), including the first appearances (FAD), last appearances (LAD) and flood abundances of key taxa.

## 2.b. East Kent (Cenomanian–Campanian)

The east Kent coast is situated above the southern margin of the London-Brabant Massif, an extensive area of shallow Palaeozoic basement that marks the northern fringe of the Cretaceous Anglo-Paris Basin. Cliff sections in east Kent near Folkestone and Dover (Fig. 1; UK national grid reference TR 26153830–38014767; N 51°05'58" E 01°13'43"–N 51°10'43" E 01°24'14"), and on the Isle of Thanet between Ramsgate and Margate (TR 3668 6408–3835 7162; N 51°19'36" E 01°23'45"–N 51°23'37" E 01°25'39"),

provide a complete and readily accessible succession of shallow-dipping Upper Cretaceous (Cenomanian–lowest Campanian) strata. These sections have a long history of study (e.g. Phillips, 1821; Price, 1877; Rowe, 1900; Jukes-Browne & Hill, 1903, 1904). Detailed locality information and logged sections have been published by Kennedy (1969), Robinson (1986), Jenkyns, Gale & Corfield (1994), Mortimore (1997) and Mortimore, Wood & Gallois (2001). The logs presented here are derived from Jenkyns, Gale & Corfield (1994) for the Cenomanian, and are based on work by Jarvis between 1984 and 2004 for the remainder of the section. The latter compilations agree well with most published logs but with some differences in thickness and lithological detail. The Cenomanian–lowest Campanian is 259 m thick.

A filtered and smoothed  $\delta^{13}\text{C}$  curve for the Cenomanian–lowest Campanian of Dover–Folkestone was published by Scholle & Arthur (1980, fig. 2), but no detailed stratigraphic framework was provided. Jarvis *et al.* (1988a) documented carbon- and oxygen-isotope curves across the Cenomanian/Turonian boundary. The isotope data reported here are those of Jenkyns, Gale & Corfield (1994), replotted against our revised logs, with additional higher resolution sample data for the Middle Cenomanian from Paul *et al.* (1994b) and Mitchell, Paul & Gale (1996), and for the Cenomanian/Turonian boundary interval from Lamolda, Gorostidi & Paul (1994).

### 2.c. Culver Cliff, Isle of Wight (Cenomanian–Campanian)

The Isle of Wight is situated towards the central part of the Anglo-Paris Basin. Cenomanian to middle Campanian chalks are well exposed on the steeply dipping (50–65°) northern limb of the Sandown Anticline at Culver Cliff (Fig. 1) and Whitecliff (SZ 6295 8550–6407 8573; N 50°39'57" W 01°06'38"–N 50°40'04" W 01°05'41'), on the eastern tip of the island. Briefly described by Rowe (1908), and reviewed by White (1921), summary logs have been published for the Cenomanian–Lower Turonian (Jarvis, Murphy & Gale, 2001), Coniacian–Campanian (Mortimore, Wood & Gallois, 2001), Santonian (Prince, Jarvis & Tocher, 1999) and Campanian (Jenkyns, Gale & Corfield, 1994). The complete Cenomanian–basal Campanian succession (300 m), logged by Jarvis during 1994–1996, is documented for the first time in this paper.

A filtered and smoothed  $\delta^{13}\text{C}$  curve for the Cenomanian–Campanian of the Isle of Wight was published by Scholle & Arthur (1980, fig. 2). Jenkyns, Gale & Corfield (1994, fig. 7) documented the  $\delta^{13}\text{C}$  profile of the Campanian at Whitecliff. Paul *et al.* (1994b, fig. 3) described carbon-isotope variation in the lower Middle Cenomanian of Culver Cliff, and Jarvis, Murphy & Gale (2001, fig. 3) published a detailed Cenomanian–Lower Turonian  $\delta^{13}\text{C}$  profile.

A composite curve for the Cenomanian–Campanian, incorporating new data for the Turonian–Santonian, is presented here.

### 2.d. Speeton, North Yorkshire (Cenomanian)

Speeton is situated close to the fault-bounded southern margin of the Cleveland Basin, a western extension of the Anglo-Dutch Basin (Fig. 1) of the southern North Sea (Cameron *et al.* 1992). Buckton Cliffs, 2 km east of Speeton, and the adjacent foreshore provide a continuous, albeit intermittently exposed, gently southerly dipping Cenomanian section (TA 1747 7487–1865 7460; N 54°09'22" W 00°12'10"–N 54°09'13" W 00°11'05") that includes an expanded succession across the Albian/Cenomanian boundary, which is unique in England (Mitchell, 1995).

Section details have been provided by Hill (1888), Jeans (1973, 1980), Paul *et al.* (1994b), Gale (1995), Mitchell (1995, 1996), Mitchell, Paul & Gale (1996) and Mortimore, Wood & Gallois (2001). A high-resolution carbon-isotope stratigraphy of the Upper Albian–basal Turonian has been documented by Mitchell and co-workers (references above); the stratigraphic and  $\delta^{13}\text{C}$  data presented here are those of Mitchell, Paul & Gale (1996, fig. 5), supplemented by additional lithological details derived from Mitchell (1995, 1996) and new logging by Gale.

### 2.e. Trunch, Norfolk (Cenomanian–Campanian)

Trunch is situated above the northern margin of the East Anglian Massif (Fig. 1). Gently easterly dipping ( $\sim 0.5^\circ$ ) Upper Cretaceous sediments occur throughout Norfolk but are generally obscured by a thick Quaternary cover. A continuously cored well sunk at Trunch (TG 2933 3455; N 52°51'34" E 01°24'19") in 1975 by the British Geological Survey (BGS; then the Institute of Geological Sciences) sampled 468 m of Cenomanian–basal Maastrichtian Chalk (Wood, Morter & Gallois, 1994). This borehole provides the most complete onshore Upper Cretaceous record in England. The lithostratigraphy and macrofossil biostratigraphy (Gallois & Morter, 1976; Wood, Morter & Gallois, 1994) have been described, but lithological logs have been published only for the Campanian (Jarvis *et al.* 2002). During the present study, the unpublished written and graphic logs of Mr A. A. Morter (BGS) were combined with our interpretation of gamma, resistivity and sonic e-log data to generate a new detailed log of the Cenomanian–Santonian succession (206 m).

A filtered and smoothed  $\delta^{13}\text{C}$  curve for the Cenomanian–Maastrichtian of Norfolk was presented by Scholle & Arthur (1980, fig. 2), but no detailed stratigraphic data were published. McArthur *et al.* (1993) included carbon and oxygen stable-isotope values for a few widely spaced samples, as part of

a strontium-isotope stratigraphy study of the borehole. Jenkyns, Gale & Corfield (1994, fig. 7) provided metre-resolution  $\delta^{13}\text{C}$  and  $\delta^{18}\text{O}$  curves for the Campanian. New data for the Cenomanian–Santonian interval are here added to the published Campanian data (Jenkyns, Gale & Corfield, 1994) to construct a complete Cenomanian–basal Campanian curve.

#### 2.f. Banterwick Barn, Berkshire (Turonian–Coniacian)

Banterwick Barn borehole 2, located (UK national grid reference SU 5134 7750; N 51°29'39" W 1°15'43") near the village of Hampstead Norries in Berkshire, was drilled by the BGS in 1996, and sampled 97 m of Turonian–Coniacian chalk (Murphy, Jarvis & Edmunds, 1997). The locality is situated close to the NW margin of the Anglo-Paris Basin (Fig. 1), in an area termed the Berkshire–Chilterns Shelf by Mortimore (1983). Here, the middle to upper Turonian becomes highly condensed and is represented by a diachronous complex of well-developed, mineralized and highly indurated hardgrounds, the Chalk Rock (Bromley & Gale, 1982; Gale, 1996; Woods & Aldiss, 2004).

Detailed lithostratigraphic, chemostratigraphic, palynological, and porewater geochemical studies have been undertaken (Murphy, Jarvis & Edmunds, 1997; A. M. Murphy, unpub. Ph.D. thesis, Kingston Univ. 1998; Pearce *et al.* 2003) on the borehole. Carbon- and oxygen-isotope curves for the succession were presented in Murphy, Jarvis & Edmunds (1997) and Pearce *et al.* (2003). These data were used in the present study. The stratigraphy of the borehole was discussed most recently by Woods & Aldiss (2004), who correlated the section with others in the Berkshire Downs.

#### 2.g. Seaford Head, East Sussex (Santonian–Campanian)

The gently folded Chalk on the East Sussex coast between Brighton and Eastbourne displays some of the thickest Cenomanian–Santonian successions in the Anglo-Paris Basin (Mortimore & Pomerol, 1987). At Seaford Head (Fig. 1) a continuously exposed and accessible Upper Turonian–Lower Campanian section (TV 5010 9750–4885 9817; N 51°39'23" E 00°10'07"–N 51°39'45" E 00°09'03"), first zoned by Rowe (1900), dips at approximately 15° to the west. The lithological succession was described by Mortimore (1986, 1997), and Jenkyns, Gale & Corfield (1994, fig. 14) published a detailed log of the Middle Santonian–Lower Campanian. The locality has been proposed as a Lower/Middle Coniacian substage boundary stratotype (Kauffman, Kennedy & Wood, 1996), and as a potential boundary stratotype section for both the Santonian (Lamolda & Hancock, 1996) and the Campanian (Hancock & Gale, 1996) stages.

The log of the uppermost Coniacian–basal Campanian (80 m) presented here, measured by Jarvis during

1993, agrees well with the recently published logs of Mortimore, Wood & Gallois (2001). Published isotope data for the Middle Santonian–Lower Campanian (Jenkyns, Gale & Corfield, 1994), replotted against our revised section, will be used in the following correlations.

#### 2.h. Eastbourne, East Sussex (Cenomanian/Turonian boundary interval)

The succession exposed at Gun Gardens (TV 5880 9543; N 50°44'12" E 00°14'57"), Beachy Head, Eastbourne (Fig. 1), affords the thickest Cenomanian/Turonian boundary section in the Anglo-Paris Basin (Jefferies, 1962, 1963; Gale *et al.* 1993, 2005; Paul *et al.* 1999). The macrofossil (Mortimore, 1986; Gale *et al.* 1993, 2000, 2005) and microfossil (Paul *et al.* 1999; Keller *et al.* 2001) biostratigraphy of the section has been documented in detail, and Paul *et al.* (1999) have published high-resolution (5–10 cm sample spacing)  $\delta^{13}\text{C}$  and  $\delta^{18}\text{O}$  curves for a 24 m section incorporating the Cenomanian/Turonian boundary. Similar but lower resolution carbon-isotope curves were presented by Leary & Peryt (1991), Gale *et al.* (1993), Jenkyns, Gale & Corfield (1994), Keller *et al.* (2001) and Tsikos *et al.* (2004).

The Gun Gardens section has become established as a reference for the Cenomanian/Turonian boundary succession in the chalk facies of NW Europe (Tsikos *et al.* 2004; Amédro, Accarie & Robaszynski, 2005; Erbacher *et al.* 2005; Kolonic *et al.* 2005; Kuhnt *et al.* 2005). Published data will be used here to illustrate the consistency of major carbon-isotope trends across the boundary interval.

### 3. Carbon-isotope stratigraphy and correlation

Scholle & Arthur (1980) recognized four key carbon-isotope ‘excursions’ in the Cenomanian–Lower Campanian: ‘light events’, close to the Albian/Cenomanian and Turonian/Coniacian boundaries, and ‘heavy events’ around the Cenomanian/Turonian and Santonian/Campanian boundaries. The remarkable coincidence between carbon-isotope events and stage boundaries was ascribed to oceanographic changes driving biotic turnover in the marine fossil record, and highlighted the potential of carbon-isotope correlation as a global stratigraphic tool. The global nature of these events, particularly the large positive excursion spanning the Cenomanian/Turonian boundary, has been confirmed subsequently by many workers (e.g. Schlanger *et al.* 1987; Arthur *et al.* 1990; Gale *et al.* 1993, 2005; Pratt *et al.* 1993; Jenkyns, Gale & Corfield, 1994; Jenkyns, Mutterlose & Sliter, 1995; Hasegawa, 1997, 2003; Voigt & Hilbrecht, 1997; DeCabrera, Sliter & Jarvis, 1999; Hasegawa & Hatsugai, 2000; Voigt, 2000; Keller *et al.* 2001; Wang *et al.* 2001; Jarvis *et al.* 2002; Tsikos *et al.* 2004; Amédro, Accarie &

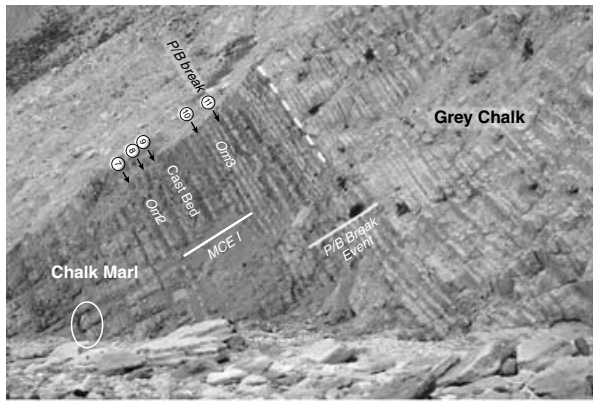


Figure 2. Lower–Middle Cenomanian Chalk of Culver Cliff, Isle of Wight. The extent of the positive carbon-isotope excursion defining Mid-Cenomanian Event I (*MCE I*) and the  $\delta^{13}\text{C}$  minimum of the P/B Break Event are indicated (white diagonal lines), along with the positions of key marker beds and macrofossil datum levels (circled black numerals; Table 1). The isotope profile is shown in Figure 3. Note the rhythmic alternations of chalk and marl that typify Cenomanian chalks, and the sharp increase in carbonate that defines the base of the Grey Chalk (dashed white line). *Om2*, *Om3*: *Orbirhynchia mantelliana* bands 2 and 3; P/B break: planktonic/benthic break (marked increase in the proportion of planktonic foraminifera). The person (circled) is 1.8 m high.

Robaszynski, 2005; Erbacher *et al.* 2005; Kolonic *et al.* 2005; Li *et al.* 2006).

Jenkyns, Gale & Corfield (1994) defined eight correlative events between east Kent and Italy for the Cenomanian–Lower Campanian. However, more detailed studies of specific intervals, such as the Middle Turonian–Lower Coniacian of Germany (Voigt & Hilbrecht, 1997; Wiese, 1999), where at least ten events can be recognized, has demonstrated the potential for further refinement. In this paper, 39 events are defined between the Albian/Cenomanian and Santonian/Campanian boundaries, providing a stratigraphic resolution of around 400 kyr; a further 33 datum levels are provisionally identified that offer potential for even greater stratigraphic refinement.

### 3.a. Cenomanian

The Cenomanian Stage (99.6–93.5 Ma) offers the possibility of the highest stratigraphic resolution for global correlation of the Upper Cretaceous stages because widely distributed ammonite species, augmented by inoceramid bivalves and planktonic foraminifera, provide a temporal resolution of 100–400 kyr (Gale *et al.* 2002). A prominent feature of Cenomanian sediments in northern and eastern Europe is the presence of clear primary bedding cyclicality, expressed as decimetre-scale marl–chalk alternations (Fig. 2). Lithological, macrofaunal and trace-fossil evidence provide a basis for correlating individual couplets on a regional scale. Cenomanian marl–chalk couplets

are interpreted to reflect Milankovitch-band climatic forcing by precession (Gale *et al.* 1999b), each couplet representing a mean duration of  $\sim 20$  kyr (cf. Berger, Loutre & Dehant, 1989). Lithological variation within couplets was probably controlled by productivity of biogenic carbonate rather than being caused by changes in clastic supply (Ditchfield & Marshall, 1989; Paul, 1992).

It has been suggested that modulation by the short eccentricity cycle has generated  $\sim 100$  kyr bundles (Gale, 1990; Mitchell & Carr, 1998; Gale *et al.* 1999b), although these are generally less well expressed. On longer time scales, third-order sequences (Vail, Mitchum & Thompson, 1977) in the Cenomanian (e.g. Robaszynski *et al.* 1998; Jarvis, Murphy & Gale, 2001) may be interpreted as a sedimentary response to sea-level changes driven by the 400 kyr long eccentricity cycle (Gale *et al.* 2002). Astronomical tuning thus offers the potential to date isotopic events to a resolution of 10–20 kyr. In this study, the cyclostratigraphic units of Gale (1990, 1995) have been identified in our sections, and are used to constrain our carbon-isotope correlations at a couplet scale. Calibration of the couplet scheme in individual sections was achieved by identifying key faunal and lithological marker beds, many of which were first defined in northern Germany (Ernst, Schmid & Siebertz, 1983), but which have been subsequently recognized in England and France (Mitchell, Paul & Gale, 1996; Robaszynski *et al.* 1998).

In southern England, the Cenomanian has traditionally been subdivided into four units (from base to summit): Glauconitic Marl, Chalk Marl, Grey Chalk and Plenus Marl (Jukes-Browne & Hill, 1903; Rawson *et al.* 1978). The glauconitic sand and marl facies at the bottom and top of the stage, respectively, represent lithologically distinct packages that can be readily distinguished throughout the area. The base of the Grey Chalk (Fig. 2) is taken at the major increase in carbonate content (calcmeter break) that occurs in the Middle Cenomanian *Acanthoceras rhotomagense* Zone. The four subdivisions are clearly expressed at Dover and Culver (Fig. 3). In northern England, the stage approximates to the Ferriby Chalk Formation of Wood & Smith (1978). Here the succession (Fig. 3) comprises red nodular chalks at the base (Hunstanton Formation), rhythmically bedded grey marly chalks with intermittent beds of calcarenitic chalk (Ferriby Formation), and a thin ( $\sim 10$  cm) black organic-rich layer within a thin interval of marls at the summit (Black Band, base of the Welton Formation). The relatively expanded section at Speeton is approximately half the thickness ( $\sim 40$  m) of its equivalent in southern England ( $\sim 80$  m). In the Trunch borehole (Fig. 3) the highly attenuated Cenomanian succession (12 m) correlates well lithostratigraphically with that at Speeton.

Based on the succession at Speeton, Mitchell, Paul & Gale (1996) described seven isotope events in the

Cenomanian: the Albian/Cenomanian Boundary Event (ACBE); three Lower Cenomanian events (LCE I–III); two Middle Cenomanian events (MCE I–II); and the Cenomanian/Turonian Boundary Event (CTBE). The uppermost three of these were correlated with southern England and Germany. These events are recognized here, and seven new events are defined.

### 3.a.1. Albian/Cenomanian Boundary Event

The base of the Cenomanian is defined by the first appearance of the planktonic foraminifera *Rotalipora globotruncanoides* Sigal (Tröger & Kennedy, 1996). In the Global boundary Stratotype Section and Point (GSSP) at Mont Risou, France (Fig. 1), this boundary lies a short distance above the first occurrence of *R. gandolfi* Luterbacher & Premoli-Silva and the last occurrence of *R. ticinensis* (Gandolfi), and a short distance below the base of the *Mantelliceras mantelli* ammonite Zone (Fig. 4) and *Neostlingoceras carcitanensis* Subzone (Gale *et al.* 1996).

A positive  $\delta^{13}\text{C}$  excursion of around  $+0.5\text{‰}$   $\delta^{13}\text{C}$ , with values up to  $2.7\text{‰}$ , occurs in the upper part of the Hunstanton Chalk Formation (Red Chalk) at Speeton, spanning the Albian/Cenomanian boundary (Mitchell, 1995). The excursion displays three separate peaks (a–c in Figs 3, 4). Mitchell (1995) placed the stage boundary in the trough between the uppermost two peaks (b, c) based largely on a correlation of the  $\delta^{13}\text{C}$  curve with that of the GSSP (Fig. 4; Gale *et al.* 1996), supplemented by evidence from the distribution of macrofossil species. Ammonites and key planktonic foraminifera are absent from the boundary interval at Speeton, but the disappearance of coarse-reticulate *Aucellina* spp. bivalves (Mortor & Wood, 1983; Mitchell, 1995) offers a possible macrofossil stage-boundary indicator that is supported by evidence from brachiopods and benthonic foraminifera.

Elsewhere in England, the boundary between the highest Albian and the Lower Cenomanian *Mantelliceras mantelli* Zone is marked by a major hiatus of up to 1.5 Myr (Gale, 1995). The well-defined  $\delta^{13}\text{C}$  peak in the lower Glauconitic Marl at Dover (Fig. 3) is here correlated with Lower Cenomanian Event I rather than the Albian/Cenomanian Boundary Event, since the first appearance datum (FAD) of *Inoceramus crippsi crippsi* Mantell (macrofossil Datum 1, Table 1) occurs a short distance above the excursion.

### 3.a.2. Lower Cenomanian Events I–III

Three well-defined positive  $\delta^{13}\text{C}$  excursions of  $+0.2$  to  $+0.5\text{‰}$  (Lower Cenomanian Events I–III), superimposed on a longer-term trend of gradually rising values, are developed in the *Mantelliceras mantelli* Zone at Speeton and Dover (Fig. 3). At Speeton, Lower Cenomanian Event I attains values up to  $2.4\text{‰}$   $\delta^{13}\text{C}$  and is associated with a weakly developed hardground

and overlying marly interval, immediately below a facies change (Fig. 3; Mitchell, 1995) from red marls and nodular chinks below (Hunstanton Chalk), to dominantly grey, less clay-rich beds above (Ferryby Chalk Formation). Following a minimum at the bottom of the Ferryby Chalk, Lower Cenomanian Event II reaches  $2.1\text{‰}$   $\delta^{13}\text{C}$  in the bed immediately above, around the LAD of *Aucellina* (Datum 2). Lower Cenomanian Events I and II are located towards the base and at the summit of the Glauconitic Marl at Dover.

Lower Cenomanian Event III, a positive excursion of  $+0.2\text{‰}$   $\delta^{13}\text{C}$  with values up to  $2.3\text{‰}$ , is developed at Speeton in the marl and chinks immediately above the *Pycnodonte* bed (Fig. 3), a prominent marker that occurs at the top of a succession of calcarenitic chinks containing abundant inoceramid bivalve shells and shell debris, particularly large *Inoceramus crippsi* (First Inoceramus Bed of Jeans, 1973). A small  $+0.1\text{‰}$  carbon-isotope peak, which occurs at the base of the beds containing a flood abundance of *I. c. crippsi* (Datum 3), is here called the Crippsi Beds Isotope Event. Lower Cenomanian Event III similarly occurs above a series of beds containing abundant *I. c. crippsi* in the upper *M. mantelli* Zone at Dover (Fig. 3). *Inoceramus c. crippsi* occurs at a comparable level in northern France (Robaszynski *et al.* 1998; Amédéo & Robaszynski, 1999) and an '*I. crippsi* event' is also recognized in northern Germany (Tröger, 1995; Wilmsen, 2003). A single peak at the base of the Chalk Marl within beds containing abundant *I. c. crippsi* at Culver (Fig. 3) is tentatively correlated with the Crippsi Beds Event.

### 3.a.3. Virgatus Beds Event

A minimum followed by a pronounced  $+0.1\text{‰}$  step in the isotope profile occurs at couplet B15 of Gale (1995; Mitchell, 1996) within beds containing abundant *Inoceramus virgatus* Schlüter of the lower *Mantelliceras dixoni* Zone at Speeton (Fig. 3), and is similarly associated with the acme occurrence of whole and fragmentary *I. ex gr. virgatus* (Datum 5) in the 3 m of chalk (couplets B13–18 of Gale, 1995) below the paired limestones with *Mantelliceras dixoni* Spath (M6 marker of Gale, 1989) at Dover. A similar step may be seen in the *I. virgatus* shell bed at 509.3 m in the Trunch borehole (Fig. 3). The step in the isotope profile defines the Virgatus Beds Isotope Event (new name).

The *Inoceramus virgatus* bioevent (Datum 5) is of regional extent, and has been recognized in northern and southern France (Gale, 1995; Robaszynski *et al.* 1998; Amédéo & Robaszynski, 1999) and northern Germany (the '*virgatus/Schloenbachia* event' of Ernst, Schmid & Siebertz, 1983; Gale, 1995; Wilmsen, 2003). A step in the  $\delta^{13}\text{C}$  profile occurring at the base of the *Inoceramus virgatus* beds of Baddeckenstedt Quarry

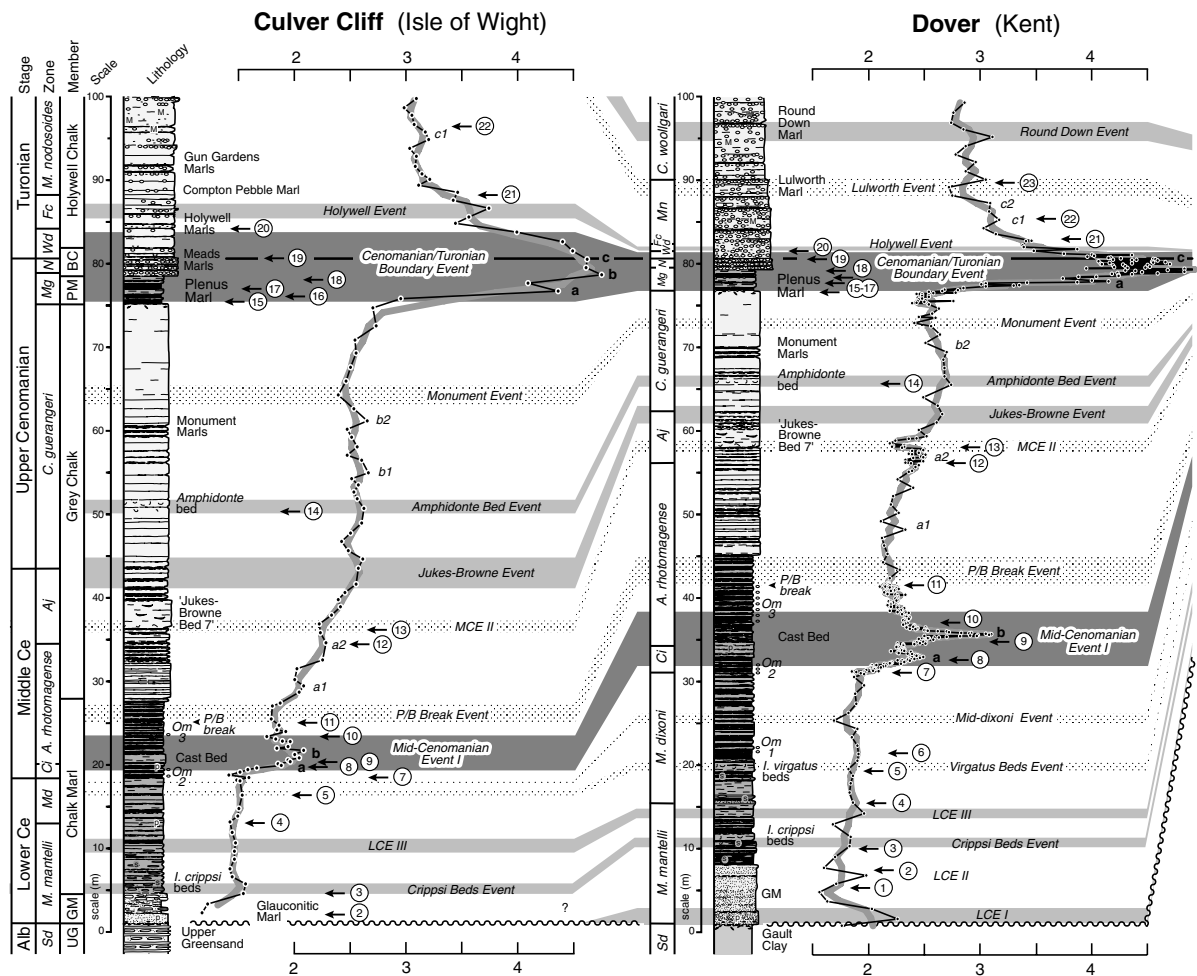


Figure 3. For legend see facing page.

in the Lower Saxony Basin (Wilmsen & Niebuhr, 2002, fig. 6) confirms the regional significance of the associated isotope event.

#### 3.a.4. Mid-dixonii Event

A  $\delta^{13}\text{C}$  minimum followed by a marked increase of around  $+0.2\text{‰}$  occurs in the mid-*Mantelliceras dixonii* Zone above *Orbirhynchia mantelliana* Band 1 (Datum 6), a well-defined marker bed that occurs throughout England (Fig. 3), northern France (Robaszynski *et al.* 1998; Amédro & Robaszynski, 1999) and northern Germany (Ernst, Schmid & Siebertz, 1983; Wilmsen, 2003). This feature is here termed the Mid-dixonii Isotope Event and is clearly developed in the profiles at Dover and Speeton (Fig. 3). The position of the isotope event at Culver is unclear, possibly due to the presence of a hiatus in the thin development of *M. dixonii* Zone represented in the section.

#### 3.a.5. Mid-Cenomanian Event I

The litho-, bio- and chemostratigraphy of the basal Middle Cenomanian in England and northern France

was described in detail by Paul *et al.* (1994b), who documented a bed-scale cyclostratigraphic and  $\delta^{13}\text{C}$  correlation between their sections. At Dover, carbon-isotope values increase sharply from the base of the *Cunningtoniceras inerme* Zone (Fig. 3) in the lower part of *Orbirhynchia mantelliana* Band 2 (Datum 7; couplet B38), rising by  $+0.5\text{‰}$   $\delta^{13}\text{C}$  to form a marked positive excursion with a value of  $2.3\text{‰}$  (Mid-Cenomanian Event Ia, Fig. 3) in the *arlesiensis* bed of couplet B41. The latter is an important NW European marker bed (Datum 8) characterized by the occurrence of the small bivalve *Lyropecten (Aequipecten) arlesiensis* (Woods), together with *Orbirhynchia mantelliana* (J. de C. Sowerby), *Oxytoma seminudum* (Dames), and *Cunningtoniceras inerme* (Pervinquier). Records of *Rotalipora ex gr. reicheli* Mornod at this level (couplets B40–41 Mitchell, 1996) provide a basis for correlation with Tethyan successions (Robaszynski & Caron, 1979a, b), although the index species apparently occurs much lower in the Cenomanian at Gubbio in Italy (see Section 4.b).

Values fall to a trough in the upper *C. inerme* Zone, couplets B42–43 (Fig. 3). They rise again by  $+0.8\text{‰}$   $\delta^{13}\text{C}$  from the base of the *Acanthoceras*

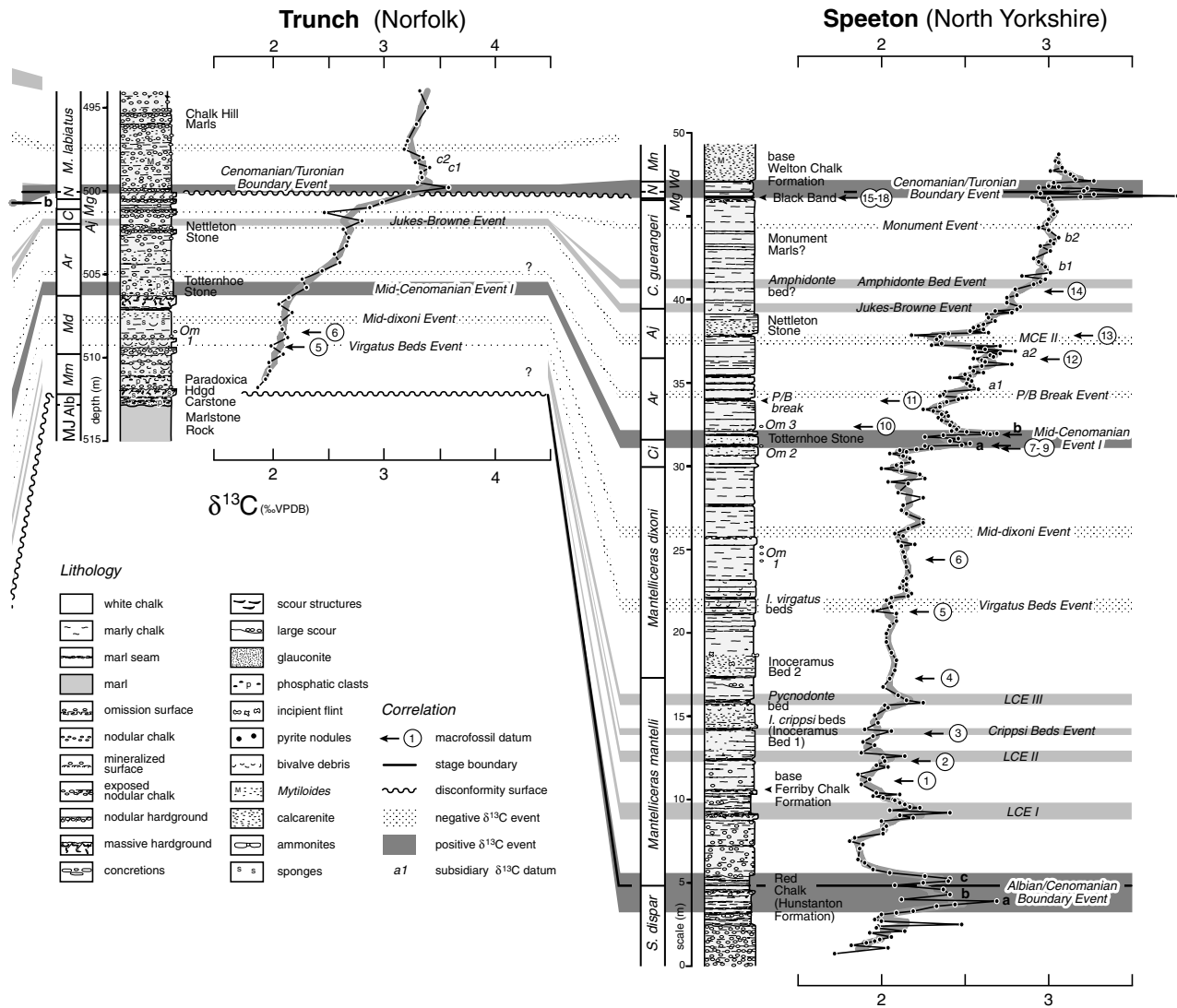


Figure 3. Correlation of English Cenomanian  $\delta^{13}\text{C}$  curves. Individual data points indicated by filled circles; thick grey lines are smoothed trends calculated as three-point moving averages. Note the expanded vertical scales used for the thinner Trunch and Speeton successions. Lithological logs are from this study. Key biostratigraphic datum levels (Table 1) indicated by circled numbers and arrows. Additional biostratigraphic sources: Culver Cliff – Jarvis, Murphy & Gale (2001); Dover – Jenkyns, Gale & Corfield (1994), Gale (1995, 1996); Trunch – Wood, Morter & Gallois (1994); Speeton – Mitchell (1996), Mitchell, Paul & Gale (1996). Isotope data sources: Culver Cliff – Paul *et al.* (1994b), Jarvis, Murphy & Gale (2001); Dover – Jenkyns, Gale & Corfield (1994); Lamolda, Gorostidi & Paul (1994), Mitchell (1996); Trunch – (this study); Speeton – Mitchell, Paul & Gale (1996). Reported  $\delta^{13}\text{C}$  values of Paul *et al.* (1994b) and Mitchell, Paul & Gale (1996) increased by +0.18 ‰ to correct offset with data of Jenkyns, Gale & Corfield (1994); all other data reported as published. Abbreviations: Alb – Albian; Ce – Cenomanian; MJ – Middle Jurassic; *Md* – *Mantelliceras dixonii*; *Mm* – *Mantelliceras mantelli*; *Mg* – *Metoicoceras geslinianum*; *N* – *Neocardioceras juddii*; *Wd* – *Watinoceras devonense*; *Fc* – *Fagesia catinus*; *Mn* – *Mammites nodosoides*; UG – Upper Greensand; GM – Glauconitic Marl; PM – Plenus Marl; BC – Ballard Cliff; *Om* 1–3 – *Orbirhynchia mantelliana* bands 1–3; *P/B break* – planktonic/benthic break (marked increase in proportion of planktonic foraminifera); LCE I–III – Lower Cenomanian Events I–III; MCE II – Mid-Cenomanian Event II.

*rotomagense* Zone, to form a second larger peak with a value of 2.9 ‰ (Mid-Cenomanian Event Ib, Fig. 3) towards the top of the Cast Bed of Price (1877), couplet C1, dropping sharply through the lower part of couplet C2. A hiatus at the base of C1 is indicated by the absence of couplets B44–45 in most sections (Gale, 1995). Carbon-isotope values then begin a long-term fall that reaches a minimum around the calcimetry break (the position of a sudden increase in carbonate

within the succession, represented by the boundary between the Chalk Marl, below, and the Grey Chalk, above, in southern England; Figs 2, 3), couplet C17, in the mid-*A. rotomagense* Zone. The Cast Bed (C1) is another regional marker (Figs 2, 3; Datum 9) that yields a unique and abundant fauna, particularly *Praeactinocamax primus* (Arkhangelsky) belemnites, *O. seminudum*, *Acanthoceras rotomagense* (Brongniart) and numerous small brachiopod species; the occurrence

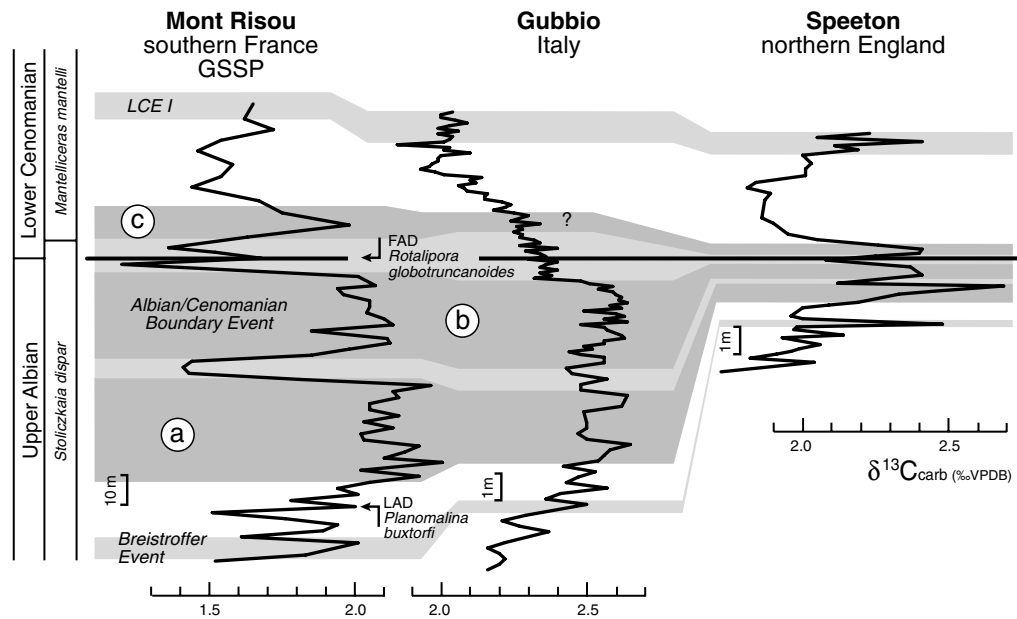


Figure 4. Correlation of Albian/Cenomanian Boundary  $\delta^{13}\text{C}$  events in Europe. The Mont Risou section near Rosans in SE France (Gale *et al.* 1996) is the Global boundary Stratotype Section and Point (GSSP) for the Cenomanian Stage (Tröger & Kennedy, 1996; Ogg, Agterberg & Gradstein, 2004). The base of the stage is defined by the first appearance datum (FAD) of the planktonic foraminifera *Rotalipora globotruncanoides*. The first appearance of *Mantelliceras mantelli* and other Cenomanian ammonites occurs 6 m higher. A complex succession of carbon-isotope events (grey shaded intervals) characterize the boundary interval: a  $\delta^{13}\text{C}$  peak coincides with the Breistroffer Level (Bréhéret, 1988), a succession containing organic-rich laminated marls; two broad peaks occur below (a, b), and one immediately above (c), the base of the Cenomanian, defining the Albian/Cenomanian Boundary Event; a positive  $\delta^{13}\text{C}$  excursion in the lower *M. mantelli* Zone, is probably correlative with Lower Cenomanian Event I (LCE I) of Mitchell, Paul & Gale (1996; Fig. 3). The base of the Cenomanian at Contessa Quarry near Gubbio in Central Italy has been placed (Stoll & Schrag, 2000) using foraminiferal assemblage data from the nearby section in the Bottaccione Gorge (Premoli Silva & Sliter, 1995). The stage boundary at Speeton (Mitchell, 1995) in NE England is defined by the disappearance of coarse reticular *Aucellina* spp. bivalves (cf. Morter & Wood, 1983), and correlation of the uppermost  $\delta^{13}\text{C}$  peak with Mont Risou. Note that the boundary succession at Mont Risou is one order of magnitude thicker than at Gubbio, and 50 times thicker than at Speeton.

of *P. primus* indicates that the bed corresponds to the 'primus Event' in Germany (Ernst, Schmid & Siebertz, 1983; Christensen, 1990).

The two  $\delta^{13}\text{C}$  peaks defining Mid-Cenomanian Events Ia and Ib are clearly distinguished at Dover and Speeton (Fig. 3), but at Culver, Mid-Cenomanian Event Ia is less well defined because most of couplet B42 and all of couplets B43–45 have been cut out by the basal Cast Bed erosion surface (Gale, 1995; Jarvis, Murphy & Gale, 2001). Mid-Cenomanian Event Ib attains a maximum value of 2.2 ‰  $\delta^{13}\text{C}$  at Culver, in the basal portion of couplet C2. At Speeton, the double  $\delta^{13}\text{C}$  peak, with values rising by +0.3 ‰ (Mid-Cenomanian Event Ia) and +0.4 ‰ (Mid-Cenomanian Event Ib) and maxima of 2.6 ‰ and 2.7 ‰, occurs in the calcarenitic chalks of the Totternhoe Stone (Fig. 3; Grey Bed of Hill, 1888). An equivalent small peak of 2.3 ‰  $\delta^{13}\text{C}$  occurs in the phosphatic calcarenites of the Totternhoe Stone at Trunch (Fig. 3). The double peaks defining Mid-Cenomanian Events Ia and Ib are well developed in northern France (Paul *et al.* 1994b), NW Germany (Mitchell, Paul & Gale, 1996; Wilmsen & Niebuhr, 2002) and central Italy (Stoll & Schrag, 2000; Tsikos *et al.* 2004).

Mid-Cenomanian Event I represents a major breakpoint on the long-term carbon-isotope profiles (Fig. 3), from the relatively constant to very slowly rising values that characterize the Lower Cenomanian, to a trend of generally increasing  $\delta^{13}\text{C}$  values through the Middle Cenomanian.

### 3.a.6. P/B Break Event

A sharp increase in the proportion of planktonic to benthonic foraminifera (P/B break, Datum 11) can be identified everywhere in England in the lower Middle Cenomanian, lower *A. rhotomagense* Zone above *Orbirhynchia mantelliana* Band 3 (Figs 2, 3, Datum 10), a succession of beds characterized particularly by common *O. mantelliana* (d'Orbigny) (in couplets C3–10 at Dover and C7–10 at Culver, with peak abundance in C9–10) and *Sciponoceras baculoides* Mantell (couplets C8–12) that is traceable throughout England (e.g. Kennedy, 1969; Jeans, 1980) and France (Gale, 1995; Amédéo & Robaszynski, 1999), Germany (the Middle Cenomanian Event of Ernst, Schmid & Siebertz, 1983; Meyer, 1990), and

the Crimea (Marcinowski, 1980; Gale, Hancock & Kennedy, 1999).

Planktonic foraminifera increase from around 5% to as much as 50% of the microfauna in couplet C11 and above, and *Rotalipora* becomes a more significant element of the planktonic foraminiferal assemblages. *Rotalipora cushmani* (Morrow) first appears at this level in England (Paul *et al.* 1994b; Mitchell, 1996), marking the base of the *R. cushmani* Zone, but appears earlier in Germany (Meyer, 1990). The P/B break has also been called the 'mid-Cenomanian non-sequence' (e.g. Carter & Hart, 1977), although no clear evidence of a sedimentary break occurs at this level in the sections studied.

A weakly developed negative  $\delta^{13}\text{C}$  excursion of up to  $-0.2\text{‰}$  or a broad  $\delta^{13}\text{C}$  minimum occur above the P/B break at Dover, Culver and Speeton (Fig. 3); at the last locality an older minimum is also developed below, in couplet C7. The main significance of the P/B Break Isotope Event (new name) is that it corresponds to a second inflection point on the long-term isotope profiles, with a change to more rapidly rising  $\delta^{13}\text{C}$  values, particularly above the calcimetry break at couplet C17. It is possible that the lower, sub-P/B break  $\delta^{13}\text{C}$  minimum at Speeton correlates to the supra-P/B break minimum at Dover and Culver, with the change in foraminiferal assemblage occurring later in northern England. This interpretation is considered to be unlikely, but higher resolution  $\delta^{13}\text{C}$  profiles for the southern England sections will be required to test this hypothesis.

### 3.a.7. Mid-Cenomanian Event II

A marked negative excursion of around  $-0.3\text{‰}$  occurs in the upper Middle Cenomanian *Acanthoceras jukesbrownei* Zone at Dover and Speeton (Fig. 3), termed Mid-Cenomanian Event II by Mitchell, Paul & Gale (1996). The isotopic signature of mid-Cenomanian Event II is located in the lower part of the calcarenitic chalks with scour structures that constitute 'Jukes-Browne Bed 7' (Jukes-Browne & Hill, 1903) at Dover and Culver (couplets D1–8), the lower beds of which (D1–3) contain abundant *Pycnodonte* oysters (Datum 13). This prominent lithological marker occurs a short distance above beds containing common *Inoceramus atlanticus* Heinz, and can be traced to northern France (Robaszynski *et al.* 1998; Amédro & Robaszynski, 1999); the *I. atlanticus* acme extends at least to the Crimea (Gale, Hancock & Kennedy, 1999). However, the isotope excursion of Mid-Cenomanian Event II is developed immediately below the Nettleton Stone calcarenites, which also have a concentration of *Pycnodonte* at their base (Nettleton *Pycnodonte* Bed; Gryphaea Bed of Bower & Farmery, 1910) at Speeton and Trunch.

In Germany, a *Pycnodonte* event (Ernst, Schmid & Siebertz, 1983) occurs around a prominent double marl

with an acme of oysters beneath, between and above the marls. The negative isotope excursion of mid-Cenomanian Event II straddles the pair of marls (e.g. at Rheine, Westphalia: Lehmann, 1999). Thus the earliest oyster occurrence in Germany would correspond to the *Pycnodonte* concentration below Jukes-Browne Bed 7 in southern England, and the latest occurrence to the *Pycnodonte* Bed below the Nettleton Stone calcarenites. However, the different lithologies of strata recording Mid-Cenomanian Event II in southern and northern England indicate that the facies change to calcarenitic chalks is diachronous between the Anglo-Paris Basin and the Cleveland–Lower Saxony Basins, with the facies change occurring later in northern England. This diachroneity is perhaps not surprising, given the time-transgressive nature of onlap surfaces, such as those inferred for the *Pycnodonte* event (Mitchell, Paul & Gale, 1996).

The interval between the P/B Break Event and Mid-Cenomanian Event II includes two broad  $\delta^{13}\text{C}$  peaks at Culver (*a1*, *a2*; Fig. 3) which are also developed at Dover and Speeton. Peak *a2* occurs at the base of the Middle Cenomanian *Acanthoceras jukesbrownei* Zone around the FADs of *Acanthoceras jukesbrownei* Spath and *Inoceramus atlanticus* (Datum 12).

### 3.a.8. Jukes-Browne Event

A broad but clearly developed maximum in  $\delta^{13}\text{C}$  values with an overlying trough occurs in the upper beds of the *Acanthoceras jukesbrownei* and lowest *Calycoceras guerangeri* zones (couplets D11–17) at Dover, Culver and Speeton (Fig. 3). The Jukes-Browne Isotope Event (new name) provides a good marker for the base of the Upper Cenomanian, at the bottom of couplet D14.

### 3.a.9. Amphidonte Bed Event

An inflection point on the long-term carbon-isotope curves from rising to constant  $\delta^{13}\text{C}$  values, the Amphidonte Bed Isotope Event (new name), occurs around the level of the Amphidonte Bed (Datum 14) at Dover and Culver (couplets D21–22 in the expanded Culver succession; Fig. 3), and an inflection point is seen at a similar position in the Speeton profile. A concentration of the small ostreid bivalve *Amphidonte* occurs around the Middle/Upper Cenomanian boundary at Speeton, immediately above the Nettleton Stone (Mitchell, Paul & Gale, 1996). However, this oyster concentration is older than the Amphidonte Bed in southern England. A higher level of *Amphidonte* has been identified elsewhere in northern England (Wood, 1992; Mortimore, Wood & Gallois, 2001), which probably correlates to that in southern England. A lower Upper Cenomanian oyster event, also characterized by the presence of *Amphidonte*, has been recognized in northern France (Amédro & Robaszynski, 1999), northern Germany (Ernst, Schmid & Siebertz, 1983;

Owen, 1996; Wilmsen, 2003) and the Crimea (Gale, Hancock & Kennedy, 1999). This bioevent can be recognized in southern England, but no corresponding isotope data are available for the sections on continental Europe.

### 3.a.10. Monument Event

A minimum in  $\delta^{13}\text{C}$  values in the upper *Calycoceras guerangeri* Zone, occurring a short distance above the Monument Marls of Jarvis, Murphy & Gale (2001), provides a clear inflection point on the profiles at Culver and Dover which may be correlated with Speeton (Fig. 3). This shift in the long-term isotope trend is here termed the Monument Isotope Event.

Two small  $\delta^{13}\text{C}$  peaks, labelled *b1* and *b2* in Figure 3, occur between the Amphidonte Bed and Monument events at Culver and Speeton, but only *b2* can be recognized in the Dover profile. These peaks also have wider potential for correlation.

### 3.a.11. Cenomanian/Turonian Boundary Event

The positive  $\delta^{13}\text{C}$  excursion spanning the Cenomanian/Turonian boundary (Fig. 3) is one of the largest and best documented carbon-isotope events in the geological record (Jenkyns, 1980, 1985; Scholle & Arthur, 1980; Schlanger *et al.* 1987). This event is conventionally interpreted as being related to accelerated burial of marine organic matter, particularly in the Atlantic, but also in other ocean basins (Herbin *et al.* 1986; Arthur *et al.* 1990; Kuypers *et al.* 2002, 2004). The phenomenon is widely referred to as the Cenomanian/Turonian Boundary Event (CTBE), or Oceanic Anoxic Event 2 (OAE2; Arthur *et al.* 1990).

Detailed studies of the Cenomanian/Turonian Boundary Event and the associated stable-isotope and biostratigraphy in England have been undertaken at Dover (Jarvis *et al.* 1988*b*; Lamolda, Gorostidi & Paul, 1994) and Eastbourne (Leary & Peryt, 1991; Gale *et al.* 1993, 2005; Paul *et al.* 1999; Keller *et al.* 2001; Tsikos *et al.* 2004), and isotope curves have also been published for Speeton (Mitchell, Paul & Gale, 1996) and Culver (Jarvis, Murphy & Gale, 2001). The Eastbourne Gun Gardens section in West Sussex (Figs 1, 5) is the most expanded boundary section in chalk facies in NW Europe (Paul *et al.* 1999), and is increasingly being used as an international reference for biostratigraphic and chemostratigraphic studies (Amédro, Accarie & Robaszynski, 2005; Erbacher *et al.* 2005; Kolonic *et al.* 2005; Kuhnt *et al.* 2005). Carbon-isotope curves for the Cenomanian/Turonian Boundary Event at Culver, Dover, Trunch and Speeton are illustrated in Figure 3, and a detailed  $\delta^{13}\text{C}$  correlation between Eastbourne and Dover is shown in Figure 6, which compares these sections with the Turonian Global boundary Stratotype Section and Point at Pueblo, Colorado, USA. The base of the Turonian

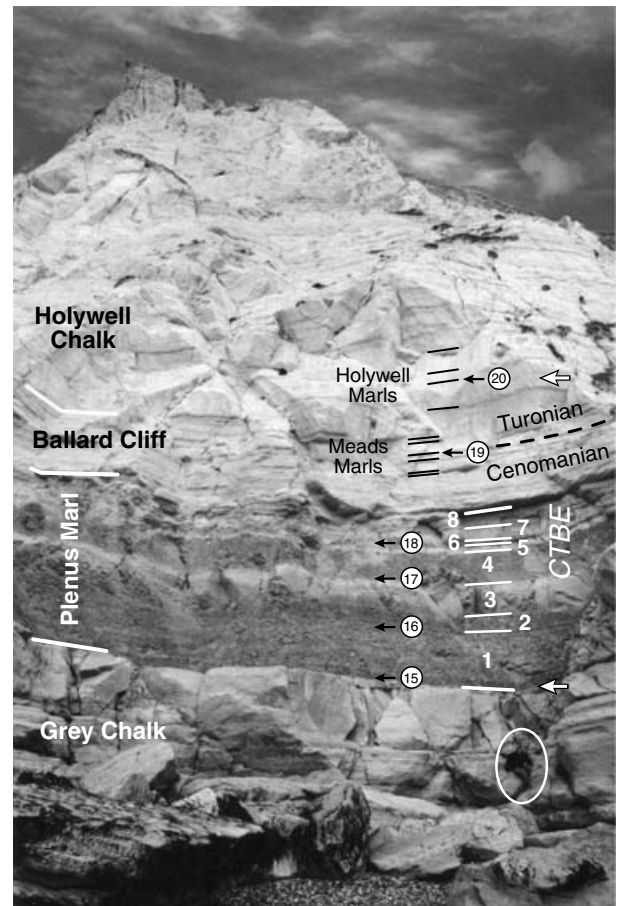


Figure 5. Cenomanian/Turonian boundary section at Eastbourne Gun Gardens, East Sussex. This locality offers the most expanded stage boundary section in the chalk facies of NW Europe (Paul *et al.* 1999) and is widely used as a reference section for stable-isotope studies. Plenus Marl bed numbers (Jefferies, 1963) are in white. Key macrofossil datum levels (Table 1) are indicated by circled black numerals. The bottom and top of the positive  $\delta^{13}\text{C}$  excursion defining the Cenomanian/Turonian Boundary Event (CTBE) are indicated by the white arrows. Carbon-isotope curves are presented in Figure 6. The person (circled) is 1.8 m high.

is defined (Bengtson, 1996; Kennedy, Walaszczyk & Cobban, 2000) as the base of Bed 86 at Pueblo (Fig. 6), which contains the first occurrence of the ammonite *Watinoceras devonense* Wright & Kennedy and the inoceramid bivalve *Mytiloides puebloensis* Walaszczyk & Cobban (Datum 19).

The positive  $\delta^{13}\text{C}$  excursion defining the Cenomanian/Turonian Boundary Event spans the Plenus Marl, Ballard Cliff Chalk and basal Holywell Chalk members (Figs 3, 5) in southern England. The stratigraphy of the Plenus Marl was described in detail by Jefferies (1962, 1963), who used a combination of lithological and faunal criteria to define eight beds (numbered 1–8, Fig. 5) that could be correlated throughout the Anglo-Paris Basin and beyond. The Plenus Marl is everywhere underlain by a strongly burrowed erosion surface at the top of the Grey Chalk, the sub-Plenus erosion surface, and is directly

overlain by white nodular chalks formerly referred to the Melbourn Rock (Jefferies, 1963; Mortimore, 1986). In expanded basinal successions, such as that at Eastbourne (Fig. 5), the latter beds show little lithological similarity to the hard nodular chalks of the Melbourn Rock in its type area of Cambridgeshire (Penning & Jukes-Browne, 1881). In recognition of this, Gale (1996) erected the Ballard Cliff Member for the interval of marly weakly nodular chalks that extends from the top of the Plenus Marl to the top of a distinctive succession containing six marls (Fig. 5), Meads Marls 1–6 of Mortimore (1986). The overlying marly chalks of the Holywell Member (Mortimore, 1986) contain a succession of marl seam marker beds, including Holywell Marls 1–7 at the base. This marker-bed stratigraphy provides a basis for detailed comparison of the study sections (Figs 3, 6).

Some remarkable similarities exist between the faunal changes accompanying the Cenomanian/Turonian Boundary Event and those associated with Mid-Cenomanian Event I, including the temporary appearance of the bivalves *Lyropecten (Aequipecten) arlesiensis* and *Oxytoma seminudum* with belemnites (*Praeactinocamax plenus* (Blainville)) (Datum 17) in Plenus Marl beds 3–6 (couplets E4–E6). Characteristic brachiopod ‘pulse’ faunas also occur in the sequence: *Orbirhynchia multicostata* Pettit in the top of Bed 1a and Bed 1b (couplet E3), and *O. wiesti* (Quenstedt) (Datum 18) in Bed 7 (couplet E6). Major faunal turnover occurred in most biotic groups through the Cenomanian/Turonian Boundary Event (e.g. Jarvis *et al.* 1988a; Paul *et al.* 1994a, 1999; Gale *et al.* 2000, 2005; Keller *et al.* 2001).

The most detailed isotope record of the Cenomanian/Turonian Boundary Event is that from Eastbourne Gun Gardens (Fig. 6; Paul *et al.* 1999, fig. 4), based on sampling a 24 m section spanning the Cenomanian/Turonian boundary at 5–10 cm intervals. Carbon-isotope values rise by +2.0‰  $\delta^{13}\text{C}$ , from 2.8‰ at the base of Plenus Marl Bed 1 to a maximum of 4.8‰ towards the top of Bed 3, and then decline again to a trough of 4.1‰ in the middle of Bed 4. This part of the curve constitutes the lowest of three main peaks (Figs 3, 6, ‘a’) forming the excursion. Values increase to a second maximum of 5.4‰  $\delta^{13}\text{C}$  at the top of Bed 8 (peak ‘b’; representing a +2.6‰  $\delta^{13}\text{C}$  increase from the base of the excursion), decline to a plateau of 4.7‰ in the Ballard Cliff Member, and peak again to 5.1‰ around Meads Marl 6 (peak ‘c’).

The base of the Turonian is marked by the coincident appearance of *Watinoceras* and *Mytiloides puebloensis* (Datum 19) immediately above Meads Marl 4 (Gale *et al.* 2005). Carbon-isotope values fall back to more constant levels of around 3.8‰ above *Roveacrinus* Bed 1 (containing abundant microcrinoids, *Roveacrinus communis* Douglas, Datum 20; couplet E23) and Holywell Marl 3 (top of the excursion of Paul *et al.* 1999). However, values continue to decline above this

at Culver and Dover, and only plateau within the upper beds of the Lower Turonian *Mammites nodosoides* Zone.

The carbon-isotope profile at Dover (Lamolda, Gorostidi & Paul, 1994) is very similar to Eastbourne, but with  $\delta^{13}\text{C}$  values shifted by around –0.4‰. The three peaks of the Cenomanian/Turonian Boundary Event excursion are clearly expressed (Fig. 6). However, at Dover the maximum defining peak ‘a’ occurs in Bed 2 and the trough is developed in Bed 3. This difference cannot be attributed to analytical or sampling error since the same positions of the peaks are evident in other published profiles for Eastbourne (Gale *et al.* 1993; Keller *et al.* 2001; Tsikos *et al.* 2004) and Dover (Jarvis *et al.* 1988a; Jeans *et al.* 1991). The low-resolution Culver profile (Jarvis, Murphy & Gale, 2001), by contrast, shows a Bed 2/3 peak and Bed 4 trough, like Eastbourne (Fig. 3).

The above differences may be due to the fact that the Eastbourne succession is more complete. For example, the last appearance of the key foraminifera index species *Rotalipora cushmani* occurs in the middle of Bed 4 at Eastbourne (Fig. 6), but at the base of the bed at Dover. This suggests that only sediment of upper Bed 4 age is represented at Dover, so the low  $\delta^{13}\text{C}$  interval that characterizes the lower part of the bed at Eastbourne is absent at Dover. The different positions of the peak ‘a’ maximum with respect to Beds 2 and 3 may be due to the middle part of Bed 3 at Eastbourne being unrepresented at Dover. Alternative explanations would be that the first peak of the excursion occurred earlier in Kent than in Sussex and the Isle of Wight, the facies change from marl (Beds 2 and 4) to chalk (Beds 3 and 5) is diachronous, or that local diagenetic factors have affected the Dover profile. The first two alternatives are judged to be unlikely, but diagenetic factors may have some influence, as indicated by the generally lower  $\delta^{13}\text{C}$  values at Dover. Much lower  $\delta^{18}\text{O}$  values characterize Bed 3 at Dover than at Eastbourne (Lamolda, Gorostidi & Paul, 1994), despite similar values through most of the section; these low  $\delta^{18}\text{O}$  values suggest selective alteration of Bed 3 at Dover.

By contrast to peak ‘a’, the peak ‘b’ maximum occurs everywhere in Bed 8 (Fig. 6), and is coincident with a marked faunal turnover: *Heterohelix* increases from 20% to >60% of the planktonic foraminifera assemblage (*Heterohelix* shift in Fig. 6) above this level, and through the higher beds of the Cenomanian/Turonian Boundary Event (Keller *et al.* 2001). The peak ‘c’ maximum at Meads Marl 6 also appears to be consistent at Dover, Eastbourne and Culver.

A lower resolution  $\delta^{13}\text{C}$  curve obtained from organic matter at Eastbourne ( $\delta^{13}\text{C}_{\text{org}}$ ) has recently been published (Gale *et al.* 2005) that broadly follows the carbonate ( $\delta^{13}\text{C}_{\text{carb}}$ ) curve (Fig. 6), and a similar  $\delta^{13}\text{C}_{\text{org}}$  curve for the Plenus Marl was presented by Tsikos

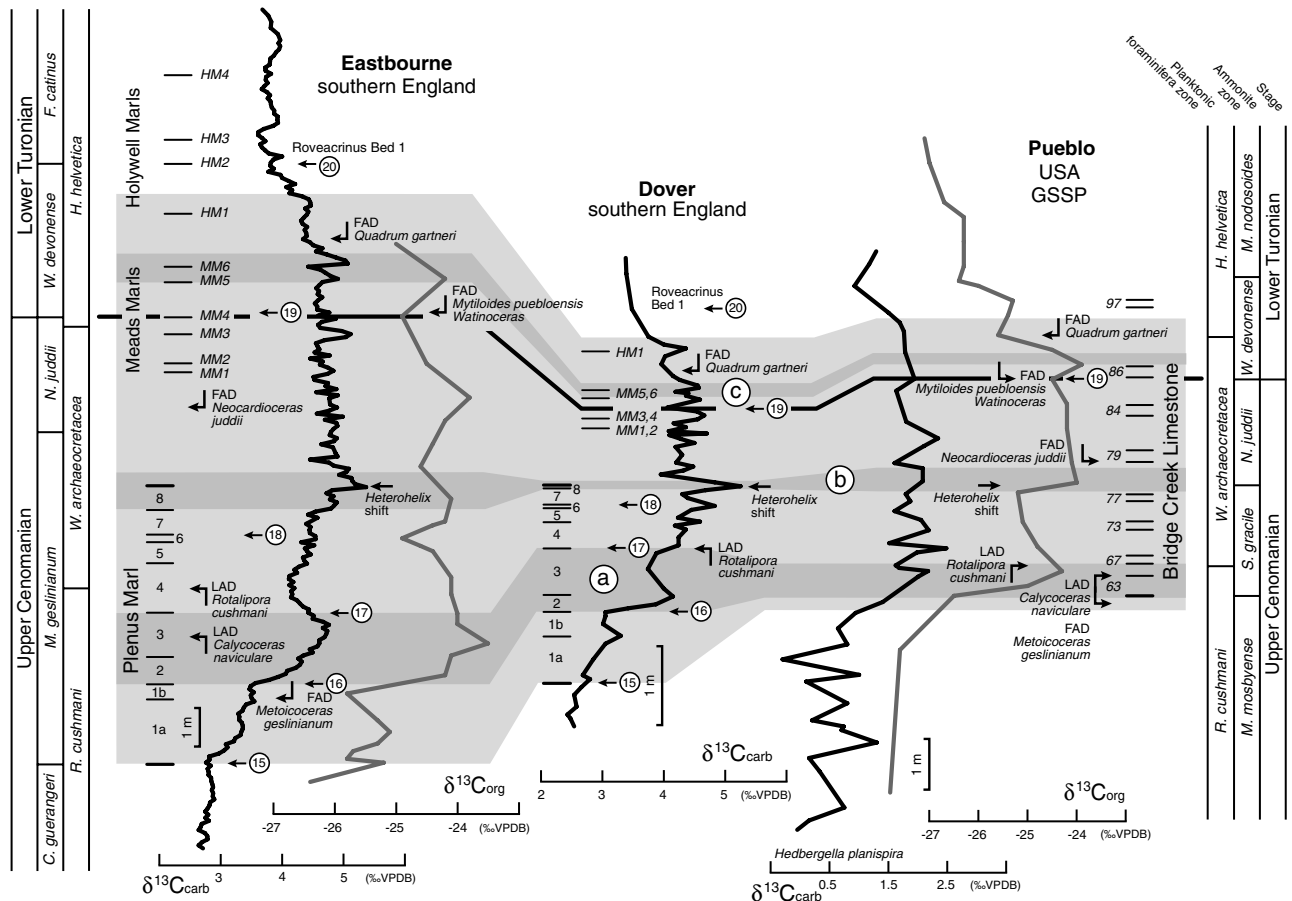


Figure 6. Correlation of the Cenomanian/Turonian Boundary  $\delta^{13}\text{C}$  event between England and the GSSP at Pueblo, Colorado, USA. The positions of stage, ammonite and planktonic foraminiferal zone boundaries, key fossil-occurrence datum levels, and key marker beds are shown for comparison. The most detailed isotope record is available for carbonate ( $\delta^{13}\text{C}_{\text{carb}}$ ) analysed in bulk sediments collected from Gun Gardens at Eastbourne, East Sussex (Paul *et al.* 1999). The Eastbourne  $\delta^{13}\text{C}$  profile (thick black line, far left) shows three carbon-isotope peaks (dark grey shaded horizons) within the overall positive excursion (pale grey shaded interval): (a) near the base, within Plenus Marl Beds 2–3 of Jefferies (1962, 1963); (b) in the middle, spanning the Plenus Marl/Ballard Cliff Member boundary (cf. Gale, 1996); and (c) at the top of the excursion, around Meads Marls 5–6 (MM5, MM6) of Mortimore (1986). Peaks are developed in similar positions on a lower resolution carbon-isotope profile (dark grey curve) obtained from organic matter ( $\delta^{13}\text{C}_{\text{org}}$ ) isolated from the sediments (Gale *et al.* 2005), although peak maxima appear to be offset slightly below those of  $\delta^{13}\text{C}_{\text{carb}}$ . The succession at Dover (Jarvis *et al.* 1988b) can be correlated at a bed scale to Eastbourne, and a detailed  $\delta^{13}\text{C}_{\text{carb}}$  profile (Lamolda, Gorostidi & Paul, 1994) shows strong similarities to the Eastbourne curve. The three carbon-isotope maxima defined in England can be correlated with the GSSP at Pueblo. The three peaks are well developed in the  $\delta^{13}\text{C}_{\text{org}}$  profile (dark grey curve) of Pratt & Threlkeld (1984). A  $\delta^{13}\text{C}_{\text{carb}}$  profile (black curve) derived from the analysis of small planktonic foraminifera (*Hedbergella planispira*) separated from the section (Keller *et al.* 2004) shows broadly similar trends, despite the lower amplitude of  $\delta^{13}\text{C}$  variation. Note, however, the similarity in the absolute  $\delta^{13}\text{C}_{\text{carb}}$  and  $\delta^{13}\text{C}_{\text{org}}$  values obtained from bulk sediments from all three sections. The isotope correlation between England and North America can be tested using last and first appearance datum levels (LAD, FAD) and floods of key fossil taxa in the reference sections. The relative positions of ammonite, inoceramid bivalve and planktonic foraminifera datum levels in the sections are consistent with the isotope correlation (Jarvis *et al.* 1988b; Gale *et al.* 1993, 2005; Paul *et al.* 1999; Keller *et al.* 2001, 2004).

*et al.* (2004, fig. 2). There is evidence from both curves that a small offset (< 10 kyr based on couplet cyclostratigraphy) exists towards earlier maxima in  $\delta^{13}\text{C}_{\text{org}}$ , and that  $\delta^{13}\text{C}_{\text{org}}$  minima occur at  $\delta^{13}\text{C}_{\text{carb}}$  plateaux that precede the rises defining peaks 'a–c'. These differences may be significant and indicate variable fractionation between organic and inorganic carbon during the Cenomanian/Turonian Boundary Event. A comparison with  $\delta^{13}\text{C}_{\text{org}}$  and  $\delta^{13}\text{C}_{\text{carb}}$  profiles for the Pueblo GSSP (Pratt & Threlkeld, 1984; Keller *et al.* 2004; Gale *et al.* 2005; Sageman, Myers &

Arthur, 2006) demonstrates that peaks 'a–c' can be recognized in North America (Fig. 6), and that they are isochronous with England within the resolution of the biostratigraphy.

The Cenomanian/Turonian Boundary Event at Trunch and Speeton is registered in highly attenuated successions. A single peak of 3.6‰  $\delta^{13}\text{C}$  at 499.75 m in the Trunch borehole (Fig. 3) suggests that only sediments from the final stages of the event are preserved. The low  $\delta^{13}\text{C}$  value of 3.2‰ in the planar hardground at 500.10 m, below, indicates that this bed

is also probably Lower Turonian (or possibly lowest *Metoicoceras geslinianum* Zone), and certainly not Upper Cenomanian *Neocardioceras juddii* Zone, as suggested by Wood, Morter & Gallois (1994).

At Speeton, erratic but elevated  $\delta^{13}\text{C}$  (up to 3.8 ‰) values are associated with the Black Band succession (Fig. 3), representing a positive excursion of +0.8 ‰. The Black Band, a thin ~10 cm bed of dark organic-rich marl containing up to 10% organic carbon (Jeans *et al.* 1991) can be traced throughout northern England into the North Sea, and is probably equivalent to the basal Turonian black shales overlying the 'Plenus Limestone' in northern Germany (Wood & Ernst, 1998). At South Ferriby, Humberside, the Black Band and the immediately underlying white chalks display a clear positive carbon excursion of up to 4.3 ‰ (Schlanger *et al.* 1987), with maximum values occurring below the organic-rich interval. Biostratigraphic evidence (Hart & Leary, 1991; Wood & Mortimore, 1995) suggests that the Black Band correlates with the Ballard Cliff Member in southern England, and beds equivalent to most of the Plenus Marl are generally thin or absent in northern England, a conclusion supported by the moderate maximum  $\delta^{13}\text{C}$  values observed at Speeton and South Ferriby. Three peaks in the profile at Speeton (Fig. 3) are separated by very low  $\delta^{13}\text{C}$  values of <3 ‰. Such anomalously low values can be attributed to overprinting by isotopically light cements precipitated during diagenesis of the organic-rich intervals.

### 3.b. Turonian

Turonian (93.5–89.3 Ma) sediments display less prominent cyclicity than those of Cenomanian age, due to the continued upwards decrease in clay content that characterizes the European Chalk. Marl–chalk couplets continue to be developed (Figs 5, 7), but marls are thinner, contain less clay and commonly display a distinct 'flaser' or 'griotte' texture. Couplets also tend to be thicker, typically around 0.5–1 m, and where more attenuated are nodular and contain abundant shell debris. Local, decimetre-deep, metre-scale scours filled with chalk pebble intraclasts and calcarenitic sediments commonly cut out parts of the succession, particularly in the Lower Turonian. Nodular flints become abundant in the upper beds, where thalassinoid burrow flints are the most prominent indicators of bedding cyclicity. Strongly cemented and mineralized hardgrounds are features of many Upper Turonian sections.

Considerable lateral variation in thickness and lithology characterizes the Turonian successions of England (Fig. 7), making cyclostratigraphic correlation considerably more difficult than in the Cenomanian. Nonetheless, a couplet stratigraphy has been successfully developed for the Lower and Middle Turonian (Gale, 1996). In southern England, sediments above the Ballard Cliff Chalk are divided into three members

(Fig. 7). These are, from base to summit: nodular intraclastic chalks containing abundant inoceramid debris (including common *Mytiloides* shell beds) of the Holywell Member (Mortimore, 1983, 1986; Gale, 1996); soft marly chalks of the New Pit Member (Mortimore, 1986; Gale, 1996); and nodular flaser chalks of the St Margaret's Member (Dowker, 1870; Robinson, 1986), which contains abundant flints in the upper part. Locally, a highly condensed succession comprising a complex of strongly cemented and mineralized hardgrounds is developed as the lateral equivalent of the upper New Pit and St Margaret's Chalks. This Chalk Rock Member (Bromley & Gale, 1982) is a distinctive but complex and highly diachronous unit (Gale, 1996). The member is strongly developed in Berkshire and is well displayed in the Banterwick Barn borehole (Fig. 7).

In northern England the lithological succession is very different, and marly, massively bedded chalks with abundant nodular flints typify the Lower and Middle Turonian: the Welton Chalk Formation of Wood & Smith (1978). The base of the Welton Chalk is taken at the erosion surface below the Black Band. The appearance of large tabular flints and a general change to more flinty sediments defines the base of the Burnham Chalk (Wood & Smith, 1978) above, approximating to the base of the *Sternotaxis plana* Zone. Trunch lies at the southern limit of northern England-type successions (Fig. 1), but shows stronger lithological similarities (Fig. 7) to successions in North Yorkshire, Humberside and Lincolnshire than those in southern England.

Gale (1996, fig. 8) plotted the Turonian carbon-isotope data of Jenkyns, Gale & Corfield (1994) from Dover against a skeleton stratigraphy and named two positive carbon-isotope excursions: the 'Pewsey Event' in the Middle Turonian uppermost *Collignonicerias woollgari* Zone, and the 'Hitch Wood Event' in the Upper Turonian upper *Subprionocyclus neptuni* Zone. These and a number of other carbon-isotope events have subsequently been widely recognized and correlated to sections throughout northern Germany and in northern Spain (Voigt & Hilbrecht, 1997; Wiese, 1999; Wiese & Kaplan, 2001). These sections include Lengerich in the Münster Basin of NW Germany, a candidate GSSP for the Middle/Upper Turonian boundary (Wiese & Kaplan, 2001), and Salzgitter-Salder in Lower Saxony, which has been proposed as a Turonian/Coniacian boundary GSSP (Wood, Ernst & Rasemann, 1984; Kauffman, Kennedy & Wood, 1996).

Detailed correlation of the Banterwick, Culver, Dover and Trunch successions (Fig. 7), supplemented by data from Germany and Spain, enables ten new named events to be defined, in addition to the Pewsey and Hitch Wood events. Fourteen other events (*c1–i3* in Fig. 7) are recognized in some sections and provide ancillary correlation points.

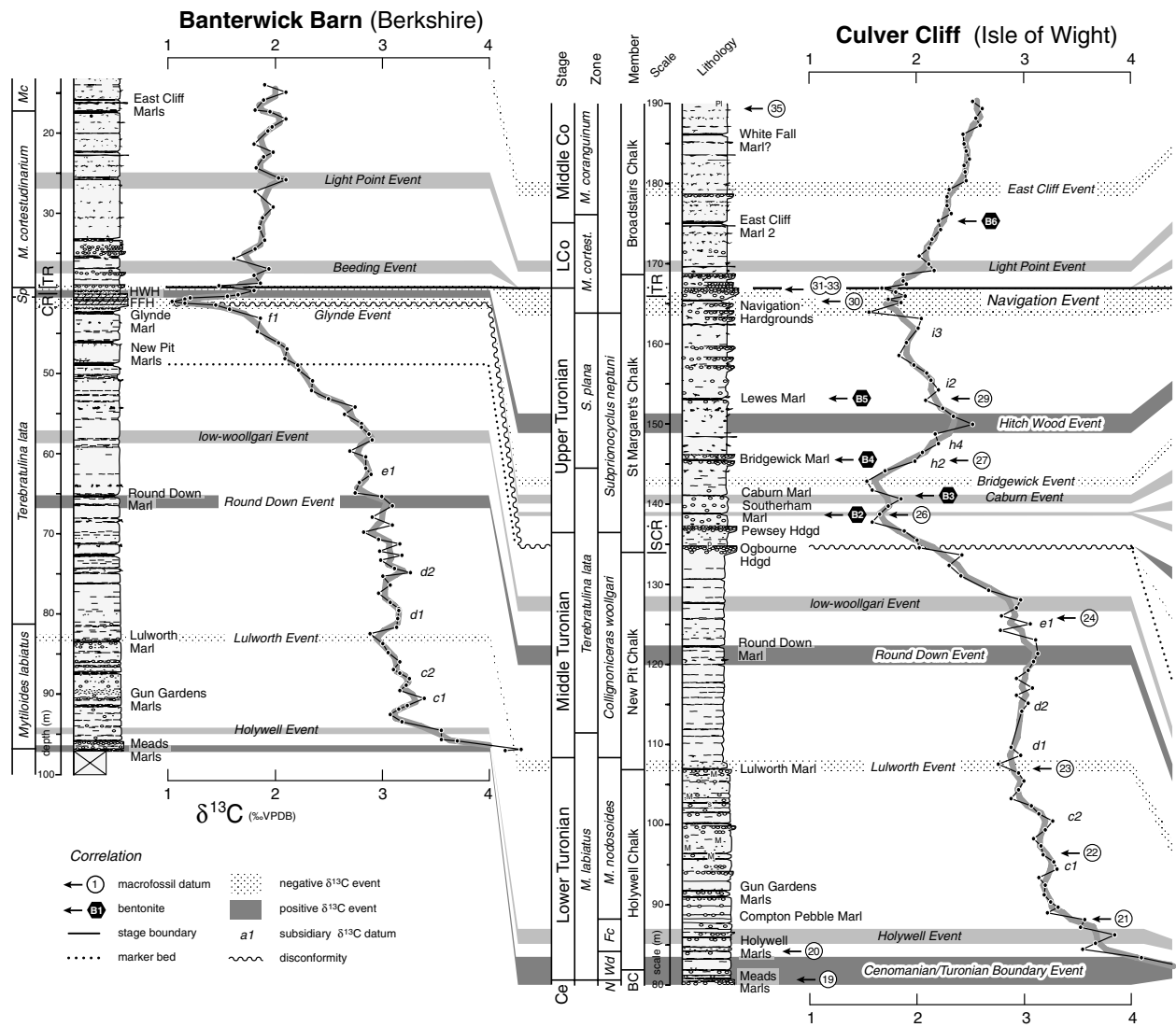


Figure 7. For legend see facing page.

### 3.b.1. Holywell Event

A small positive  $\delta^{13}\text{C}$  excursion of +0.2‰ occurring above Holywell Marl 4 at Culver and Eastbourne (couplet E25) is superimposed on the general trend of falling carbon-isotope values above the Cenomanian/Turonian Boundary Event (Figs 6, 7). A similar peak occurs at the same stratigraphic position between macrofossil Datum levels 20 and 21 at Dover. This Holywell Isotope Event (new name), which is also recognizable at Banterwick (Fig. 7), provides a useful correlation point within the basal Turonian.

### 3.b.2. Lulworth Event

The basal marker of the New Pit Chalk is the Lulworth Marl (Gale, 1996), which is overlain by *Roveacrinus* Bed 2 (together constituting couplet F1). A significant

inflection point occurs at this level in the carbon-isotope curves, with a change from falling  $\delta^{13}\text{C}$  values to rising values above. The  $\delta^{13}\text{C}$  minimum occurs within *Roveacrinus* Bed 2 (Datum 23, uppermost Lower Turonian *Mammites nodosoides* Zone) at Culver, and is apparently slightly lower (couplet E52) in the more attenuated nodular chalks at Dover, although this difference may be due to a combination of low-resolution sampling and analytical error. The  $\delta^{13}\text{C}$  minimum and associated -0.2‰ negative excursion, with values of around 3‰, defines the Lulworth Isotope Event (new name). The event lies in the uppermost Lower Turonian, the base of the Middle Turonian being placed 2 m above the Lulworth Marl at Culver, at the first occurrence of *C. woollgari* (Mantell) in couplet F3. An identical inflection point is seen in the Lower Turonian profile at Söhlde in northern Germany (Voigt & Hilbrecht, 1997).

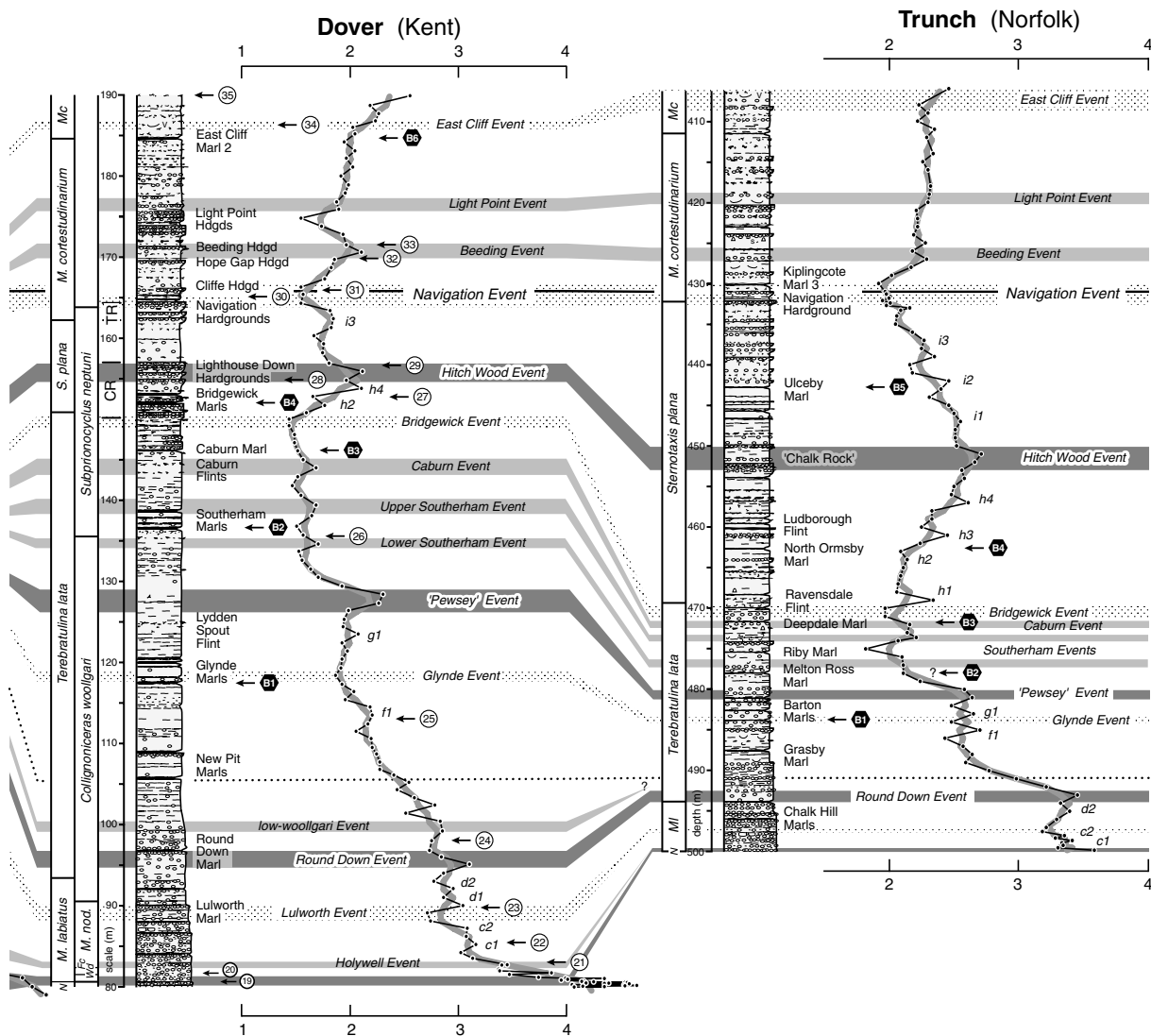


Figure 7. Correlation of English Turonian  $\delta^{13}\text{C}$  curves. See Figure 3 for plotting details. Additional biostratigraphic data sources: Banterwick Barn – Pearce *et al.* (2003), Woods & Aldiss (2004); Culver – this study; Dover – Jenkyns, Gale & Corfield (1994), Gale (1996); Trunch – Wood, Morter & Gallois (1994). Isotope data sources: Banterwick Barn – Murphy, Jarvis & Edmunds (1997); Culver – this study; Dover – Jenkyns, Gale & Corfield (1994); Trunch – this study. Abbreviations: *Fc* – *Fagesia catinus*; *Mc* – *Micraster coranguinum*; *M. cortest.* – *Micraster cortesudinarium*; *Ml* – *Mytiloides labiatus*; *M. nod.* – *Mammites nodosoides*; *N* – *Neocardioceras juddii*; *Sp* – *Sternotaxis plana*; *Wd* – *Watinoceras devonense*; BC – Ballard Cliff Member; CR – Chalk Rock; FFH – Fognam Farm Hardground; HWH – Hitch Wood Hardground; SCR – ‘Southern Chalk Rock’; TR – Top Rock.

Between the Holywell Event, with  $\delta^{13}\text{C}$  values approaching 4 ‰, and the Lulworth Event, where values fall to 3 ‰, isotope profiles in all four study sections are characterized by two small  $\delta^{13}\text{C}$  peaks superimposed on the general long-term falling trend. These +0.1 to +0.2 ‰ peaks (*c1* and *c2* in Fig. 7) occur in couplet E37 (a short distance below Datum 22) and couplet E44 of the expanded succession at Culver, and lie within sampling error of these positions at Dover.

### 3.b.3. Round Down Event

Carbon-isotope values above the level that records the Lulworth Event rise very gradually towards a

low Middle Turonian maximum (typically around 3.1 ‰  $\delta^{13}\text{C}$ ) in the lower *C. woollgari* Zone, below the Round Down Marl (Fig. 7) of Robinson (1986; base of couplet F20). This marl is a distinctive marker that can be traced from Kent into Dorset and Wiltshire, and is overlain by several levels containing abundant small fragmentary *Inoceramus cuvieri* (J. Sowerby). The underlying carbon-isotope maximum is here termed the Round Down Isotope Event.

Within the succession between the levels of the Lulworth and Round Down events, two small (+0.1 to +0.2 ‰) weakly developed  $\delta^{13}\text{C}$  peaks (*d1*, *d2*) occur that may be significant, but inadequate sampling resolution and the irregular nature of the profiles makes it impossible to resolve their positions with respect to the cyclostratigraphy.

Table 2. Key bentonite marker beds used to constrain the carbon-isotope chemostratigraphy

Bentonite	Marl marker bed equivalence
Coniacian	
B6	unknown, East Cliff Marl 2 (Shoreham Marl 2), Little Weighton Marl 2
Turonian	
B5	T <sub>F</sub> tuff, Lewes Marl, Ulceby Marl
B4	T <sub>E</sub> tuff, Bridgewick Marl 1, North Ormsby Marl
B3	T <sub>D1</sub> tuff, Caburn Marl, Deepdale Lower Marl
B2	T <sub>C2</sub> tuff, Southerham Marl 1, Melton Ross Marl
B1	T <sub>C</sub> tuff, Glynde Marl 1, Barton Marl 1

Marl equivalence after Wray (1999). Marker beds named are from northern Germany, southern England, and northern England, respectively.

### 3.b.4. Low-woollgari Event

A further significant break point in the carbon-isotope profiles occurs in the Middle Turonian low-*C. woollgari* Zone, mid-way between the Round Down Marl and New Pit Marls at Dover, with a change from gradually to more steeply falling  $\delta^{13}\text{C}$  values. This inflection point is here called the Low-woollgari Isotope Event, and provides a valuable correlation line between Banterwick, Culver and Dover (Fig. 7). A minor carbon-isotope peak in the underlying succession (*e1*) also occurs at Banterwick and Culver, a short distance below Datum 24 (Table 1) at the latter locality.

The condensed nature of the Lower Turonian at the Trunch and inadequate sampling mean that the Round Down and Low-woollgari events cannot be clearly differentiated in the borehole succession; only a single inflection point is seen in the carbon-isotope profile. This point is correlated with the Round Down Event in Figure 7, based on the overall shape of the isotope curve, which defines a clear  $\delta^{13}\text{C}$  maximum at this level.

### 3.b.5. Glynde Event

A  $\delta^{13}\text{C}$  minimum of 1.9‰ occurs above Glynde Marl 3 at Dover. This Glynde Isotope Event (new name) marks a prominent inflection point on the long-term isotope profile from falling to rising values. A similar isotope trend (but with higher absolute values) occurs at the level of the Barton Marls at Trunch (Fig. 7), confirming the lateral equivalence of these deposits to the Glynde Marls of southern England. The geochemical signatures of Barton Marl 1 and Glynde Marl 1, and the stratigraphically equivalent T<sub>C</sub> tuff of northern Germany (Wray, 1999), indicate that they represent the first in a series of Turonian–Coniacian bentonites (B1 in Fig. 7, Table 2) that provide a framework for international correlation in NW Europe.

The Glynde Marls and their isotope event are cut out by an erosion surface associated with the Ogbourne Hardground at Culver (Fig. 7), and only the basal marl remains at Banterwick, below the Fognam Farm Hardground of the Chalk Rock. A minor  $\delta^{13}\text{C}$  peak (*f1*)

occurs between the New Pit and Glynde marls at Dover and Banterwick, the maximum occurring immediately above Datum 25 at Dover. This isotopic feature is also present at Trunch, but has been cut out by an erosion surface at Culver.

### 3.b.6. 'Pewsey' Event

The +0.4‰ positive  $\delta^{13}\text{C}$  excursion with a maximum value of 2.3‰ occurring at the summit of the Middle Turonian *C. woollgari* Zone at Dover (Fig. 7) was termed the 'Pewsey Event' by Gale (1996), who suggested that this correlates with the phosphatized Pewsey Hardground in the Chalk Rock. The 'Pewsey' Isotope Event is a valuable marker that has been correlated with intervals in Germany and Spain (Fig. 8), where it has been referred to as 'Peak -4' (Wiese, 1999; Wiese & Kaplan, 2001).

At Culver, where the 'Southern Chalk Rock' (SCR; incorporating the Ogbourne and Pewsey Hardgrounds, Fig. 7) is well developed, the Pewsey Hardground is associated with a low  $\delta^{13}\text{C}$  value of 1.9‰, and a similar value of 2.0‰ occurs in the underlying Ogbourne Hardground. Correlation with Dover (Fig. 7) shows that sediments characteristic of the 'Pewsey' positive carbon-isotope event are absent at Culver, having been cut out by an erosion surface associated with the development of the Ogbourne Hardground (see also Gale, 1996). High  $\delta^{13}\text{C}$  values do not occur at the Pewsey Hardground, but the term 'Pewsey' Event is retained for the positive isotope excursion to ensure consistency with previous work. The isotope event is also unrepresented at Banterwick, presumably due to erosion associated with the formation of the Chalk Rock, but is clearly seen above the Barton Marls at Trunch.

### 3.b.7. Lower and Upper Southerham events

Carbon-isotope values fall sharply immediately above the level of the 'Pewsey' Event at Dover and Trunch (Fig. 7), and form a relative plateau through the lower Upper Turonian *S. neptuni* Zone. Three small positive carbon-isotope excursions of +0.1 to +0.2‰ occur within the plateau region: one 1 m above and one 2 m below the Southerham Marls, and a third at the level of the Caburn Flints. The first two of these are called the Lower and Upper Southerham Isotope events (new names). Macrofossil Datum 26 occurs immediately above the level of the Lower Southerham Isotope Event at Dover (Fig. 7).

The individual Southerham events cannot be resolved at Culver (Fig. 7) due to inadequate sampling resolution and the relatively condensed nature of this part of the succession, and the entire sediment package is either absent or only partly represented in the highly condensed Chalk Rock at Banterwick. The Melton Ross Marl of northern England is equivalent

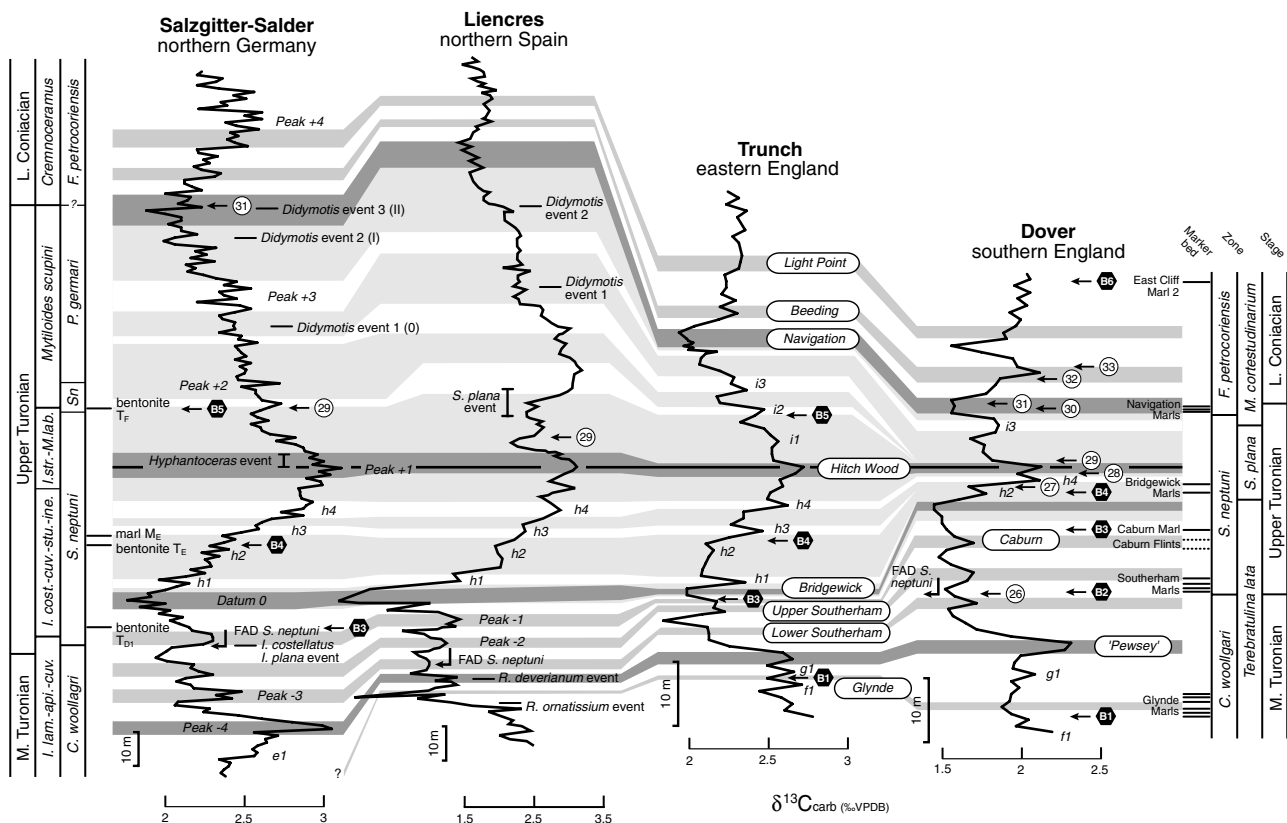


Figure 8. Correlation of Upper Turonian  $\delta^{13}\text{C}$  events between England, Germany and Spain. Salzgitter-Salder in northern Germany is a candidate GSSP for the Turonian/Coniacian boundary (Kauffman, Kennedy & Wood, 1996). The positions of stage, macrofossil zonal boundaries, key fossil-occurrence datum levels, and key marker beds are shown for comparison. Numbers in parentheses after *Didymotis* events 1–3 at Salzgitter-Salder are the original designations of Wiese (1999). Isotope data sources: Salzgitter-Salder – Voigt & Hilbrecht (1997); Liencres Wiese (1999); Trunch – this study; Dover – Jenkyns, Gale & Corfield (1994). Stratigraphic data sources: Salzgitter-Salder – Ernst, Schmid & Siebertz (1983), Wood, Ernst & Rasemann (1984), Wiese & Kröger (1998); Liencres – Wiese (1997); Trunch – this study; Dover – Jenkyns, Gale & Corfield (1994), Gale (1996), this study. Abbreviations: *I. lam.-api.-cuv.* – *Inoceramus lamarcki-apicalis-cuvieri*; *I. cost.-cuv.-stu.-ine.* – *Inoceramus costellatus-cuvieri-stuemckei-inaequivalvis*; *I.str.-M.lab.* – *Inoceramus striatoconcentricus-Mytiloides labiatoidiformis*; *Sn* – *Subprionocyclus neptuni*.

to the Southerham Marl 1 in the southern province (Wray, 1999), the two marls equating to Bentonite B2 (Table 2). The isotope profile at Trunch (Fig. 7) is more consistent with the ‘Riby Marl’ identified in the borehole representing this level, although it is acknowledged that the sampling resolution is not high.

Despite patchy development in England caused by regional erosion surfaces, the Southerham events are prominent features of isotope profiles from Germany and Spain (Fig. 8), correlating with Turonian carbon-isotope ‘Peak -3’ and ‘Peak -2’ (Wiese, 1999, fig. 4; Wiese & Kaplan, 2001, fig. 6).

3.b.8. Caburn Event

The third  $\delta^{13}\text{C}$  peak in the mid-Turonian plateau interval at Dover occurs between the Caburn Flints, 2 m below the Caburn Marl. The Caburn Marl is equivalent to the Deepdale Lower Marl of northern England and the T<sub>D1</sub> Tuff of northern Germany, representing Bentonite B3 (Figs 7, 8, Table 2; Wray *et al.* 1996; Wray, 1999).

The isotope peak, here called the Caburn Event, is well developed at Culver and Trunch (Fig. 7); it correlates to ‘Peak -1’ in Spain and Germany (Fig. 8).

3.b.9. Bridgewick Event

One of the most prominent features of Turonian carbon-isotope curves (Figs 7, 8) is the  $\delta^{13}\text{C}$  minimum occurring low in the Upper Turonian *S. neptuni* Zone, which marks the end of the plateau interval, and a change to rising  $\delta^{13}\text{C}$  values above. This minimum, which defines the Bridgewick Isotope Event (new name), has a value of 1.5‰ at Dover and occurs immediately below the Bantam Hole Hardgrounds constituting the bottom of the ‘Dover Chalk Rock’, and < 1 m below the Bridgewick Flint and Bridgewick Marls. At Culver, an identical 1.5‰  $\delta^{13}\text{C}$  minimum occurs in the beds containing abundant cyclostome bryozoans, *Bicavea rotaformis* Gregory, below the Bridgewick Marl. Macrofossil Datum 27 occurs between Bridgewick Marls 1 and 2 at Dover. The equivalent interval at Trunch lies between the Deepdale

and Ravensdale flints, but with a higher  $\delta^{13}\text{C}$  value of 2.0 ‰. The lowest  $\delta^{13}\text{C}$  value at Banterwick, 1.0 ‰ in the middle of the Chalk Rock, occurs at the surface of the Fognam Farm Hardground.

The Bridgewick Event is equivalent to 'Datum 0' (Fig. 8), the key level used for  $\delta^{13}\text{C}$  correlation of the Middle–Upper Turonian in Germany and Spain (Wiese, 1999, fig. 4; Wiese & Kaplan, 2001, fig. 6), where minima of around 2.0 ‰ are also typical of pelagic sections, although values of < 1 ‰ are recorded from hemipelagic sediments in Spain. An equivalent level at Gubbio, Italy, displays  $\delta^{13}\text{C}$  values that are identical to those in southern England (Stoll & Schrag, 2000; see Section 4.a)

### 3.b.10. Hitch Wood Event

A positive carbon-isotope excursion with values of 2.1 ‰ in the upper *S. neptuni* Zone at Dover was called the Hitch Wood Event by Gale (1996), who correlated it with the phosphatized Hitch Wood Hardground of the Chalk Rock. The  $\delta^{13}\text{C}$  maximum (Fig. 7) occurs in the middle of Lighthouse Down Hardground complex (Robinson, 1986) that forms the top of the 'Dover Chalk Rock', at the level of the lower Lewes Flints.

In the more expanded sections at Culver and Trunch (Fig. 7) the Hitch Wood Event is seen to lie at the summit of a much broader long-term  $\delta^{13}\text{C}$  peak that spans the entire *S. plana* Zone. At Culver, a 2.5 ‰ maximum occurs in flinty white chalks, mid-way between the Bridgewick and Lewes marls. At Trunch, a 2.7 ‰ peak occurs between two hardground complexes at 450–453 m, referred to as the 'East Anglia Chalk Rock' by Wood, Morter & Gallois (1994). The Hitch Wood Hardground is well developed at Banterwick (Fig. 7). Here,  $\delta^{13}\text{C}$  values rise steadily from 1.0 ‰ at the surface of the Fognam Farm Hardground to a peak of 1.8 ‰ in the glauconitic chalks above the Hitch Wood Hardground, falling back to 1.5 ‰ in the Top Rock hardground, above. The  $\delta^{13}\text{C}$  maximum thus post-dates the Hitch Wood Hardground.

The Hitch Wood Isotope Event is the most prominent Turonian positive  $\delta^{13}\text{C}$  excursion. Although only characterized by a modest short-term excursion of +0.2 ‰  $\delta^{13}\text{C}$  (Fig. 7), it also represents both the maximum and the inflection point on a larger long-term Upper Turonian peak of up to 1.0 ‰ that rises from the minimum of the Bridgewick Event below, and falls to the minimum of the Navigation Event above.

Four small positive  $\delta^{13}\text{C}$  excursions of around +0.2 ‰ occur between the Bridgewick and Hitch Wood events which are most clearly developed in the most expanded Trunch section (*h1*–*h4*), but *h2* and *h4* can also be recognized at Culver and Dover. Event *h1* occurs at the level of the Ravensdale Flint at Trunch (Fig. 7); this event probably correlates with an unnamed low Upper Turonian peak in profiles from Germany and Spain (Fig. 8). Event *h2* represents a small peak

occurring below Bridgewick Marl 1 and Datum 27 at Culver and Dover, and is situated in nodular chalks 2 m below the North Ormsby Marl at Trunch. Peak *h3* occurs in nodular chalks above the North Ormsby Marl at Trunch, and *h4* occurs 4 m higher. The *h4* maximum is situated 1 m above Bridgewick Marl 2 at Dover and 2 m above the Bridgewick Marl at Culver. The *h3* and *h4* events are well represented in profiles from Germany and Spain, and the isotope correlation (Fig. 8) is consistent with equivalence between the North Ormsby Marl, Bridgewick Marl 1 and the T<sub>E</sub> Tuff in Germany (Table 2), which represent bentonite B4.

The  $\delta^{13}\text{C}$  peak and inflection point defining the Hitch Wood Event are very well developed in Germany and Spain (Voigt & Hilbrecht, 1997; Wiese, 1999, fig. 4; Wiese & Kaplan, 2001, fig. 6). This event corresponds to the upper part of 'Peak + 1' (Fig. 8), a broad maximum which at most localities has a doublet structure, the lower peak of which corresponds to our event *h4*. The Hitch Wood Event is also clearly distinguishable in Turonian carbon-isotope profiles from Italy (Jenkyns, Gale & Corfield, 1994; Stoll & Schrag, 2000).

### 3.b.11. Navigation Event: the Turonian/Coniacian boundary

The uppermost Turonian is marked by the disappearance of common *Mytiloides* group inoceramids, closely followed by the first occurrence of *Cremonoceramus* (Walaszczyk & Wood, 1998; Walaszczyk & Cobban, 2000). The base of the Coniacian stage is currently defined (Kauffman, Kennedy & Wood, 1996) by the first occurrence of *Cremonoceramus deformis erectus* (Meek) (previously referred to its junior synonym, *C. rotundatus* (*sensu* Tröger *non* Fiege)). This datum level lies slightly below the first occurrence of the ammonite *Forresteria* (*Harleites*) *petrocoriensis* (Coquand), the previously favoured basal Coniacian index (Birkelund *et al.* 1984; Kennedy, 1984a, b).

At Dover and on the Isle of Wight, the change in the inoceramid fauna occurs at the Navigation Hardgrounds ('Dover Top Rock' of Stokes 1975, 1977), with the disappearance of a *Mytiloides*-dominated assemblage immediately below, and the appearance of *Cremonoceramus* (including *C. waltersdorfensis hannovrensis* Collom, Datum 30) within the Navigation Marls (Fig. 7), immediately above the hardground complex. A sole record of the Turonian/Coniacian boundary marker inoceramid *Didymotis* (Lee *in* Mortimore, 1997) also originates from within this hardground complex at Dover, and a fragment of *F.(H.) petrocoriensis* was recorded from within Navigation Hardground 3 by Gale & Woodroof (1981). Definitive *C. deformis erectus* (Datum 31) first occur above the Navigation Marls in the Cliffe Hardground at Downley, West Sussex (Wood *et al.* 2004), so the base of the Coniacian is now placed (Fig. 7) at the base of the cemented chalk forming this hardground.

The Turonian/Coniacian boundary interval is characterized by a prominent  $\delta^{13}\text{C}$  minimum at the end of a long-term fall within the Upper Turonian *S. neptuni* Zone, above the Hitch Wood Event (Figs 7, 8). At both Dover and Culver, a small +0.2 ‰ positive  $\delta^{13}\text{C}$  excursion, with values around 2 ‰, peaks in the uppermost Turonian Navigation Hardground complex, and is followed by a sharp fall of around -0.4 ‰ to a minimum of 1.6 ‰. The  $\delta^{13}\text{C}$  minimum is here termed the Navigation Isotope Event. At Dover, the minimum spans Navigation Hardground 3, the Navigation Marls and the Cliffe Hardground, 2 m above. The base of the Coniacian thus falls towards the top of the negative  $\delta^{13}\text{C}$  excursion. At Culver, however, the fall in  $\delta^{13}\text{C}$  values occurs at 'Navigation Hardground 2', indicating some diachroneity in hardground development between Dover and Culver. A similar lateral variation in hardground development at this level is seen locally in the Dover area between Langdon Stairs and St Margaret's Bay.

At Trunch, only a single hardground is developed and the isotope step is less well expressed, with a peak of 2.2 ‰ situated around 1 m lower than a minimum of 2.0 ‰ spanning the Navigation Hardground and overlying *Cremonoceramus-Didymotis* marls to Kiplingcote Marl 3 (Fig. 7). The isotope stratigraphy confirms the equivalence of the Navigation Hardgrounds and Navigation Marls with these beds (Wood, 1992; Mortimore, Wood & Gallois, 2001). The  $\delta^{13}\text{C}$  minimum (1.5 ‰) occurs in the 'Top Rock' hardground at Banterwick.

Three small  $\delta^{13}\text{C}$  excursions (*i1-i3*) of +0.1 to +0.2 ‰ are developed in the interval between the Hitch Wood and Navigation events in the expanded Trunch section. These are less well defined in the thinner successions at Dover and Culver, although the most prominent peak (*i2*) is correlated with small peaks occurring above the Lewes Marl and Datum 29 at Culver and in the Ulceby Oyster Bed above the Ulceby Marl at Trunch (Fig. 7). These marls represent bentonite B5 (Table 2) and are the lateral equivalent of German Tuff  $T_F$  (Fig. 8). The bentonite is absent at Dover and Banterwick, being represented by hiatuses at the surfaces of Lighthouse Down Hardground 5 at Dover and the Hitch Wood Hardground at Banterwick (cf. Gale, 1996, fig. 7).

The  $\delta^{13}\text{C}$  minimum defining the Navigation Event is well developed at Salzgitter-Salder, northern Germany (Fig. 8). Here, the minimum also occurs in the uppermost Turonian (Wiese, 1999, fig. 4; Wiese & Kaplan, 2001, fig. 6), based on the first appearance of *C. deformis erectus* (Datum 31), in flood abundance, a short distance above *Didymotis* event 3 (= *Didymotis* Event II of Wiese, 1999; Wood *et al.* 2004). An identical isotope minimum in the profile at Liencres (Fig. 8), northern Spain, has previously been assigned to the Lower Coniacian (Wiese, 1997), with the base of the Coniacian being placed at *Didymotis* event 2 in that

section. However, *C. deformis erectus* is absent in material collected from Liencres (Wiese, 1999), and the isotope correlation (Fig. 8) places the stage boundary significantly higher.

Events *i1-i3* can be correlated with isotope profiles from Germany and Spain (Fig. 8): peak *i1* broadly corresponds to Peak +2 and *i3* to Peak +3, although none of these are developed as simple peaks and the correlation remains equivocal. Three acme occurrences of *Didymotis* cf. *costatus* Fritsch provide potential correlation points between Salzgitter-Salder and Liencres that support the carbon-isotope correlation (Fig. 8), although interpretation of these events remains controversial (Wiese, 1999).

### 3.c. Coniacian

The Coniacian (89.3–85.8 Ma) in southern England typically comprises soft fine white chalks with inconspicuous omission surfaces and numerous horizons of nodular flints (Fig. 9). Nodular chalks and hardgrounds occur everywhere in the Lower Coniacian (top St Margaret's Chalk), but nodularity decreases upwards and is uncommon above East Cliff Marl 2. The disappearance of nodular chalks, which marks the base of the Broadstairs Chalk (Whitaker, 1865a; Whitaker, Bristow & Hughes, 1872; Robinson, 1986), is diachronous (Fig. 9), occurring earlier in basal sections like Culver, than in more marginal areas, like Dover. Nodularity is less developed in northern England. Here, the flinty Burnham Chalk continues up to the middle Coniacian where common marls appear, marking the base of the Flamborough Chalk Formation (Wood & Smith, 1978). The succession at Trunch (Fig. 9) displays a transitional facies with nodularity in the lower Coniacian and only weakly developed marls.

The first occurrence of the inoceramid genus *Volviceras*, specifically *V. koeneni* (G. Müller), is used to define the base of the Middle Coniacian (Kauffman, Kennedy & Wood, 1996). *Volviceras koeneni* first appears immediately above East Cliff Marl 2 (Fig. 9), coincident with the base of the *Micraster coranguinum* Zone, and an acme occurs in the overlying beds (Datum 34). Above this, the inoceramid fauna is abundant, and dominated by *V.* cf. *involutus* (J. de C. Sowerby) and *Platyceras* (Datum 35) up to a few metres above the East Cliff Semitabular Flint (Fig. 9).

The base of the Upper Coniacian is defined (Kauffman, Kennedy & Wood, 1996) by the first occurrence of *Megadiceramus subquadratus* (Schlüter). *Megadiceramus* is rarely found in chalk facies and *M. subquadratus* is unrecorded from the study sections. However, *Volviceras* disappears in the middle Kingsdown Beds (Fig. 9) of Kent. The genus last occurs in the lowest Upper Coniacian, suggesting that the base of the Upper Coniacian lies within the lower Kingsdown Beds.

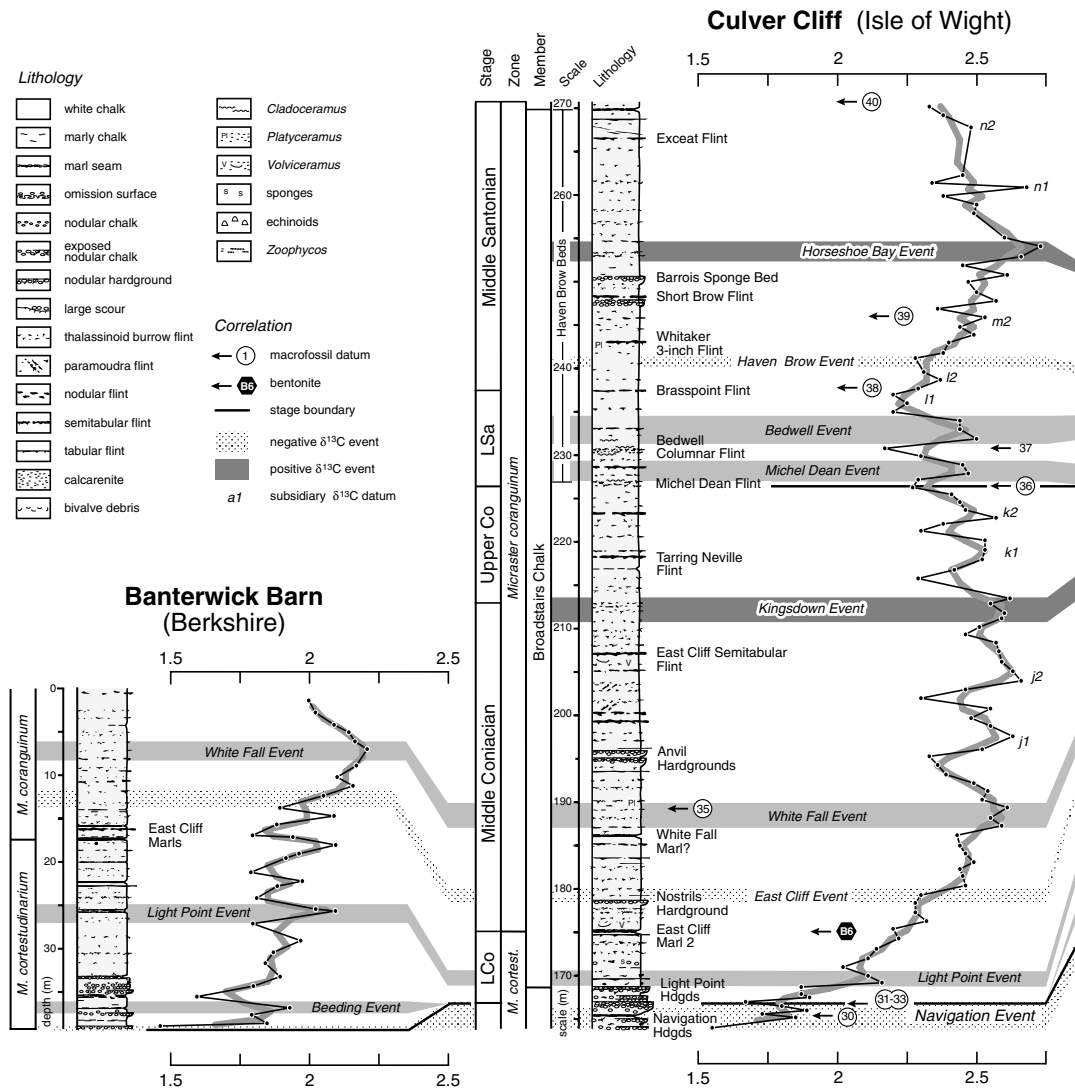


Figure 9. For legend see facing page.

There has been little previous work on the carbon-isotope stratigraphy of the Coniacian. The summary curves of Scholle & Arthur (1980) show no structure in the Coniacian. Jenkyns, Gale & Corfield (1994) plotted data for Dover against a skeleton stratigraphy but did not attempt a detailed stratigraphic analysis. However, correlation of their data with new results for Culver and Trunch, plus limited published data from Banterwick (Murphy, Jarvis & Edmunds, 1997), enable the recognition of six prominent Coniacian isotope events, including the negative  $\delta^{13}\text{C}$  excursion of the Navigation Event (see Section 3.b.11) at the base. Four other numbered events ( $j1$ – $k2$ ) may also be significant.

### 3.c.1. Beeding Event

Carbon-isotope values rise sharply everywhere above the minimum defining the Navigation Event. A positive  $\delta^{13}\text{C}$  excursion of +0.5‰ to maximum values of 2.1‰ occurs around the level of the Beeding

Hardground at Dover (Fig. 9). Less prominent peaks are developed in the thinner successions elsewhere, probably because of insufficient sampling resolution or the presence of hiatuses. Isotope values fall back to around 1.6‰ in the nodular chalks above Light Point Hardgrounds 1–3 at Dover, in the lower Top Rock at Culver, and in the youngest nodular chalks at Banterwick.

### 3.c.2. Light Point Event

A sharp increase in  $\delta^{13}\text{C}$  values by up to +0.3‰ occurs immediately above the top of the Lower Coniacian nodular chalk and hardgrounds at all localities (Fig. 9). The prominence of the isotope shift may be due partly to sediment omission associated with the top of the hardground sequences. However, a small excursion terminating the positive shift is well developed at Culver. The sharp increase and subsequent excursion are here termed the Light Point Isotope Event.

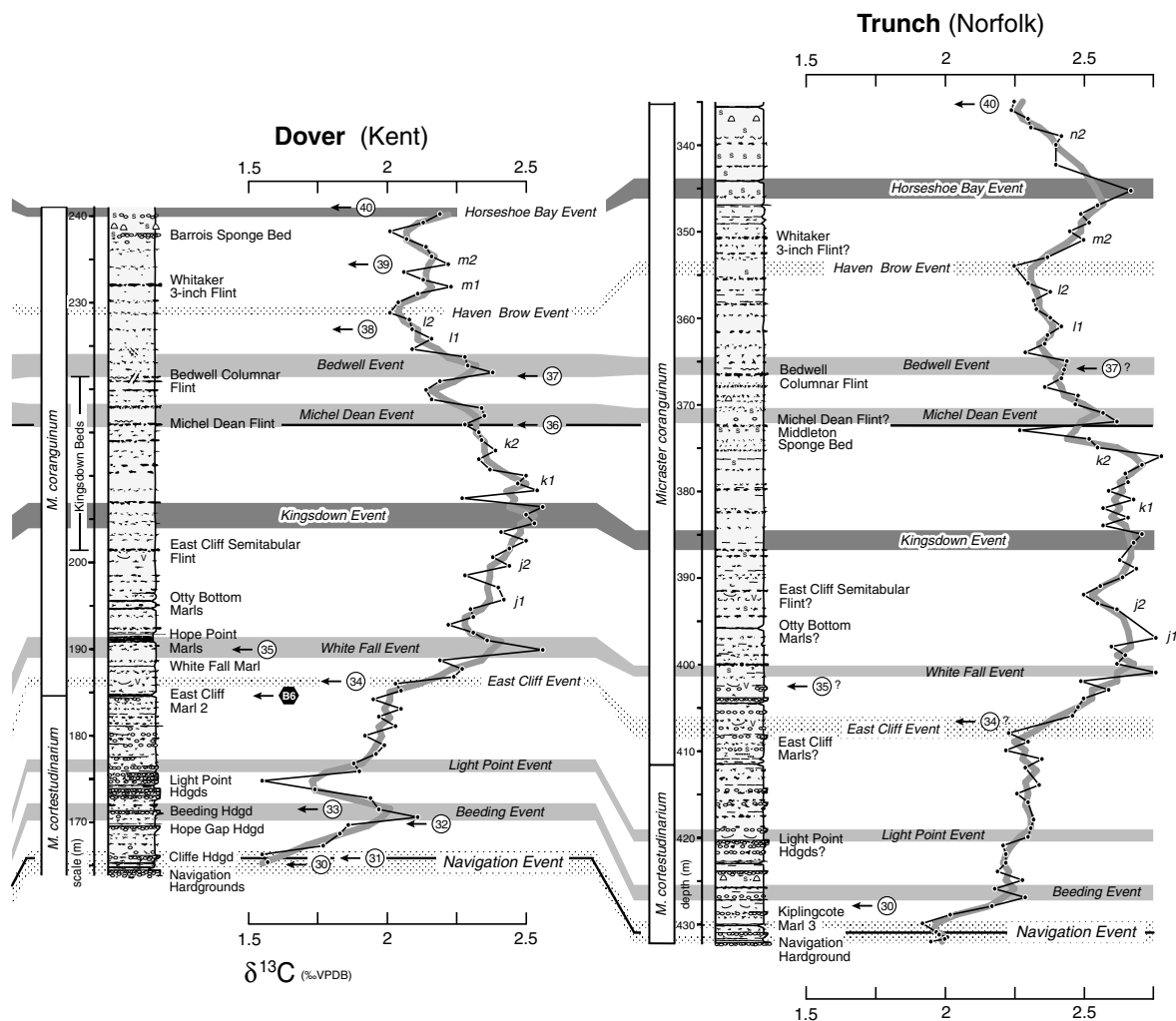


Figure 9. Correlation of English Coniacian  $\delta^{13}\text{C}$  curves. See Figure 3 for plotting details; data sources as Figure 7. Abbreviations: *M. cortest.* – *Micraster cortestudinarium*; Co – Coniacian; Sa – Santonian.

3.c.3. East Cliff Event

Carbon-isotope values rise steadily above the Light Point Event, up to a small trough and large positive step of +0.3 ‰ from 2.0 to 2.3 ‰  $\delta^{13}\text{C}$ , 1–2 m above East Cliff Marl 2 (Shoreham Marl 2 of Mortimore, 1986) at Dover (Fig. 9); this feature occurs immediately above the level yielding abundant Middle Turonian index species *V. koeneni* (Datum 34) and *Platyceramus*, with the former being essentially restricted to these beds. East Cliff Marl 2 has been identified as a bentonite (Wray, 1999) that correlates to Little Weighton Marl 2 of northern England (bentonite B6, Table 2). The small  $\delta^{13}\text{C}$  trough and large positive step defines the East Cliff Isotope Event (new name). A similar shift occurs 1 m above a marly interval and a bed with *V. koeneni* at Trunch (Fig. 9).

The main shift in the more expanded Culver section occurs 5 m above East Cliff Marl 2, 1 m above the limonitic Nostrils Hardground (new name derived from ‘The Nostrils’, a pair of caves at the southern end of Whitecliff; the hardground crops out between these

two caves; Fig. 9). The isotope trend is more erratic at Banterwick, but a marked shift above a pair of marls may be an equivalent event.

3.c.4. White Fall Event

The carbon-isotope curve continues to rise above the East Cliff Event, and displays a +0.3 ‰ positive excursion with values of 2.6 ‰ in the lower Middle Coniacian (Fig. 9), mid-way between the White Fall and Hope Point marls (Belle Tout Marls 1 and 2 of Mortimore, 1986) at Dover, within beds containing *Platyceramus* and *Volvicceramus* debris. This is the White Fall Isotope Event (new name). A similar but broader peak with an identical  $\delta^{13}\text{C}$  value occurs in the thicker Culver section, 1–3 m above a marl, at the base of a thick succession of beds containing very abundant *Platyceramus* and *Volvicceramus involutus* (J. de C. Sowerby). The first appearance of *V. cf. involutus* (Datum 35) consistently occurs around the White Fall Event (Fig. 9).

A similar +0.3‰ rise but a higher  $\delta^{13}\text{C}$  maximum of 2.8‰ is developed at Trunch within an interval containing several marls, and 2 m above a bed yielding *V. cf. involutus*. A semitabular flint at 400.0 m has previously been correlated with the East Cliff Semitabular (Wood, Morter & Gallois, 1994), which the isotope correlation places higher, at 391.5 m (Fig. 9; see below). A broad  $\delta^{13}\text{C}$  peak towards the top of the Banterwick core (Fig. 9) probably equates with the White Fall Event.

### 3.c.5. Kingsdown Event

Above the White Fall Event at Dover,  $\delta^{13}\text{C}$  values continue a long-term rise through the Middle Coniacian, reaching a maximum around the Middle/Upper Coniacian boundary, before beginning a long-term fall through the Upper Coniacian into the Lower Santonian. A double peak of +0.1‰ with a  $\delta^{13}\text{C}$  maximum of 2.5‰ occurs around the inflection point on the long-term isotope curve, in the lower Kingsdown Beds of Robinson (1986). The peak is situated 5 m above the East Cliff Semitabular Flint (Seven Sisters Flint of Mortimore, 1986), a distinctive marker bed containing abundant *Platyceramus* and *Volvicceramus*. We term this  $\delta^{13}\text{C}$  maximum the Kingsdown Isotope Event (Fig. 9). A similar maximum occurs 6 m above the East Cliff Semitabular at Culver, and the same distance above a semitabular flint associated with *V. cf. involutus* at Trunch, correlated here with the East Cliff Semitabular.

The Middle/Upper Coniacian boundary  $\delta^{13}\text{C}$  maximum corresponds to a facies change from chalks containing abundant macrofossil remains, particularly inoceramid bivalves, to the relatively unfossiliferous beds of the Upper Coniacian ('Barren Beds' of Mortimore, Wood & Gallois, 2001). Carbon-isotope profiles in the Middle Coniacian between the White Fall and Kingsdown events show considerable structure on overall flat to rising trends (Fig. 9). Two broad +0.3‰  $\delta^{13}\text{C}$  peaks are seen in the Culver curve, the lower (*j1*) with a maximum above the limonitic Anvil Hardgrounds 1–3 (Fig. 9; new name derived from 'The Anvil', a local name for White Horse Headland at Whitecliff, where the hardgrounds are well displayed on the southern side), and the second (*j2*) occurring in a series of paramoudra flint beds. These peaks are less well defined on the Dover and Trunch profiles but appear to be represented in the sections.

### 3.d. Santonian

The Santonian (85.8–83.5 Ma) in southern England (Figs 10, 11) consists of soft fine white chalks with inconspicuous omission surfaces and numerous horizons of nodular flints in the lower and middle parts (upper Broadstairs Chalk). In basinal areas like Sussex and the Isle of Wight, marls become common in the flinty white chalks of the Upper Santonian (Fig. 11), reflected

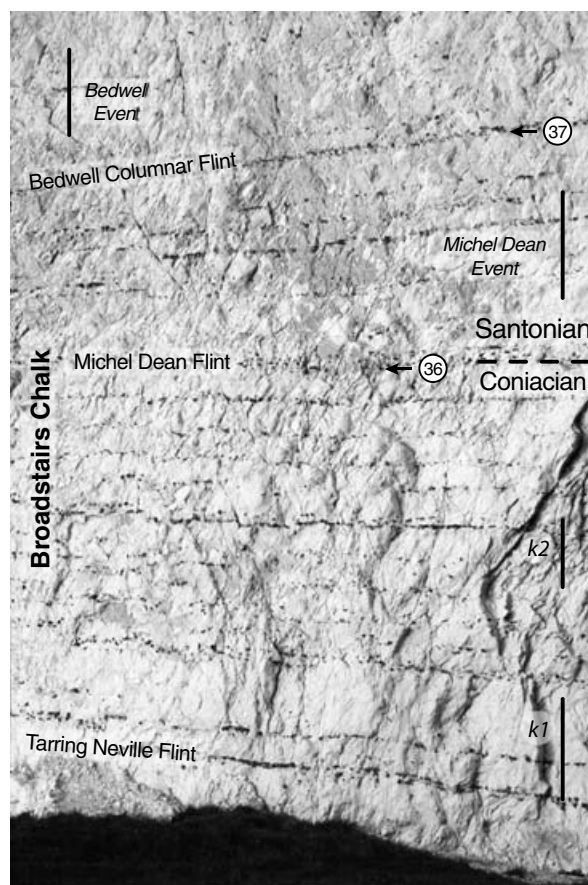


Figure 10. Coniacian/Santonian boundary succession, Culver Cliff, Isle of Wight. The grass at the base of the photo is the top of White Horse Headland. The photograph is reoriented from a succession dipping at around 60° to the north. Circled numerals indicate the bases of *Cladoceramus* beds 1 (Datum 36, base Santonian) and 2 (Datum 37). The black bars indicate the extent of positive  $\delta^{13}\text{C}$  excursions defining the *k1*, *k2*, Michel Dean and Bedwell Isotope events. The distance between the Michel Dean and Bedwell Columnar flints is 4 m.

in the passage to the Newhaven Chalk (Mortimore, 1983) at Buckle Marl 1. In Kent, the facies changes in the Upper Santonian to very soft white chalks with few flints above the Barrois Sponge Bed (Fig. 11), the Margate Chalk of Whitaker (1865*a*; Whitaker, Bristow & Hughes, 1872). In northern England, the flinty Flamborough Chalk continues up into the Campanian, although marls become less common upwards. At Trunch, the Upper Santonian is characterized by a reduction in the abundance of both flint and marl (Fig. 11).

As currently defined (Lamolda & Hancock, 1996), the base of the Santonian is marked by the first occurrence of *Cladoceramus undulatoplicatus* (Roemer). This species is an excellent marker that first appears in the lower *Cladoceramus* band, associated with the Michel Dean Flint (Datum 36; Figs 10, 11) throughout southern England. No substages have been formally agreed for the Santonian, but the base of the Middle Santonian is currently placed at the last appearance

of *C. undulatoplicatus*, and the base of the Upper Santonian at the first occurrence of *Uintacrinus socialis* Grinnell. *Cladoceramus undulatoplicatus* ranges several metres above the upper *Cladoceramus* band, a second flood of inoceramids at the level of the Bedwell Columnar Flint (Datum 37; Figs 10, 11). *Uintacrinus socialis* first occurs in the lower beds of the Margate Chalk in Kent, and in the basal Newhaven Chalk in Sussex and on the Isle of Wight.

As is the case with the Coniacian, there has been little previous work on the carbon-isotope stratigraphy of the Santonian stage. Jenkyns, Gale & Corfield (1994) plotted data from Dover and Seaford Head (Sussex), but did not attempt detailed stratigraphic analysis or correlation. Their data will be compared here with new results from Culver and Trunch to develop a carbon-isotope stratigraphy for the Santonian. Seven named isotope events are defined in addition to the positive carbon-isotope excursion associated with the Santonian/Campanian Boundary Event (Jarvis *et al.* 2002). Eleven other events (*l1–q1* in Fig. 11) provide potential additional correlation points.

#### 3.d.1. Michel Dean Event

A clearly resolved positive  $\delta^{13}\text{C}$  excursion of +0.1 ‰ occurs immediately above the Michel Dean Flint at the base of the Santonian (Figs 10, 11), with values approaching 2.5 ‰ at Dover and Culver, and a bigger peak occurs in the same position at Trunch. This excursion is here named the Michel Dean Isotope Event. Two small positive excursions occurring in the Upper Coniacian between the Kingsdown and Michel Dean events, which are less consistently developed in the study sections, are informally numbered events *k1* and *k2* (Fig. 10).

#### 3.d.2. Bedwell Event

A second and larger excursion of +0.3 ‰  $\delta^{13}\text{C}$  occurs in the Lower Santonian immediately above the Bedwell Columnar Flint (Figs 10, 11), with values rising to around 2.5 ‰ at Dover and Culver; a smaller peak occurs in the same position at Trunch. This Bedwell Isotope Event (new name) is the last of four equally spaced positive  $\delta^{13}\text{C}$  excursions (*k1*, *k2*, Michel Dean and Bedwell events) superimposed on the long-term falling isotope trend above the Kingsdown Event maximum.

The identical asymmetric shapes of the  $\delta^{13}\text{C}$  peaks of the Bedwell Event at Culver and Dover suggest that a significant hiatus occurs above the Bedwell Columnar Flint in both sections. A smaller peak occurs above a flint at 366.5 m in the Trunch borehole associated with *C. undulatoplicatus*, identified by Wood, Morter & Gallois (1994) as being the equivalent of the Bedwell Columnar Flint. This places the base of the Santonian somewhat lower, at 372.4 m, a short distance above the Middleton Sponge Bed (Fig. 11).

#### 3.d.3. Haven Brow Event

The carbon-isotope profile continues its long-term fall following the Bedwell Event (Fig. 11). A  $\delta^{13}\text{C}$  long-term minimum of 2.2 ‰ at Culver occurs in the upper Lower Santonian, with a second trough of 2.3 ‰ in the lower Middle Santonian. Based on the marker-bed correlation, the second trough correlates with the long-term minimum of 2.0 ‰  $\delta^{13}\text{C}$  and inflection point in the Dover  $\delta^{13}\text{C}$  curve. The lower Middle Santonian minimum, which lies within the lower Haven Brow Beds of Mortimore (1986), is here termed the Haven Brow Isotope Event. A well-defined minimum of 2.3 ‰ and inflection point at 353.9 m in the Trunch borehole correlates with this event.

Two minor peaks (*l1*, *l2*) between the Bedwell and Haven Brow events can be correlated between the three sections (Fig. 11).

#### 3.d.4. Horseshoe Bay Event

The long-term  $\delta^{13}\text{C}$  profile through the Middle Santonian at Culver displays a broad symmetrical peak reaching a maximum of 2.7 ‰ in the middle Middle Santonian (Fig. 11). The maximum occurs in a succession of flinty chalks, 3 m above the Barrois Sponge Bed, in the middle of Horseshoe Bay. The carbon-isotope maximum is here called the Horseshoe Bay Event. An identical symmetrical peak of 2.7 ‰ occurs at 345.2 m at Trunch, and a 2.5 ‰ maximum occurs at Seaford, both associated with a succession of sponge beds. The Event represents a +0.4 ‰ positive excursion above the underlying and overlying minima.

At Dover, a lesser maximum of 2.3 ‰ lies 3 m above the Barrois Sponge Bed but the upper half of the Middle Santonian long-term peak is not seen (Fig. 11), indicating substantial condensation or a major hiatus in the basal Margate Chalk. It is likely that this condensation is related to the development of the Barrois Sponge Bed and the associated sponge beds immediately above this, around the Rowe Echinoid Band. This degree of condensation implies that the Horseshoe Bay Event may be unrepresented, and that sediments yielding the highest carbon-isotope values are high Middle Santonian.

Two small isotope peaks, one immediately below and one above the Whitaker 3-inch Flint (*m1*, *m2*), are clearly developed in the Dover profile (Fig. 11), the latter coincident with the *Echinocorys* aff. *elevata* Bed (Datum 39). Possible correlative peaks occur at Trunch, and the higher peak may also be seen around the Short Brow Flint in the Culver and Seaford profiles.

#### 3.d.5. Buckle Event

The broad  $\delta^{13}\text{C}$  maximum characterizing the Middle Santonian (Fig. 11) declines up-section to a minimum of around 2.2 ‰ in the basal Upper Santonian, lower

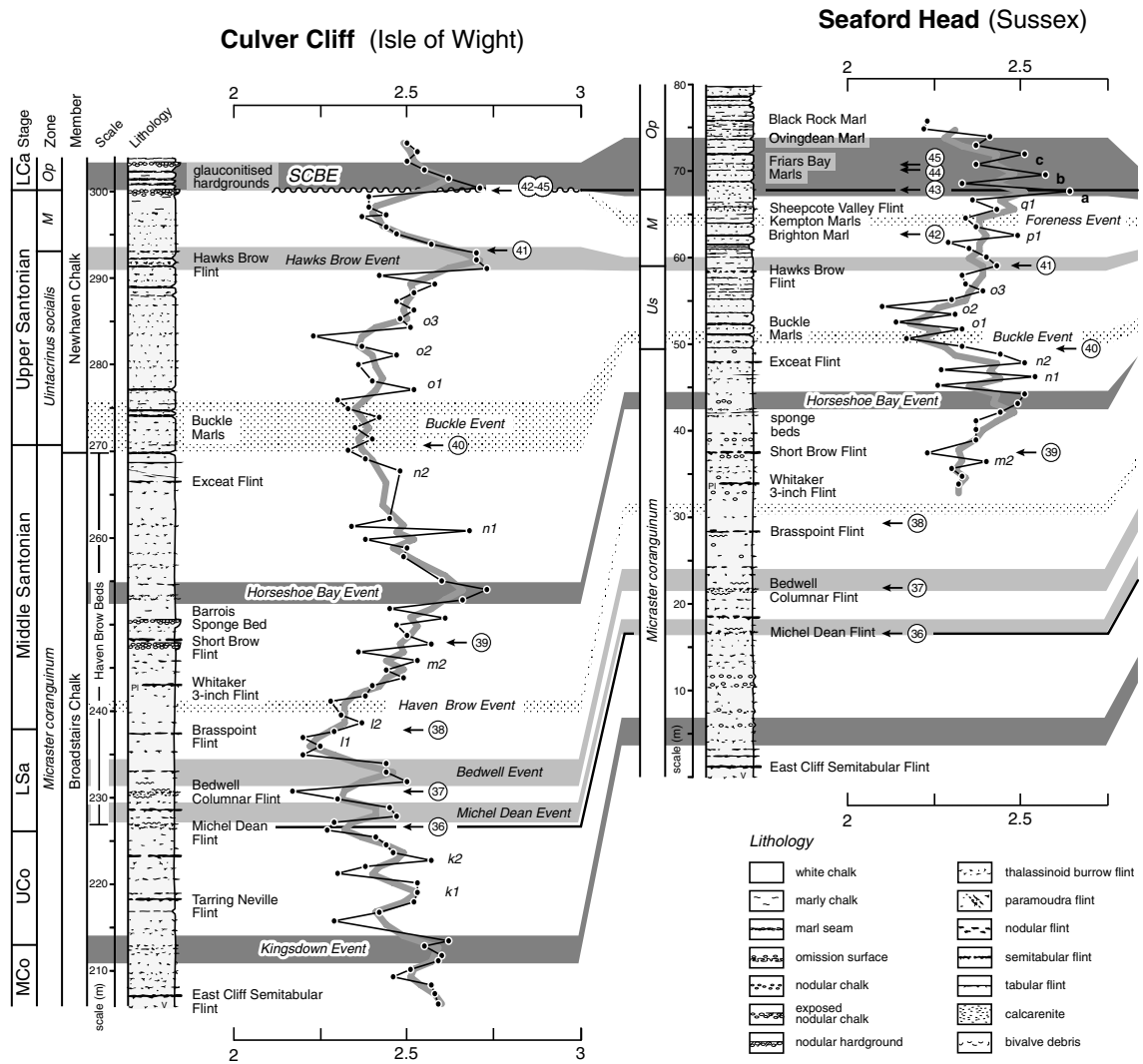


Figure 11. For legend see facing page.

*U. socialis* Zone at Culver, Seaford and Trunch, at the level of the Buckle Marls. A similar minimum occurs in the basal *U. socialis* Zone at Dover. This isotope minimum is here called the Buckle Event (new name).

Two small peaks (*n1*, *n2*) between the Horseshoe Bay and Buckle events, the second at the Exceat Flint (Fig. 11), have potential correlation value. These peaks are not resolved in the more attenuated succession at Dover.

3.d.6. *Hawks Brow Event*

A broad positive  $\delta^{13}C$  excursion of +0.3 ‰ with a maximum value of 2.7 ‰ occurs at the top of the *U. socialis* Zone at Culver, at the level of the Hawks Brow Flint (Fig. 11). Similar peaks occur around the first appearance of *Marsupites laevigatus* (Datum 41) at Seaford, Dover and Trunch; the associated carbon-isotope excursion defines the Hawks Brow Isotope Event. The carbon-isotope trends between the Buckle and Hawks Brow events are remarkably similar at all

four localities, displaying upwards-stepping profiles with three discrete  $\delta^{13}C$  peaks (*o1*–*o3*).

3.d.7. *Foreness Event*

A  $\delta^{13}C$  minimum and inflection point is developed in the Upper Santonian mid-*Marsupites* Zone at Seaford, Dover and Trunch (Fig. 11). A minimum of 2.2 ‰ is particularly well developed above the Foreness Flint at Foreness Point Kent, and the negative isotope excursion is here named the Foreness Isotope Event. The minimum lies within the Kempton Marls at Seaford. A small positive isotope excursion (*p1*) occurs between the Hawks Brow and Foreness events at Seaford, Dover and Trunch, which approximates to the level of the first appearance of *Marsupites testudinarius* (Schlotheim), Datum 42. At Culver, a prominent  $\delta^{13}C$  minimum occurs above the Hawks Brow Event, immediately below a pair of glauconitized hardgrounds at the top of the *Marsupites* Zone. The *p1* excursion is not represented, despite the presence

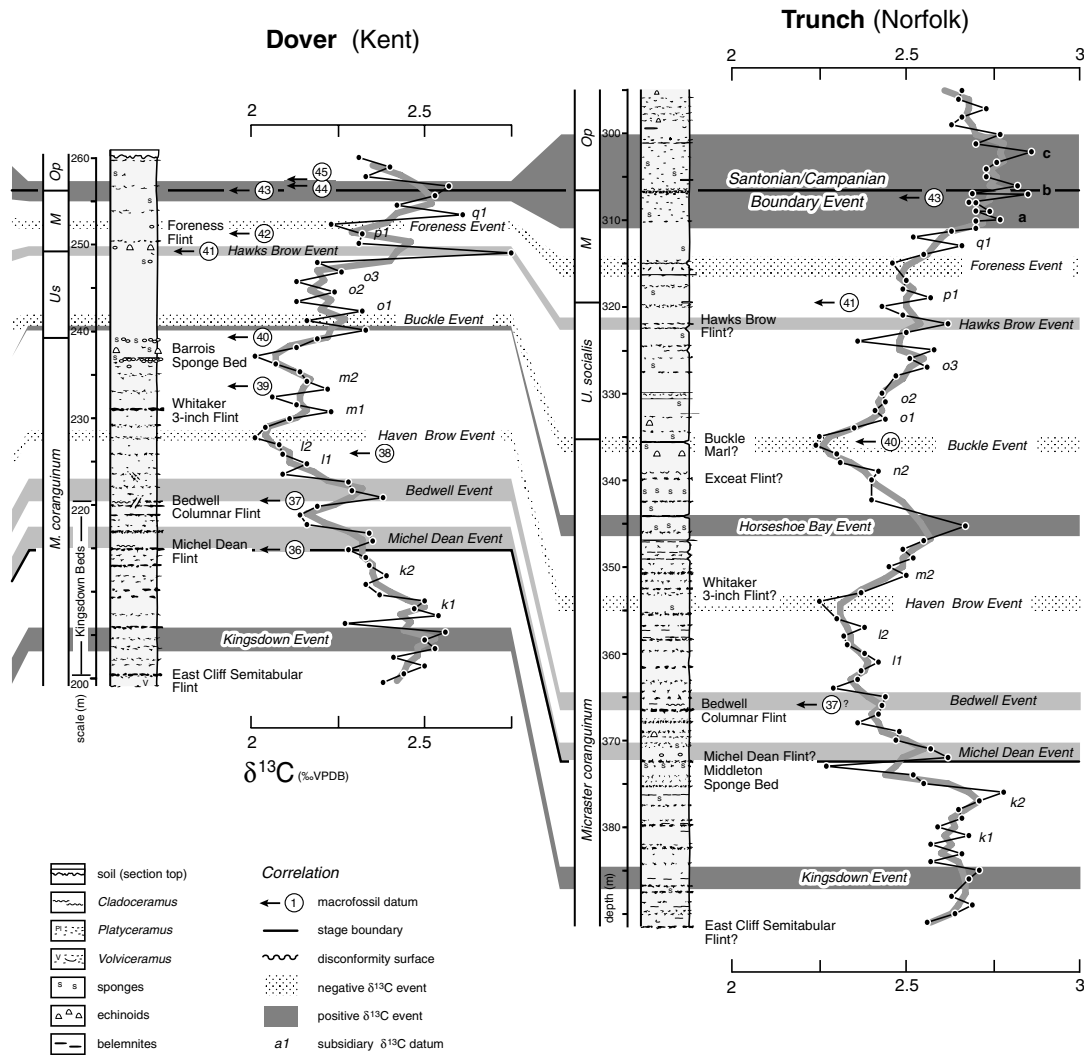


Figure 11. Correlation of English Santonian  $\delta^{13}\text{C}$  curves. See Figure 3 for plotting details; Seaford Head isotope data from Jenkyns, Gale & Corfield (1994), see Figure 7 for other data sources. Abbreviations: *Us* – *Uintacrinus socialis*; *M* – *Marsupites*; *Op* – *Offaster pilula*; *Co* – Coniacian; *Sa* – Santonian; SCBE – Santonian/Campanian Boundary Event.

of a considerably thicker section, suggesting that the Foreness Event is absent at Culver and that the observed minimum at the top of the Upper Santonian correlates to the sub-*p1* trough elsewhere.

3.d.8. Santonian/Campanian Boundary Event

The Santonian/Campanian boundary interval is characterized everywhere by a positive  $\delta^{13}\text{C}$  excursion of around + 0.3 ‰ with maximum values up to 2.9 ‰. The base of the Campanian is best defined by the disappearance of *M. testudinarius*, macrofossil Datum 43 (Grossouvre, 1901; Gale *et al.* 1995; Hancock & Gale, 1996). It is likely that the extinction of *Marsupites* is nearly coincident with the first appearances of *Placenticerus bidorsatum* (Roemer) and *Goniot euthis granulataquadrata* (Stolley), and lies close to the extinction level of the *Dicarinella asymetrica-concavata* group of planktonic foraminifera (but see Section 4.b for an alternative correlation). *Uintacrinus anglicus*

Rasmussen (Rasmussen, 1961) is a widespread and short-ranging basal Campanian marker species (Hancock & Gale, 1996; Datum levels 44, 45) that extends to Texas in the USA, Kazakhstan and Australia, and *Offaster pilula* (Lamarck) typically first appears a few metres above the base of the stage.

The boundary successions display considerable differences between the four study sections (Fig. 11). At Culver, the basal Campanian consists of a distinctive 17 m thick interval of marly chalks containing few flints, several nodular chalks, glauconitized chalk pebble beds, and beds of granular phosphate and glauconite, which is restricted to the eastern Isle of Wight (I. Jarvis, unpub. D.Phil. thesis, Univ. Oxford, 1980; Gale, Wood & Bromley, 1987; Prince, Jarvis & Tocher, 1999). This unit is referred to as the Whitecliff Ledge Beds (Gale, Wood & Bromley, 1987). The last occurrence of *M. testudinarius* lies in the second of a pair of nodular hardgrounds with glauconitized surfaces at the base of this succession.

At Seaford, the boundary interval consists of flinty chalks with numerous marl seams (Fig. 11). Inoceramid and oyster shell debris is abundant through the uppermost Santonian and lowest Campanian, particularly in the beds immediately underlying the Friars Bay Marls. The last occurrence of *M. testudinarius* (Datum 43) occurs in Friars Bay Marl 1. Above this, *U. anglicus* Rasmussen occurs between Friars Bay Marls 2 and 3 (Datum levels 44, 45), and the first *O. pilula* appears 5 m higher (Mortimore, Wood & Gallois, 2001), at the Black Rock Marl.

At Trunch, the boundary succession is largely free of flints and consists of calcarenitic chalks containing abundant inoceramid and oyster shells from 309 m (Fig. 11), around the last occurrence of *Marsupites* at 307.4 m, up to 300 m depth. *Goniot euthis* belemnites are common in the basal Campanian section, and *O. pilula* first appears at 297 m. The calcarenitic chalk facies developed at Trunch and to some extent at Seaford is characteristic of Santonian/Campanian boundary successions in northern Germany, the so-called 'Grobkreide' facies, which is typical of the *Goniot euthus granulataquadrata* Zone (Schulz *et al.* 1984).

In Kent, the soft white chalks of the uppermost Margate Chalk contain widely spaced, weakly developed burrow flints and scattered discontinuous sponge horizons (Fig. 11). *Marsupites testudinarius* disappears 4 m below the top of the preserved Chalk section, and *U. anglicus* occurs in the basal Campanian chalk. *Offaster pilula* is unrecorded from the coastal outcrops.

The base of the Santonian/Campanian positive carbon-isotope excursion (Santonian/Campanian boundary event) lies in the uppermost Upper Santonian at the top of the *Marsupites* Zone at Seaford, Dover and Trunch (Fig. 11), and its top lies in the basal Campanian below the first occurrence of *O. pilula* in all three sections. The thickest Santonian/Campanian Boundary Event interval occurs at Trunch (11 m), closely followed by Seaford (7 m), sections that contain calcarenitic chalk facies. At Culver and Dover, the isotope event is limited to < 2 m of chalk, emphasizing the attenuated nature of the successions in the eastern Isle of Wight and Kent.

The Santonian/Campanian Boundary Event isotope profiles at Seaford and Trunch are very erratic (Fig. 11), suggesting that substantial structure exists within the overall positive excursion, which is poorly resolved by the relatively coarse 1 m sampling used in this study. Three possible maxima within the overall Santonian/Campanian Boundary Event at Seaford and Trunch are labelled a–c in Figure 11. The narrow symmetrical peak at Dover is indicative of reduced sedimentation. At Culver, the sharp step in  $\delta^{13}\text{C}$  values at the surface of the lower glauconitized hardground and the gradual decline above, demonstrate the presence of a significant hiatus at the hardground surface. Based on the absence

of the Foreness Event below (Fig. 11, see above) and faunal records, this hiatus must be equivalent to the upper half of the *Marsupites* Zone and the basal *O. pilula* Zone, including all of the lower beds containing *U. anglicus*.

A marked  $\delta^{13}\text{C}$  peak (*q1*) immediately overlies the isotope minimum defining the Foreness Event at Seaford, Dover and Trunch, and provides a useful subsidiary correlation point (Fig. 11).

### 3.e. A Cenomanian–Santonian $\delta^{13}\text{C}$ reference curve

The detailed correlations described above demonstrate that substantial variation in thickness and facies occurs in the English Chalk, and no single section contains a complete Cenomanian–Santonian succession. However, carbon-isotope trends and values in the various successions are remarkably consistent. To construct a high-resolution carbon-isotope reference curve, the Cenomanian–Santonian succession was subdivided into nine intervals, and  $\delta^{13}\text{C}$  data were taken from the most complete sections to produce a stacked composite profile (Fig. 12). Isotope data were plotted against the time scale of Ogg, Agterberg & Gradstein (2004), supplemented by data in Hardenbol *et al.* (1998); ages were assigned to samples, assuming a constant accumulation rate between age datum levels (Table 3).

In two cases, small offsets in the absolute  $\delta^{13}\text{C}$  values were apparent between adjacent data sets on the composite profile. Similar offsets between sections are apparent on the Cenomanian–Turonian composite  $\delta^{13}\text{C}$  plot of Voigt (2000, fig. 4). Such offsets might be caused by primary differences in the isotopic composition of regional water masses, they might be due to minor differential diagenetic overprinting associated with different burial and uplift histories of the study areas, or they might result from analytical bias between different stable-isotope laboratories. In this study, 0.2 ‰ offsets in the Albian–Lower Cenomanian and Middle–Upper Turonian data were corrected by applying constant correction factors to these data sets (see below).

#### 3.e.1. Cenomanian

Correlation of the English Cenomanian carbon-isotope curves (Figs 3, 4, 6) demonstrates that the thickest and most complete Lower Cenomanian (*M. mantelli* and *M. dixoni* Zones) is developed at Speeton, the thickest Middle Cenomanian (*C. inerme*–*A. jukesbrownei* Zones) at Dover, the thickest lower Upper Cenomanian (*C. guerangeri* Zone) at Culver, and the thickest and most complete Cenomanian/Turonian boundary succession (*M. geslinianum*–*F. catinus* Zones) is developed at Eastbourne. The composite  $\delta^{13}\text{C}$  curve (Fig. 12) was constructed using data from these intervals in these sections.

The  $\delta^{13}\text{C}$  values from Speeton are consistently + 0.2 ‰ higher throughout the Cenomanian than are

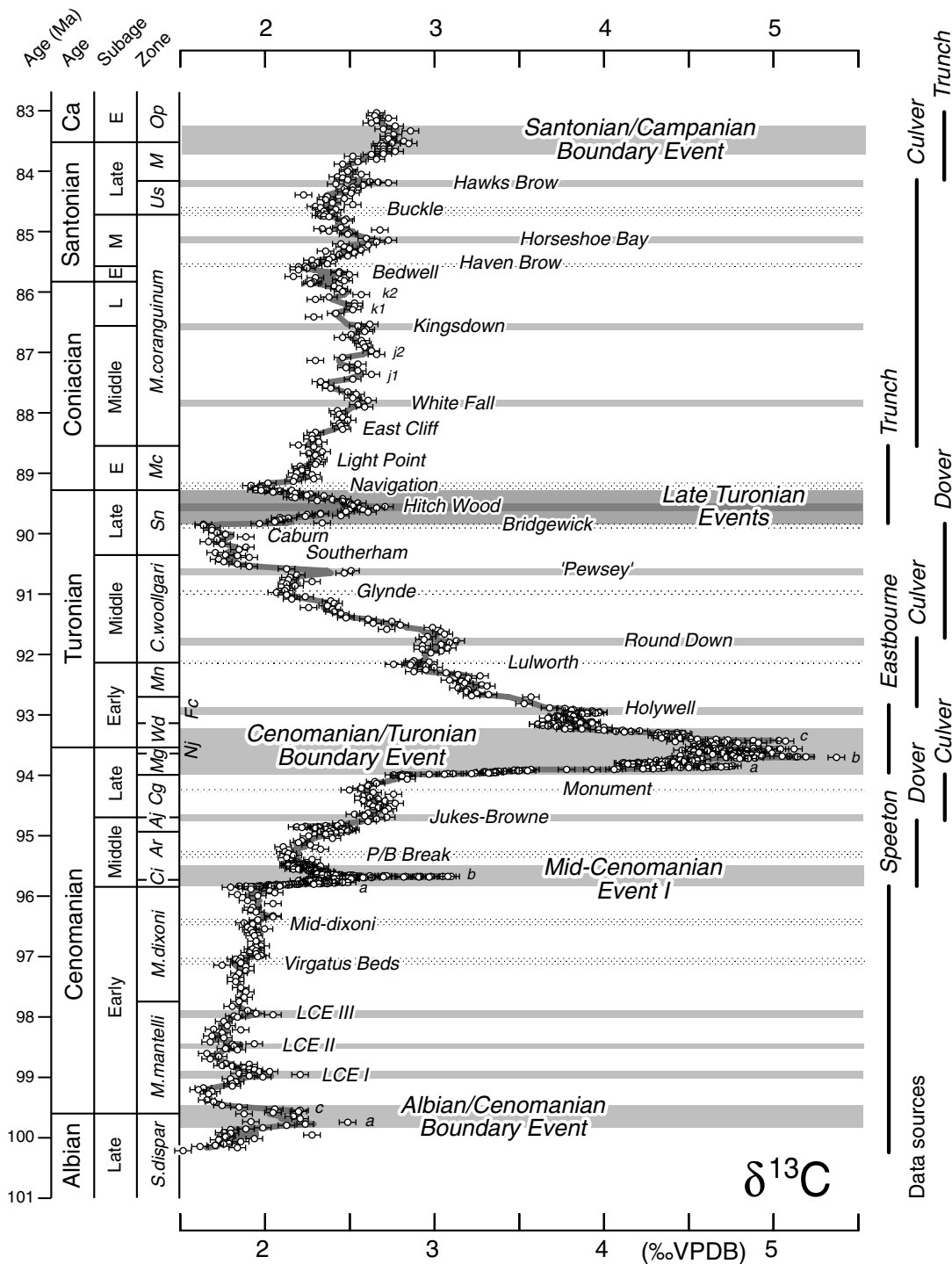


Figure 12. A carbon-isotope reference curve for the Cenomanian–Santonian ages based on the English Chalk. The curve is a stacked composite incorporating data from the most complete sections studied. Sources of data for different intervals are indicated on the right of the figure. The curve has been calibrated using the age assignments of Ogg, Agterberg & Gradstein (2004) and Hardenbol *et al.* (1998); see Table 3 and text for details. Individual data points are indicated by circles. ‘Error’ bars of 0.1 ‰  $\delta^{13}\text{C}$  are qualitative estimates of the maximum range of replicate samples; circle diameters (0.03 ‰) represent typical  $3\sigma$  sample reproducibility. The dark grey smoothed curve is a 3-point moving average illustrating long-term trends. The positions of key positive (grey) and negative (stippled) isotope events are indicated. Abbreviations: Ca – *Cunningtoniceras inerme*; Ar – *Acanthoceras rhotomagense*; Aj – *A. jukesbrowni*; Cg – *Calycoceras guerangeri*; Mg – *Metoicoceras geslinianum*; Nj – *Neocardioceras juddii*; Wd – *Watinoceras devonense*; Fc – *Fagesia catinus*; Mn – *Mammites nodosoides*; Sn – *Subprionocyclus neptuni*; Mc – *Micraster cortestudinarium*; Us – *Uintacrinus socialis*; M – *Marsupites*; Op – *Offaster pilula*.

Table 3. Ages determined for biostratigraphic datum levels (stage and zone bases unless stated)

Datum level	Age (Ma)			
	This study	Ogg, Agterberg & Gradstein (2004)	Voigt (2000)	Hardenbol <i>et al.</i> (1998)
Lower Campanian (top <i>Marsupites</i> )	<b>83.53</b>	<b>83.53</b>	nd	83.46
<i>Marsupites</i> Zone	84.14	nd	nd	nd
Upper Santonian ( <i>U. socialis</i> )	84.71	nd	nd	nd
Middle Santonian (upper <i>M. coranguinum</i> )	85.57	nd	nd	nd
Lower Santonian ( <i>C. undulatoplicatus</i> )	<b>85.85</b>	<b>85.85</b>	nd	85.79
Upper Coniacian ( <i>M. subquadratus</i> )	86.56	nd	nd	87.49
Middle Coniacian ( <i>V. koeneni</i> )	<b>88.55</b>	nd	nd	<b>88.55</b>
Lower Coniacian ( <i>C. deformis erectus</i> )	<b>89.27</b>	<b>89.27</b>	89.0	88.96
Upper Turonian ( <i>S. neptuni</i> )	<b>90.36</b>	nd	90.4	<b>90.36</b>
Middle Turonian ( <i>C. woollgari</i> )	<b>92.13</b>	<b>92.13</b>	92.2	91.88
<i>M. nodosoides</i> Zone	<b>92.70</b>	<b>92.70</b>	92.8	92.43
<i>F. catinus</i> Zone	93.20	nd	nd	nd
Lower Turonian ( <i>W. devonense</i> )	<b>93.55</b>	<b>93.55</b>	93.5	93.49
<i>N. juddii</i> Zone	<b>93.64</b>	<b>93.64</b>	93.7	93.73
<i>M. geslinianum</i> Zone	<b>93.99</b>	nd	93.95	<b>93.99</b>
Upper Cenomanian ( <i>C. guerangeri</i> )	<b>94.71</b>	nd	94.7	<b>94.71</b>
<i>A. jukes-brownei</i> Zone	94.93	nd	94.9	94.86
<i>A. rhotomagense</i> Zone (ex <i>C. inerme</i> )	95.72	nd	nd	nd
Middle Cenomanian ( <i>C. inerme</i> )	<b>95.84</b>	nd	95.8	<b>95.84</b>
<i>M. dixoni</i> Zone	97.74	nd	97.5	97.39
Lower Cenomanian ( <i>M. mantelli</i> )	<b>99.60</b>	<b>99.60</b>	98.9	98.94

nd – no data; values in bold are age calibration values used in this study.

equivalent values at Dover and elsewhere. Lower Cenomanian values plotted on the composite profile (Fig. 12) were hence corrected by  $-0.2\%$ . Age datum levels used to calibrate the isotope curve are listed in Table 3. The calculated age of the base of the *M. dixoni* Zone of 97.74 Ma is slightly older than previous estimates (Hardenbol *et al.* 1998; Voigt, 2000) due to the greater age assigned to the base of the Cenomanian by Ogg, Agterberg & Gradstein (2004). The calculated age of the base of the *A. jukesbrownei* Zone at 94.93 Ma agrees closely with previous estimates.

### 3.e.2. Turonian

The Turonian composite  $\delta^{13}\text{C}$  curve (Fig. 12) was constructed using data from Eastbourne up to the base of the *M. nodosoides* Zone at the Compton Pebble Marl (base couplet E28), then data from Culver up to the Round Down Marl (base couplet F20), data from Dover up to the top of the Bridgewick Event  $\delta^{13}\text{C}$  minimum at the base of the *S. plana* echinoid Zone, and data from the Trunch borehole for the uppermost Turonian. Correlation between the sections was achieved using the detailed biostratigraphic, marker-bed, couplet and carbon-isotope correlations summarized in Figure 7.

An age of 93.20 Ma was calculated for the base of the *F. catinus* Zone at Holywell Marl 2 (couplet E23) at Eastbourne (Table 3). The Eastbourne and Culver  $\delta^{13}\text{C}$  profiles were stacked at the Compton Pebble Marl with an age of 92.70 Ma for the base of the *M. nodosoides* Zone (Ogg, Agterberg & Gradstein, 2004). Stacking of the Culver and Dover profiles in the low *C. woollgari* Zone employed an age of 91.748 Ma for the Round Down Marl, calculated from Culver using an accumulation rate determined for the

*M. nodosoides* Zone applied to the low *C. woollgari* Zone. This figure is only an approximation because the sedimentological differences between the calcarenitic weakly nodular Holywell Chalk and the marly New Pit Chalk indicate a change in depositional regime in the upper *M. nodosoides* Zone, although these differences are less pronounced in the expanded section at Culver than elsewhere in southern England. The Dover and Trunch profiles were stacked in the mid-*S. neptuni* Zone using an age of 89.835 Ma for the top of the Bridgewick Event, calculated from Dover using a sedimentation rate based on the *C. woollgari* Zone applied to the lower *S. neptuni* Zone. This part of the succession displays relatively uniform lithological characteristics.

The stacked  $\delta^{13}\text{C}$  profiles (Fig. 12) displayed excellent continuity except for the Dover data that showed an offset of  $-0.2\%$ . Turonian values from Dover were corrected for this offset by adding  $0.2\%$ .

### 3.e.3. Coniacian

Data from the Trunch borehole were used to represent the upper Upper Turonian and Lower Coniacian intervals because this section is least affected by the condensation, omission and erosion accompanying the formation of the Chalk Rock facies of southern England. Culver was chosen to represent the Middle and Upper Coniacian because the biostratigraphic and marker-bed stratigraphy are far better constrained in the outcrop section. The two  $\delta^{13}\text{C}$  profiles were stacked at East Cliff Marl 2 (Fig. 12) with an age of 88.55 Ma assigned to the base of the Middle Coniacian *V. koeneni* Zone (Hardenbol *et al.* 1998).

The estimated age for the base of the Late Coniacian at 86.56 Ma (Table 3) is significantly younger than

a previous estimate of 87.49 Ma (Hardenbol *et al.* 1998; base of the *M. subquadratus* Zone). However, as noted previously, the Upper Coniacian index species *Megadiceramus subquadratus* is unrecorded in southern England, and the base of the substage is placed at the last appearance of *Volviceras*, below part of the succession that contains few macrofossils. Large potential errors exist therefore in the placement of the Upper Coniacian substage boundary in England.

#### 3.e.4. Santonian

The Culver data were chosen to represent the Lower Santonian to middle Upper Santonian portion of the composite  $\delta^{13}\text{C}$  curve (Fig. 12). However, the uppermost Upper Santonian is absent at Culver due to erosion associated with the glauconitized hardgrounds at the base of the Whitecliff Ledge Beds (base Campanian), and reliable ages for the bases of the Early and Middle Santonian are currently unavailable. To calculate the amount of missing Santonian section at Culver, the sediment thicknesses between two key marker beds, the Exceat Flint and the Hawks Brow Flint, were measured at Culver (25.1 m) and Seaford (10.4 m), and the amount of expansion in the former section (Fig. 11) calculated ( $\times 2.41$ ). This factor was then applied to the thickness of sediment between the Hawks Brow Flint and base Campanian (Friars Bay Marl 1) at Seaford (10.5 m) to calculate the projected position of the base Campanian at Culver, relative to the Hawks Brow flint (+ 25.3 m). The projected position (315.9 m) was used to calculate the average accumulation rate for the Santonian at Culver, prior to Campanian erosion. This accumulation rate was applied to generate an age model for the Culver Santonian  $\delta^{13}\text{C}$  curve.

Calculated ages for the bases of the Middle (top *C. undulatopticatus* inoceramid Zone) and Late (base *U. socialis* Zone) Santonian were 85.57 and 84.71 Ma (Table 3). The uppermost Upper Santonian to lowest Campanian portion of the composite  $\delta^{13}\text{C}$  curve uses data from the expanded Trunch borehole succession. These data were stacked on the Culver profile at the Hawks Brow Event in the uppermost *U. socialis* Zone, using an age of 84.179 Ma for the Hawks Brow Flint calculated at Culver. An age estimate of 84.14 Ma for the base of the *Marsupites* Zone (Table 3) calculated from Culver, compares favourably to an age of 84.11 Ma derived from the Trunch borehole.

#### 4. International correlation

Filtered and smoothed low-resolution carbon- and oxygen-isotope curves for the Albian–Palaeocene at Gubbio, Italy, were published by Scholle & Arthur (1980, fig. 2). A higher resolution stable-isotope study was undertaken by Corfield *et al.* (1991), and this work was enhanced further for the Cenomanian–Campanian

by 1 m sampling and re-logging of the Bottaccione Gorge section by Jenkyns, Gale & Corfield (1994, fig. 10). The isotope stratigraphy at Gubbio was constrained by a published foraminiferal biostratigraphy (Cresta, Monechi & Parisi, 1989), that was later revised by Premoli Silva & Sliter (1995), with the addition of a previously unpublished nannofossil zonation. Comparable carbon-isotope data were subsequently presented for equivalent levels in the Piobbico area of the same region (Erbacher, Thurow & Littke, 1996; Erbacher & Thurow, 1997; Coccioni & Galeotti, 2003).

Much higher resolution carbon- and oxygen-isotope curves for the Albian–Santonian (10–20 cm sampling), were published by Stoll & Schrag (2000, figs 2, 3), based on sampling at Contessa Quarry around 4 km from the Bottaccione Gorge. The biostratigraphy of Premoli Silva & Sliter (1995) from Bottaccione was applied to the Contessa section (cf. Stoll & Schrag, 2000) by translating the depths of biostratigraphic boundaries using the base of the Livello Bonarelli black shales (uppermost Cenomanian) as a reference level. Most recently, Tsikos *et al.* (2004) published  $\delta^{13}\text{C}$  data at 10 cm resolution for the Middle Cenomanian–Lower Turonian from the Gubbio S2 core taken from Vispi Quarry, Contessa Gorge, together with new biostratigraphic data for the Cenomanian/Turonian boundary interval.

#### 4.a. Boreal–Tethyan carbon-isotope correlation

Carbon-isotope curves from Gubbio are correlated to the English Chalk age-calibrated reference  $\delta^{13}\text{C}$  curve in Figures 13 and 14. It is notable that the two high-resolution Gubbio curves for the Cenomanian–Turonian are in excellent agreement (Fig. 13), with a slightly thicker Cenomanian section represented in the S2 core. A small + 0.1‰  $\delta^{13}\text{C}$  offset in the core data might reflect weathering of outcrop samples or analytical bias. This offset has no significant effect on the shapes of the curves which record identical fine detail.

The carbon-isotope events defined in the Cenomanian–Turonian of the English Chalk are readily identified at Gubbio. Key tie points are provided by the Albian/Cenomanian Boundary Event, Mid-Cenomanian Event I, the Cenomanian/Turonian Boundary Event, and the Bridgewick, Hitch Wood and Navigation events of Late Turonian age. The fidelity of the Middle–Upper Cenomanian and Middle–Upper Turonian records in the two areas is remarkable, with identical profiles and absolute  $\delta^{13}\text{C}$  values (Fig. 13). Correlation of the Albian–Lower Cenomanian interval is less certain, although the main features of the two records are comparable.

The uppermost Cenomanian at Gubbio is characterized by ~ 1 m of black shale and radiolarian sand, forming the Livello Bonarelli. This interval is essentially carbonate free, and is represented by a gap

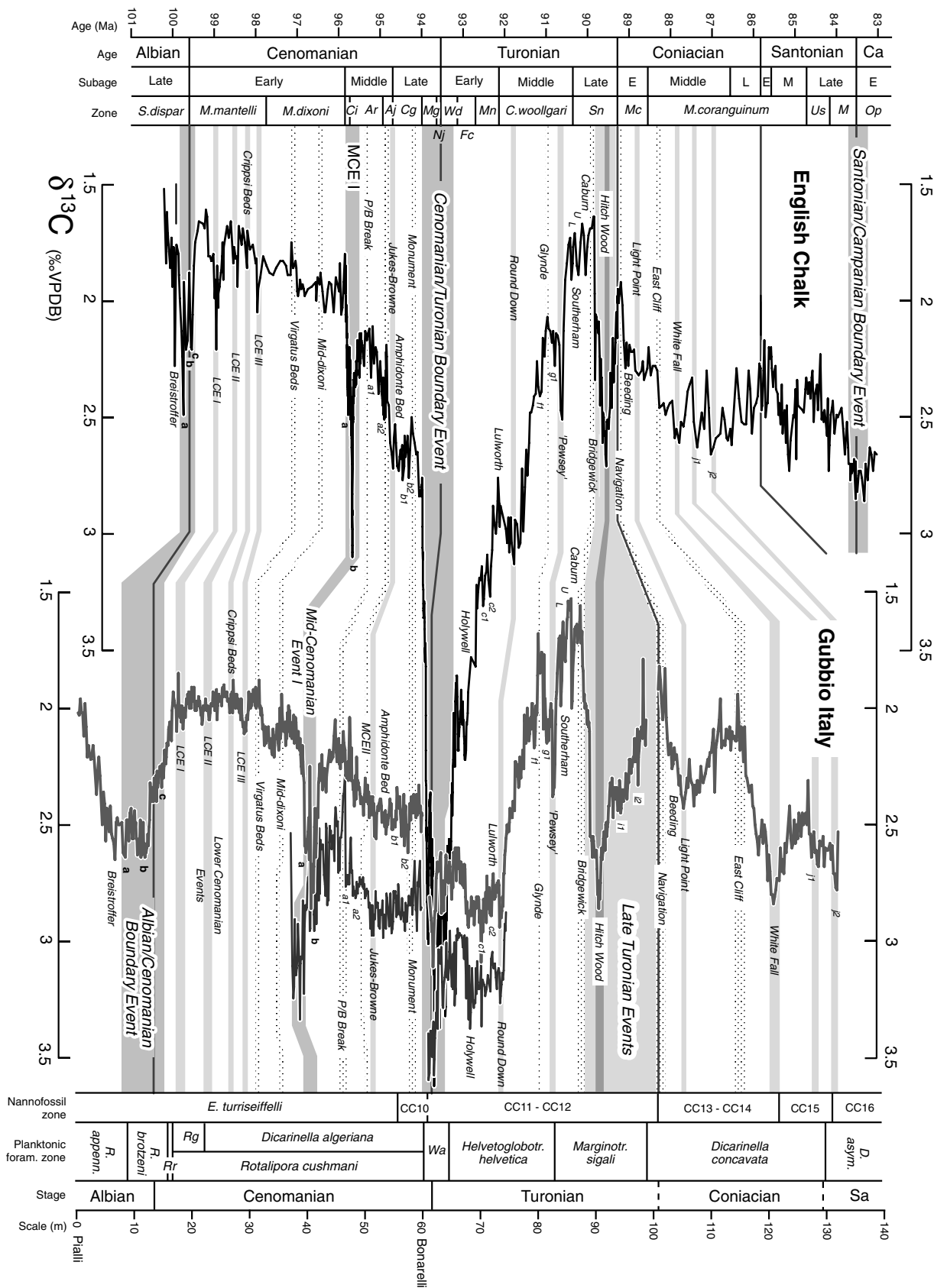


Figure 13. For legend see facing page.

in the  $\delta^{13}\text{C}$  carbonate records (Fig. 13). In the Chalk,  $\delta^{13}\text{C}$  values at this level rise rapidly by +2‰ to form the base of the large positive excursion characterizing the Cenomanian/Turonian Boundary Event. A positive excursion of the same magnitude is recorded by organic matter from the Livello Bonarelli (Tsikos *et al.* 2004, fig. 6).

Carbonate  $\delta^{13}\text{C}$  values immediately above the Livello Bonarelli are relatively low at around 3‰, and they do not show the high and sharply falling values seen in England (Fig. 13), possibly due to overprinting associated with diagenesis of the underlying black shales. Values remain relatively low through the Lower Turonian at Gubbio but, despite this, the main carbon-isotope events defined in England can be readily identified.

The  $\delta^{13}\text{C}$  minimum defining the Navigation Event at the Turonian/Coniacian boundary provides a robust correlation point between England and Italy (Fig. 13). Above this, the carbon-isotope record displays less variation with broader lower amplitude peaks and troughs that make correlation less certain. Details of a proposed Coniacian–Santonian correlation between the Chalk reference curve and the medium-resolution Gubbio curve of Jenkyns, Gale & Corfield (1994) are shown in Figure 14. There is excellent agreement between the Albian–Coniacian portion of the Jenkyns, Gale & Corfield (1994) curve and the higher resolution data of Stoll & Schrag (2000), confirming the validity of the lower resolution data. The tops of the English and Italian curves have been pinned on the  $\delta^{13}\text{C}$  maxima defining the Santonian/Campanian Event. The latter is placed at the top of the Gubbio curve, not at the base of the *G. elevata* Zone established by Premoli Silva & Sliter (1995), because elsewhere in Europe  $\delta^{13}\text{C}$  values generally fall through the Lower Campanian (Scholle & Arthur, 1980; Schönfeld & Burnett, 1991; Pratt *et al.* 1993; Jenkyns, Gale & Corfield, 1994; Jarvis *et al.* 2002) above a boundary-event maximum.

The isotope correlation presented in Figure 14 offers good correspondence between the English and Italian curves in both shape and absolute values, while maintaining relatively constant sedimentation rates through the Coniacian–Santonian at Gubbio. It

is notable that the correlation is consistent with the position of the base of Chron 33r, the termination of the long normal geomagnetic polarity interval of the Aptian–Santonian (Chron 34n; the ‘Cretaceous Quiet Zone’), at the top of the Buckle Event (Fig. 14). In England, the Chron 34n/33r boundary occurs a short distance above the base of the Upper Santonian in the lower *Uintacrinus* Zone (Gale *et al.* 1995; Montgomery *et al.* 1998), consistent with its position in Russia (Pechersky, Naidin & Molotovskiy, 1983). In Italy, the reversal has generally been regarded as occurring immediately above the base of the Campanian (Alvarez *et al.* 1977; Lowrie & Alvarez, 1977; Alvarez & Lowrie, 1978; Cresta, Monechi & Parisi, 1989; Premoli Silva & Sliter, 1995).

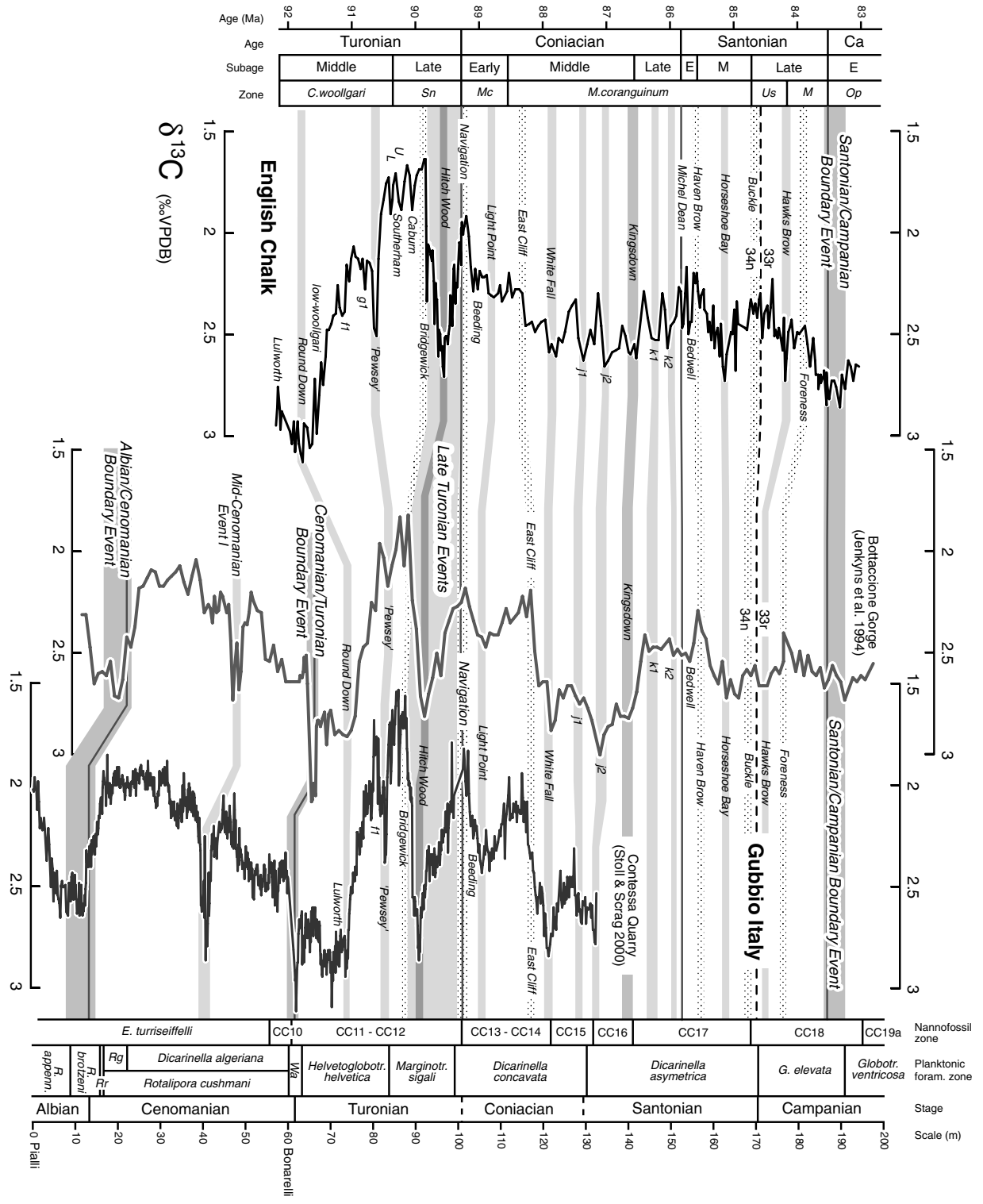
#### 4.b. Equivalence of Boreal and Tethyan biostratigraphy

The lack of integrated litho-, bio-, magneto- and chemostratigraphic analysis of the Gubbio sections offers the possibility of metre-scale errors in the placement of zonal boundaries with respect to the carbon-isotope stratigraphy. For example, the base of the *R. brotzeni* Zone and the base of the Cenomanian Stage were placed close to the bottom of the positive  $\delta^{13}\text{C}$  excursion defining the Albian/Cenomanian Boundary Event at Bottaccione Gorge by Jenkyns, Gale & Corfield (1994, fig. 10), and near the top of the excursion at Contessa Quarry by Stoll & Schrag (2000, fig. 2). Correlation of the  $\delta^{13}\text{C}$  curve from the Cenomanian Global boundary Stratotype Section and Point at Risou with that from Gubbio (Fig. 4; Gale *et al.* 1996) indicates that the base of the Cenomanian Stage lies above the  $\delta^{13}\text{C}$  maximum defining peak b of the Albian/Cenomanian Boundary Event. *Rotalipora globotruncanoides*, the base Cenomanian index species, has not been recorded at Gubbio, but in Bottaccione Gorge the last occurrence of *Rotalipora ticinensis* occurs around 1 m above the base of the *R. brotzeni* Zone (Premoli Silva & Sliter, 1995), indicating that the base of the Cenomanian lies immediately above this, at a level that is consistent with our carbon-isotope correlation (Figs 4, 13).

The base of Mid-Cenomanian Event I, a short distance above the base of the Middle Cenomanian Substage, provides a robust correlation point between

Figure 13. Correlation of Cenomanian–Coniacian  $\delta^{13}\text{C}$  events between England and Italy. The English Chalk reference curve in black is an unsmoothed composite plotted against age; see Figure 12, Table 3 and text for details. High-resolution profiles from Gubbio are plotted against stratigraphic height for Contessa Quarry (Stoll & Schrag, 2000, medium grey curve, left) and the Gubbio S2 core from Vispi Quarry, Contessa Gorge (Tsikos *et al.* 2004, dark grey curve, right). The S2 curve has been offset by +0.25‰  $\delta^{13}\text{C}$  relative to the Contessa data to facilitate comparison. Gubbio biostratigraphy after Premoli Silva & Sliter (1995), derived from the Bottaccione section, transposed to Contessa Quarry using stratigraphic heights relative to the Livello Bonarelli, with additional data from Tsikos *et al.* (2004). ‘Late Turonian Events’ represent the succession of isotope events defining the long-term positive  $\delta^{13}\text{C}$  excursion in the Upper Turonian, with the Bridgewick and Navigation negative excursions defining the bottom and top of the interval and the Hitch Wood Event representing the carbon-isotope maximum. Abbreviations as in Figure 12, plus: LCE I–III – Lower Cenomanian Events I–III; MCE I – Mid-Cenomanian Event I; *R. appenn.* – *Rotalipora appenninica*; *Rr* – *Rotalipora reicheli*; *Rg* – *Rotalipora greenhornensis*; *Wa* – *Whiteinella archaeocretacea*; *Helvetoglobotr.* – *Helvetoglobotruncana*; *Marginotr.* – *Marginotruncana*; *D. asym.* – *Dicarinella asymetrica*; *Sa* – Santonian.

Figure 14. For legend see facing page.



the Boreal and Tethyan sections (Fig. 13). This apparently lies in the mid-*R. cushmani* Zone at Gubbio (Premoli Silva & Sliter, 1995; Coccioni & Galeotti, 2003), the base of which is generally regarded as being Middle Cenomanian (Ogg, Agterberg & Gradstein, 2004). This major discrepancy in the relative positions of the *R. cushmani* and *R. reicheli* zones requires urgent investigation. The isotope correlation (Fig. 13) offers considerable potential for refining the poorly resolved Cenomanian biostratigraphy at Gubbio.

The correspondence between Boreal and Tethyan biozonations for the Cenomanian–Turonian boundary interval is well established (e.g. Tsikos *et al.* 2004; Ogg, Agterberg & Gradstein, 2004; Amédéo, Accarie & Robaszynski, 2005; Gale *et al.* 2005) and is consistent with the carbon-isotope correlation (Figs 6, 13). In the Middle and Upper Turonian the Round Down, Glynde, ‘Pewsey’, Bridgewick, Hitch Wood and Navigation events provide excellent tie points (Figs 8, 13) that confirm the placement of the *M. sigali* Zone in the upper Middle Turonian and the base of the *D. concavata* Zone high in the Upper Turonian (Ogg, Agterberg & Gradstein, 2004). The positions of the ‘Pewsey’ Event at the top of the *H. helvetica* Zone, the Hitch Wood Event in the mid-*M. sigali* Zone, and the Navigation Event of the basal *D. concavata* zones, all provide potentially robust international markers.

The Coniacian–Santonian correlation is more problematic. The location of the East Cliff and White Fall events in the Middle Coniacian, mid-*D. concavata* Zone is consistent with the established biostratigraphy (Ogg, Agterberg & Gradstein, 2004), but the isotopic correlation (Figs 13, 14) places the base of the *D. asymetrica* Zone at the summit of the Middle Coniacian rather than at the base of the Santonian. The basal Santonian Michel Dean Event lies in the mid-*D. asymetrica* Zone, and the basal Upper Santonian Buckle Event and the base of Chron 33r correlate with the top of the Zone. If correct, this correlation places the Santonian/Campanian boundary in the upper *G. elevata* Zone and not at the base of the zone, as currently assumed (Ogg, Agterberg & Gradstein, 2004).

It is clear that significant anomalies exist in established relationships between the Boreal and Tethyan Cenomanian, Coniacian and Santonian biostratigraphic schemes. Further work is required to confirm the placement of the macrofossil-defined zones and stage boundaries with respect to planktonic foraminiferal and nannofossil biostratigraphies.

## 5. Carbon isotopes and sea-level change

Carbon-isotope stratigraphy based on the analysis of bulk samples of hemipelagic and pelagic carbonates provides a robust means of correlating Cenomanian–Santonian strata on a global scale, with coeval successions displaying remarkably similar trends and  $\delta^{13}\text{C}$  values. Major positive and negative excursions together with significant inflection points on the isotope curves have enabled the definition of a carbon-isotope event stratigraphy that can be used for international correlation.

The tight stratigraphic framework provided by the combination of biostratigraphy and chemostratigraphy allows carbon-isotope profiles to be compared with regional and presumed global sea-level curves, and other palaeoenvironmental proxies, to investigate the forcing mechanisms and feedbacks involved.

### 5.a. Eustatic sea-level

There is considerable evidence for a relationship between positive shifts in Cretaceous  $\delta^{13}\text{C}$  records and first-order rises in eustatic sea-level (e.g. Scholle & Arthur, 1980; Berger & Vincent, 1986; Arthur, Schlanger & Jenkyns, 1987; Weissert, 1989; Jenkyns, Gale & Corfield, 1994; Mitchell, Paul & Gale, 1996; Voigt & Hilbrecht, 1997; Weissert *et al.* 1998; Jarvis, Murphy & Gale, 2001; Jarvis *et al.* 2002). This association is generally attributed to changes in the partitioning of carbon between organic and carbonate carbon sinks caused by sea-level rise and consequent transgression. However, the Exxon global Mesozoic–Cenozoic sea-level curve (Haq, Hardenbol & Vail, 1987, 1988), which is commonly used to assess eustatic influences on regional sequence stratigraphy and sea-level change, has insufficient stratigraphic resolution to test these relationships with any rigour (Miall, 1992; Jarvis *et al.* 2002).

A quantitative sea-level curve, interpreted as eustatic, for the Middle Jurassic–Cretaceous was developed by Sahagian *et al.* (1996), based on sequences on the supposedly tectonically stable Russian Platform, supplemented by data from Siberia. These authors employed a combination of sediment geometry, lithology, sediment structure, mineralogy, macrofossil palaeoecology and taphonomy, and trace-fossil assemblages (ichnofacies) to estimate water-depth changes on the Platform, which were assumed to be predominantly a response to accommodation space provided by

Figure 14. Correlation of Middle Turonian–Santonian  $\delta^{13}\text{C}$  events between England and Italy. The age-calibrated English Chalk unsmoothed reference curve in black (this study), is compared with a medium-resolution stratigraphic height profile for Gubbio from Bottaccione Gorge (Jenkyns, Gale & Corfield, 1994, medium grey curve) and a higher resolution stratigraphic height curve from Contessa Quarry (Stoll & Schrag, 2000, dark grey curve). Gubbio biostratigraphy after Premoli Silva & Sliter (1995), derived from the Bottaccione section. The position of the base of Chron 33r (dashed horizontal line) is indicated (Alvarez *et al.* 1977; Montgomery *et al.* 1998), marking the termination of the Cretaceous Long Normal (Chron 34n). The Bottaccione  $\delta^{13}\text{C}$  data display a systematic offset of around +0.1‰ compared to the Contessa Quarry and English Chalk data. See Figure 13 for abbreviations.

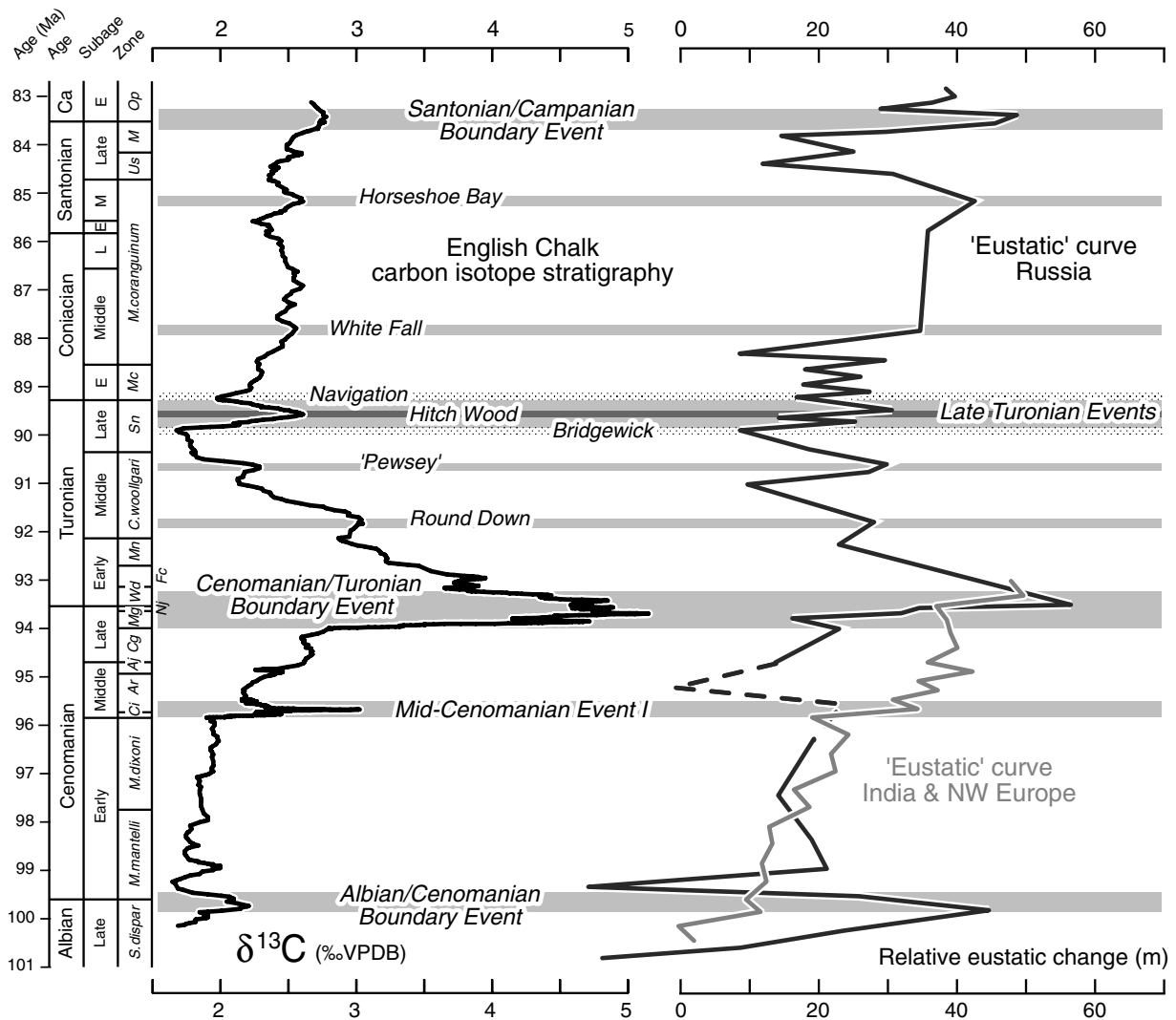


Figure 15. Relationship between carbon-isotope stratigraphy and sea level. A smoothed (5-point moving average) version of the English Chalk  $\delta^{13}\text{C}$  composite age-calibrated curve (this study) is compared with biostratigraphically well-constrained sea-level curves, interpreted as eustatic, based on data from the Russian Platform and Siberia (Sahagian *et al.* 1996), India and NW Europe (Gale *et al.* 2002). The sea-level curves have been recalibrated to the time scale of Ogg, Agterberg & Gradstein (2004) using macrofossil zone, substage and stage data. Abbreviations as in Figure 12.

eustatic sea-level rise. The curve was constrained by macrofossil biostratigraphy with episodes of major sea-level fall being indicated by regional hiatuses in the succession. Back-stripping techniques that accounted for palaeodepth variations, sediment loading, compaction and basin subsidence were used to generate relative sea-level curves for multiple sections, which were then combined to produce a composite eustatic curve (Sahagian *et al.* 1996, fig. 11). Subsequently, a more detailed supposedly eustatic curve for the Cenomanian, constrained by high-resolution ammonite biostratigraphy, was presented by Gale *et al.* (2002, fig. 4) based on sequence stratigraphic analysis of sections in SE India and NW Europe, and Miller *et al.* (2003, 2004) presented a sea-level curve for the entire Upper Cretaceous based on an analysis of the New Jersey Coastal Plain, USA.

The Sahagian *et al.* (1996) and Gale *et al.* (2002) 'eustatic' curves, rescaled against the time scale of Ogg, Agterberg & Gradstein (2004) using stage and ammonite zone data, are compared to the English Chalk composite  $\delta^{13}\text{C}$  profile in Figure 15. Detailed comparison with the data of Miller *et al.* (2003, 2004) is hampered by relatively poor stratigraphic control on the Cenomanian–Santonian portion of their curve; strontium isotopes were found to be diagenetically altered in this interval, and ages were constrained by limited nannofossil records supplemented by pollen and some planktonic foraminiferal data (Sugarman *et al.* 1999).

The composite  $\delta^{13}\text{C}$  curve shows remarkable similarities to the 'eustatic' curves (Fig. 15). The long-term rise in  $\delta^{13}\text{C}$  values, from around 1.5‰ in the latest Albian to nearly 3‰ at the Santonian/Campanian

boundary, is matched by a sea-level rise of around 40 m. Medium-term peaks and troughs on the isotope curve correspond well with highstands and lowstands, respectively. For example, the Cretaceous sea-level maximum at the Cenomanian/Turonian boundary is matched by a  $\delta^{13}\text{C}$  maximum of 5‰. The latest Albian sea-level highstand is equated with the Albian/Cenomanian Boundary Event isotope maximum and the latest Santonian highstand with the Santonian/Campanian boundary Event, although stratigraphic uncertainties exist around these intervals.

The similarity between the Cenomanian isotope profile and the supposedly eustatic curve of Gale *et al.* (2002) is particularly striking (Fig. 15), but both the Sahagian *et al.* (1996) and the Gale *et al.* (2002) sea-level curves independently demonstrate a rise of 50 m through the Cenomanian, corresponding to a +3‰ positive shift in  $\delta^{13}\text{C}$  values. Miller *et al.* (2003, 2004), on the other hand, estimated a sea-level rise of only 20 m through the stage but predicted higher sea-levels in the middle Cenomanian. The rate of long-term sea-level rise during the Cenomanian, therefore, was 3–8 m Myr<sup>-1</sup>, which is well below the 30 m Myr<sup>-1</sup> maximum imposed by tectonic as opposed to glacio-eustatic forcing. However, the amplitude of medium- to short-term sea-level change of 2–20 m estimated by Gale *et al.* (2002), although less than the 50 m calculated by Sahagian *et al.* (1996) and >25 m determined by Miller *et al.* (2003, 2004), indicates rates of short-term sea-level change during the Cenomanian of 10–100 m Myr<sup>-1</sup>. It is notable that the lower amplitude sea-level variation documented by Gale *et al.* (2002) correlates well with the amplitude of variation displayed by the  $\delta^{13}\text{C}$  curve (Fig. 15).

The calculated rates of short-term sea-level change are difficult to explain without invoking glacio-eustasy, yet new evidence for high Arctic Ocean palaeotemperatures appears to preclude any possibility of a northern hemisphere ice sheet during the Late Cretaceous (Jenkyns *et al.* 2004). Antarctic glaciation on high-altitude sites remains possible (cf. DeConto & Pollard, 2003). It has been calculated that a 4 km thick icecap on Antarctica would be required to lower sea level by 100 m (Dewey & Pitman, 1998), but Miller *et al.* (2003, 2004) have argued that a restricted ephemeral inland Antarctic ice sheet of 5–10 × 10<sup>6</sup> km<sup>3</sup> would be sufficient to drive 25 m amplitude short-term changes.

A strong correspondence between the shape of Cenomanian carbon-isotope profiles and the Exxon (Haq, Hardenbol & Vail, 1988) and other supposedly eustatic sea-level curves has been noted previously (e.g. Mitchell, Paul & Gale, 1996). This relationship has been attributed to the increased area of productive shallow seas available after marine transgression, with the consequent increased global burial flux of <sup>12</sup>C-enriched marine organic carbon and elevated  $\delta^{13}\text{C}$  values in ocean waters recorded in biogenic carbonates (Jenkyns, Gale & Corfield, 1994). Lower rates of

organic carbon burial and the oxidation of previously deposited organic matter accompanied sea-level fall, producing falling  $\delta^{13}\text{C}$  values during regressions.

By contrast, Voigt (2000) demonstrated poor agreement between the Exxon sea-level curve for the Turonian and a composite  $\delta^{13}\text{C}$  profile derived from sections in England and Germany. The observed differences were explained by periods of enhanced inorganic carbon burial increasing the ratio of global inorganic to organic carbon fluxes and shifting the <sup>13</sup>C/<sup>12</sup>C ratio to more negative values. However, the Exxon curve differs substantially from the better constrained Turonian sea-level data of Sahagian (1996, fig. 13). For example, the marked late Middle Turonian lowstand of Haq, Hardenbol & Vail (1988) is much less pronounced and is dated as early Middle Turonian by both Sahagian *et al.* (1996) and Miller *et al.* (2003, 2004).

A relative sea-level rise around the Early/Middle Turonian boundary (Fig. 15) corresponds to a broad  $\delta^{13}\text{C}$  maximum culminating in the Round Down Event. This sea-level maximum, dated as low-*woollgari* Zone by Hancock (2000), is particularly well developed in the US Western Interior. A latest Middle Turonian transgression (corresponding to the ‘Pewsey’ Event) and the subsequent sea-level highstand correlate well with the isotope profile (Fig. 14). The Late Turonian sea-level fall and lowstand (Gale, 1996; Sahagian *et al.* 1996; Miller *et al.* 2003, 2004) is matched by a broad carbon-isotope minimum culminating in the Bridgewick Event. There is corresponding evidence of widespread regression at this time in NW Europe, the North American Gulf Coast and Western Interior, North and West Africa, eastern Brazil and Western Australia (e.g. Matsumoto, 1980). The latest Turonian  $\delta^{13}\text{C}$  maximum of the Hitch Wood Event is coincident with a transgressive pulse in many areas.

A marked early Middle Coniacian transgression (Fig. 15) is correlated with the step towards more positive  $\delta^{13}\text{C}$  values above the East Cliff Event, culminating in the White Fall Event, above. A widespread Coniacian transgressive maximum (Hancock & Kauffman, 1979; Hancock, 2000) correlates with a broad  $\delta^{13}\text{C}$  maximum between the White Fall and Kingsdown events. Early and Late Santonian transgressions (Sahagian *et al.* 1996; Miller *et al.* 2003, 2004) correspond to the Horseshoe Bay and Santonian/Campanian boundary positive carbon-isotope events (Fig. 15).

### 5.b. Feedbacks and forcing mechanisms

Similarities between the shape of the long-term Cenomanian–Santonian  $\delta^{13}\text{C}$  profile and sea-level curves that are of at least regional significance (Fig. 15) support the argument that  $\delta^{13}\text{C}$  might be considered as an independent method for estimating first-order eustatic sea-level (Mitchell, Paul & Gale, 1996; Voigt & Hilbrecht, 1997; Grant, Coe & Armstrong, 1999). However, it must be acknowledged that even

using the stratigraphically better constrained sea-level curves now available for different continents, the exact temporal relationships between sea-level change and variations in the carbon-isotope record remain uncertain. Furthermore, the effects of sea-level change on the global carbon cycle and the partitioning of carbon-isotopes in organic versus inorganic reservoirs are undoubtedly complex. For example, rates of sea-level rise/transgression and fall rather than the magnitude of sea-level change may affect the amplitude of carbon-isotope variation, so exact agreement is unlikely (Jenkyns, Gale & Corfield, 1994).

Variations in the area of shallow seafloor provide a simple mechanism for changing organic-carbon burial fluxes and  $\delta^{13}\text{C}$  values in response to sea-level rise and fall. However, other factors may be significant (Jarvis *et al.* 2002). Increased rates of formation of isotopically light methane hydrate on continental margins during transgressions, and reduced rates of formation and/or their dissociation during periods of sea-level fall, tectonic activity on continental margins, or a rise in bottom-water temperatures, may also play a role (Kvenvolden, 1998; Ripperdan, 2001; Jarvis *et al.* 2002; Jenkyns, 2003). At times of rapid sea-level rise, reworking of sediments and soils on previous land areas might promote increased nutrient fluxes to epicontinental seas, which would have supported increased local productivity and enhanced organic-carbon burial rates (Jenkyns, Gale & Corfield, 1994; Hilbrecht *et al.* 1996). Higher nutrient supply to surface waters would have favoured organic and siliceous plankton production and reduced rates of calcareous plankton rain. If sea-level rise were rapid, carbonate platforms would have been flooded and shallow-water carbonate factories closed down, potentially (assuming a constant output of global sedimentary carbon) increasing the relative proportion of the organic-carbon flux; major carbonate platform crises are documented (Skelton, 2003, fig. 5.1) in the Middle Cenomanian, at the Cenomanian/Turonian boundary, in the early Coniacian, and around the Santonian/Campanian boundary, each coincident with major eustatic transgressions and increased  $\delta^{13}\text{C}$  values (Fig. 15). Terrestrial environments would also be affected by the transgression, with higher water tables during sea-level rise leading to increased peat accumulation and  $^{12}\text{C}$  removal in deltaic and other coastal margin settings.

As the rates of sea-level rise declined, and new sediments covered the drowned land masses, the nutrient flux would have decreased, reducing productivity. An increased area of pelagic carbonate deposition, a relative increase in calcareous plankton production, and new carbonate platform development would have changed the balance in favour of the inorganic carbon flux and (once again, assuming a constant output of global sedimentary carbon) shifted  $\delta^{13}\text{C}$  to lower values. During regressions, rates of organic-carbon burial would have fallen, and lower base levels would

have led to reworking of previously deposited organic-rich marine and terrestrial strata, returning isotopically light carbon to the global reservoir. Accompanying changes in oceanic circulation might also have had an effect. Increased oceanic circulation due to more efficient deep-water formation during times of low sea level would enhance  $^{12}\text{C}$  recycling, which would increase the residence time of  $^{12}\text{C}$  in the water column. This phenomenon would increase the size of the oceanic C reservoir, decrease the organic-carbon flux into sediments, and further reduce seawater  $\delta^{13}\text{C}$  values.

## 6. A carbon-isotope reference curve for the Cenomanian–Campanian ages

The work described in this paper complements that of Jarvis *et al.* (2002), who studied the carbon-isotope stratigraphy of the Campanian (83.5–70.6 Ma) based on sections in England, France and Tunisia. As with the current study, those authors demonstrated good agreement between carbon-isotope curves from Tethyan and Boreal areas, and argued for a close relationship between  $\delta^{13}\text{C}$  curves and eustatic sea level. Jarvis *et al.* (2002) used the isotopic data of Jenkyns, Gale & Corfield (1994) from the Trunch borehole to plot a Campanian reference curve. It is straightforward, therefore, to take the Santonian/Campanian boundary interval  $\delta^{13}\text{C}$  data from Trunch (Jenkyns, Gale & Corfield, 1994), used in the construction of the present stacked Cenomanian–Santonian reference curve (Fig. 12), and to extend this up through the Campanian. The resulting  $\delta^{13}\text{C}$  composite curve for the entire Cenomanian–Campanian ages is shown in Figure 16, calibrated against the timescale of Ogg, Agterberg & Gradstein (2004).

In addition to the positive  $\delta^{13}\text{C}$  excursion defining the Santonian/Campanian boundary event, a prominent positive shift of +0.2‰ occurs at the base of the Upper Campanian *Belemnitella mucronata* Zone (Fig. 16). This Mid-Campanian Event (Jarvis *et al.* 2002) coincides with the *mucronata* transgression recognized in northern Germany (Niebuhr, 1995; Niebuhr, Wood & Ernst, 2000) and elsewhere. The base of the Mid-Campanian Event also presents a major inflection point in the long-term Campanian stable-isotope curve; relatively stable  $\delta^{13}\text{C}$  values of around 2.4‰ in the Lower Campanian fall progressively through the Upper Campanian to 2.0‰ at the top of the stage. This drop corresponds to a phase of falling long-term supposedly eustatic sea level through the Late Campanian (Haq, Hardenbol & Vail, 1987, 1988).

A negative shift of –0.4‰  $\delta^{13}\text{C}$ , occurring in the middle of the Upper Campanian (Fig. 16), represents a major feature of the Cenomanian–Campanian isotope curve. This Late Campanian Event (Jarvis *et al.* 2002) correlates with the sea-level fall associated with the *polyplacum* regression in Germany; the subsequent

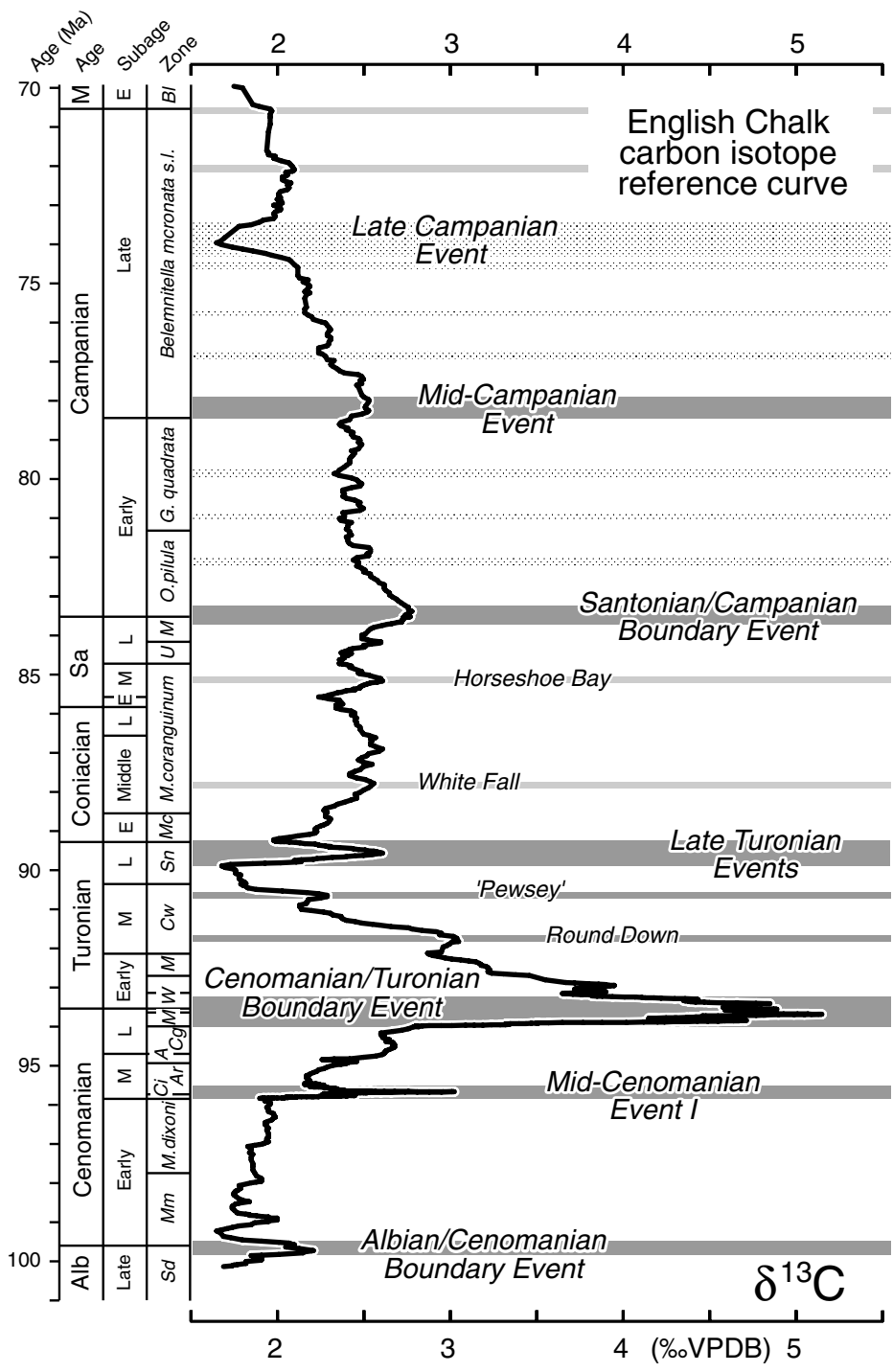


Figure 16. A carbon-isotope reference curve for the Cenomanian–Campanian ages based on the English Chalk. The curve is a 5-point moving average based on a stacked composite for the Cenomanian–Santonian (Fig. 12), with additional Campanian–Maastrichtian isotope data from the Trunch borehole (Jenkyns, Gale & Corfield, 1994). The curve has been calibrated using the age assignments of Ogg, Agterberg & Gradstein (2004). Abbreviations as in Figure 12, plus: M – Maastrichtian; Bl – *Belemnella lanceolata*.

transgression is marked by a return to previous  $\delta^{13}\text{C}$  values but no positive excursion. An inflection point at the base of the Maastrichtian, marking a shift to more rapidly falling carbon-isotope values, offers a possible criterion for recognizing the Campanian/Maastrichtian boundary on the isotope curve, but the reliability of this marker remains unproven. Seven further informally defined inflection points (Fig. 16) on the Campanian

isotope curve were used by Jarvis *et al.* (2002) to refine their Tethyan–Boreal correlation.

The 29 Myr long carbon-isotope record illustrated in Figure 16 is the first stratigraphically well-constrained high-resolution  $\delta^{13}\text{C}$  curve and associated isotope-event stratigraphy for the entire Cenomanian–Campanian interval of the Cretaceous Period. It offers potential for improved global correlation, and can be

employed to test the synchronicity of biotic events on a regional to global scale, and the equivalence of biostratigraphic schemes in different floral and faunal realms. Calibration of the  $\delta^{13}\text{C}$  curve to the geological timescale further provides a means of assigning absolute ages to well-characterized chemostratigraphic events, which can in turn be used to constrain rates of sedimentation or biotic turnover in sections anywhere in the world.

## 7. Conclusions

Carbon-isotope variation determined from bulk pelagic and hemipelagic carbonate sediments collected through the Cenomanian–Santonian stages shows consistent stratigraphic trends and commonly identical  $\delta^{13}\text{C}$  values, which provide a sound basis for high-resolution international correlation. Positive and negative  $\delta^{13}\text{C}$  excursions and inflection points on isotope profiles enable the definition of a succession of carbon-isotope events that are isochronous within a framework provided by key macrofossil biostratigraphic datum levels, bentonite horizons, and traditional macrofossil zonal boundaries within the UK and elsewhere in NW Europe.

Major chemostratigraphic datum levels are provided by 100 kyr-scale positive  $\delta^{13}\text{C}$  excursions: the Albian/Cenomanian Boundary Event; Mid-Cenomanian Event I; the Cenomanian/Turonian Boundary Event; a maximum of Late Turonian age defined by the Bridgewick, Hitch Wood and Navigation events; and the Santonian/Campanian Boundary Event. The detailed isotope stratigraphy based on the recognition of 72 events has been successfully applied to published isotope profiles from France, Germany, Italy and Spain, and provides a sound basis for high-resolution international correlation.

The diagenetically immature Chalk successions of southern, northern and eastern England offer some of the best-documented Cenomanian–Santonian pelagic-carbonate sections in the world, but substantial regional variation in thickness and stratigraphic completeness is demonstrated by detailed carbon-isotope correlation of seven English sections. None of the study localities offers a complete stratigraphic record. However, a composite  $\delta^{13}\text{C}$  reference curve based on the English Chalk has been successfully constructed using data from Culver, Dover, Eastbourne, Speeton and Trunch, calibrated against the 2004 geological timescale (Ogg, Agterberg & Gradstein, 2004). The locations of stage and substage boundaries are tightly constrained by macrofossil biostratigraphy.

Based on the English Chalk composite reference curve, carbon-isotope values in marine carbonates generally rise from 1.5‰  $\delta^{13}\text{C}$  in the Upper Albian to 2.9‰ in the uppermost Santonian, with a large broad symmetrical peak between the base of the Middle Cenomanian and the middle Upper Turonian

that attains a maximum of 5.4‰  $\delta^{13}\text{C}$  in the uppermost Cenomanian (Cenomanian/Turonian Boundary Event) and a minimum of 1.6‰ in the middle Upper Turonian (Bridgewick Event). Positive and negative carbon-isotope excursions and inflection points on the longer-term curve that define the isotope events have amplitudes ranging from 0.1 to 1‰ and occur throughout the succession.

The carbon-isotope stratigraphy based on English Boreal sections enables detailed correlation with Tethyan sections in central Italy. The Cenomanian–Turonian correlation is particularly well constrained and generally agrees well with established relationships between Tethyan planktonic foraminiferal and Boreal macrofossil biozonations, although important anomalies exist with respect to the positions of Cenomanian planktonic foraminiferal biozones. Correlation of the Coniacian–Santonian is less clear-cut. Magnetostratigraphic evidence for placing the base of Chron 33r near the base of the Upper Santonian is in good agreement with the carbon-isotope correlation, but generates significant anomalies regarding the placement of the Santonian and Campanian stage boundaries with respect to Tethyan planktonic foraminiferal and nannofossil zones. These discrepancies require further investigation.

The Cenomanian–Santonian carbon-isotope reference curve is remarkably similar in shape to recently published supposedly eustatic sea-level curves based on quantitative data from biostratigraphically well-constrained sections in Russia and India. Sea level appears to represent a major control on Cretaceous carbon-isotope variation with increasing  $\delta^{13}\text{C}$  values accompanying sea-level rise and transgression, and decreasing  $\delta^{13}\text{C}$  values characterizing sea-level fall and regression.

The direct correlation between carbon isotopes and sea level is most easily explained by variations in epicontinental sea area affecting organic-matter burial fluxes. Increasing shallow seafloor area and increased accommodation space accompanying sea-level rise allowed more efficient burial of marine organic matter, with the preferential removal of  $^{12}\text{C}$  from the marine carbon reservoir. Pelagic carbonates record the resulting increase in seawater  $\delta^{13}\text{C}$  values. During sea-level fall, reduced seafloor area, marine erosion of previously deposited sediments, and exposure of basin margins led to reduced organic-carbon burial fluxes and oxidation of previously deposited organic matter, causing falling  $\delta^{13}\text{C}$  values.

The carbonate carbon reservoir may also have played a role. Assuming that the global output of sedimentary carbon remained constant, drowning of carbonate platforms during periods of rapid sea-level rise would have reduced the inorganic carbon flux, while renewed platform growth during late transgressions and highstands would have prompted a major increase in carbonate deposition. Both processes would effectively

amplify the positive and negative  $\delta^{13}\text{C}$  shifts, respectively, driven by flux changes to the organic carbon reservoir. Other factors such as variations in nutrient supply, rates of oceanic turnover, and the sequestration or liberation of methane from gas hydrates in response to sea-level change, are also likely to have contributed to the observed carbon-isotope variation, but are harder to quantify.

The Cenomanian–Santonian composite  $\delta^{13}\text{C}$  curve has been stacked with a previously published reference curve for the Campanian (Jarvis *et al.* 2002) to present a complete composite carbon-isotope curve for the 29 Myr interval of the Cenomanian–Campanian ages. High-resolution carbon-isotope stratigraphy is a robust method for the correlation of pelagic carbonates, and the reference curve developed here provides valuable calibration points for future chemostratigraphic studies. When combined with biostratigraphy, chemostratigraphy offers potential for significantly improving global correlation and may provide a proxy for eustatic sea-level variation.

**Acknowledgements.** Research support to IJ and MAP by Statoil Norway is gratefully acknowledged. Samples and unpublished data from the Banterwick Barn and Trunch boreholes were supplied by the British Geological Survey. Dr Heather Stoll (Williams College) kindly provided digital isotope data for Gubbio. Julie Cartlidge operated the PRISM mass spectrometer at the University of Oxford where the isotopic data were generated. Constructive reviews were provided by Drs Silke Voigt (University of Cologne) and Peter Ditchfield (University of Oxford).

## References

- ALVAREZ, W., ARTHUR, M. A., FISCHER, A. G., LOWRIE, W., NAPOLEONE, G., PREMOLI SILVA, I. & ROGGENTHEN, W. M. 1977. Upper Cretaceous–Paleocene magnetic stratigraphy at Gubbio, Italy V. Type section for the Late Cretaceous–Paleocene geomagnetic reversal time-scale. *Geological Society of America Bulletin* **88**, 383–9.
- ALVAREZ, W. & LOWRIE, W. 1978. Upper Cretaceous magnetic stratigraphy at Moria (Umbrian Apennines, Italy): verification of the Gubbio section. *Geophysical Journal of the Royal Astronomical Society* **55**, 1–17.
- AMÉDRO, F., ACCARIE, H. & ROBASZYNSKI, F. 2005. Position de la limite Cénomaniens–Turonien dans la Formation Bahloul de Tunisie centrale: apports intégrés des ammonites et des isotopes du carbone ( $\delta^{13}\text{C}$ ). *Eclogae Geologicae Helveticae* **98**, 151–67.
- AMÉDRO, F. & ROBASZYNSKI, F. 1999. Les craies cénomaniennes du Boulonnais. Comparaison avec l'Aube (France) et le Kent (Royaume Uni). *Géologie de la France* **2**, 33–53.
- ARTHUR, M. A., JENKYN, H. C., BRUMSACK, H. J. & SCHLANGER, S. O. 1990. Stratigraphy, geochemistry, and paleoceanography of organic carbon-rich Cretaceous sequences. In *Cretaceous Resources Events and Rhythms: Background and Plans for Research* (eds R. N. Ginsburg and B. Beaudoin), pp. 75–119. NATO Science Series C: Mathematical and Physical Sciences no. 304. Dordrecht, The Netherlands: Kluwer Academic Publishers.
- ARTHUR, M. A., SCHLANGER, S. O. & JENKYN, H. C. 1987. The Cenomanian/Turonian Oceanic Anoxic Event, II: Palaeoceanographic controls on organic matter production and preservation. In *Marine Petroleum Source Rocks* (eds J. Brooks and A. J. Fleet), pp. 401–20. Geological Society of London, Special Publication no. 26. Oxford: Blackwell.
- BENGTSON, P. 1996. The Turonian stage and substage boundaries. In *Proceedings "Second International Symposium on Cretaceous Stage Boundaries" Brussels 8–16 September 1995* (eds P. F. Rawson, A. V. Dhondt, J. M. Hancock and W. J. Kennedy), pp. 69–79. Bulletin de l'Institut Royal des Sciences Naturelles de Belgique Sciences de la Terre no. 66, supplement.
- BERGER, A., LOUTRE, M. F. & DEHANT, V. 1989. Pre-Quaternary Milankovitch frequencies. *Nature* **323**, 133.
- BERGER, W. H. & VINCENT, E. 1986. Deep-sea carbonates: reading the carbon isotope signal. *Geologische Rundschau* **75**, 249–69.
- BIRKELUND, T., HANCOCK, J. M., HART, M. B., RAWSON, P. F., REMANE, J., ROBASZYNSKI, F., SCHMID, F. & SURLYK, F. 1984. Cretaceous stage boundaries – proposals. *Bulletin of the Geological Society of Denmark* **33**, 3–20.
- BOWER, C. R. & FARMERY, J. R. 1910. Zones of the Lower Chalk of Lincolnshire. *Proceedings of the Geologists' Association* **21**, 333–59.
- BRÉHÉRET, J.-G. 1988. Episodes de sédimentation riche en matière organique dans les marnes bleues d'âge aptien et albien de la partie pélagique de bassin vocontien. *Bulletin de la Société Géologique de France* **4**, 349–86.
- BRISTOW, C. R. 1999. *The Stratigraphy of the Chalk Group of the Wessex Basin*. British Geological Survey Technical Report, WA/99/08. Keyworth: British Geological Survey, 19 pp.
- BRISTOW, C. R., MORTIMORE, R. N. & WOOD, C. J. 1997. Lithostratigraphy for mapping the Chalk of southern England. *Proceedings of the Geologists' Association* **108**, 293–315.
- BROMLEY, R. G. & GALE, A. S. 1982. The lithostratigraphy of the English Chalk Rock. *Cretaceous Research* **3**, 273–306.
- CAMERON, T. D. J., CROSBY, A., BALSON, P. S., JEFFERY, D. H., LOTT, G. K., BULAT, J. & HARRISON, D. J. 1992. *The Geology of the Southern North Sea*. United Kingdom Offshore Regional Report. London: HMSO for the British Geological Survey.
- CARTER, D. J. & HART, M. B. 1977. Aspects of mid-Cretaceous stratigraphic micropalaeontology. *Bulletin of the British Museum of Natural History (Geology)* **29**, 1–135.
- CHRISTENSEN, W. K. 1990. *Actinocamax primus* Arkhangel'sky (Belemnitellidae; Upper Cretaceous). Biometry, comparison and biostratigraphy. *Paläontologische Zeitschrift* **64**, 75–90.
- COCCIONI, R. & GALEOTTI, S. 2003. The mid-Cenomanian Event: prelude to OAE 2. *Palaeogeography, Palaeoclimatology, Palaeoecology* **190**, 427–40.
- CORFIELD, R. M., CARTLIDGE, J. E., PREMOLI SILVA, I. P. & HOUSLEY, R. A. 1991. Oxygen and carbon isotope stratigraphy of the Palaeogene and Cretaceous limestones in the Bottaccione Gorge and the Contessa Highway sections, Umbria, Italy. *Terra Nova* **3**, 414–22.

- CRESTA, S., MONECHI, S. & PARISI, G. 1989. *Stratigrafia del Mesozoico e Cenozoico nell' area Umbro-Marchigiana (Mesozoic-Cenozoic Stratigraphy in the Umbria-Marche area)*. Memorie descrittive della Carta Geologica d'Italia no. 39. Roma, 185 pp.
- DECABRERA, S. C., SLITER, W. V. & JARVIS, I. 1999. Integrated foraminiferal biostratigraphy and chemostratigraphy of the Querecual Formation (Cretaceous), eastern Venezuela. *Journal of Foraminiferal Research* **29**, 487–99.
- DECONTO, R. M. & POLLARD, D. 2003. Rapid Cenozoic glaciation of Antarctica induced by declining atmospheric CO<sub>2</sub>. *Nature* **421**, 245–9.
- DEWEY, J. F. & PITMAN, W. C. 1998. Sea-level changes: mechanisms, magnitudes and rates. In *Paleogeographic Evolution and Non-glacial Eustasy* (eds J. L. Pindell and C. Drake), pp. 1–16. SEPM Special Publication no. 58. Tulsa: SEPM (Society for Sedimentary Geology).
- DITCHFIELD, P. & MARSHALL, J. D. 1989. Isotopic variation in rhythmically bedded chalks: Paleotemperature variation in the Upper Cretaceous. *Geology* **17**, 842–5.
- DOWKER, G. 1870. On the Chalk of Thanet, Kent, and its connection with the Chalk of East Kent. *Geological Magazine* **7**, 466–72.
- ERBACHER, J., FRIEDRICH, O., WILSON, P. A., BIRCH, H. & MUTTERLOSE, J. 2005. Stable organic carbon isotope stratigraphy across Oceanic Anoxic Event 2 of Demerara Rise, western tropical Atlantic. *Geochemistry Geophysics Geosystems* **6**, Q06010, doi:10.1029/2004GC000850.
- ERBACHER, J. & THUROW, J. 1997. Influence of oceanic anoxic events on the evolution of mid-Cretaceous radiolaria in the North Atlantic and western Tethys. *Marine Micropaleontology* **30**, 139–58.
- ERBACHER, J., THUROW, J. & LITKE, R. 1996. Evolution patterns of radiolaria and organic matter variations: a new approach to identify sea-level changes in mid-Cretaceous pelagic environments. *Geology* **24**, 499–502.
- ERNST, G., SCHMID, F. & SIEBERTZ, E. 1983. Event stratigraphie im Cenoman und Turon von NW Deutschland. *Zitteliana* **10**, 531–54.
- GALE, A. S. 1989. Field meeting at Folkestone Warren, 29th November, 1987. *Proceedings of the Geologists' Association* **100**, 73–82.
- GALE, A. S. 1990. A Milankovitch scale for Cenomanian time. *Terra Nova* **1**, 420–5.
- GALE, A. S. 1995. Cyclostratigraphy and correlation of the Cenomanian stage in Western Europe. In *Orbital Forcing Timescales and Cyclostratigraphy* (eds M. R. House and A. S. Gale), pp. 177–97. Geological Society of London, Special Publication no. 85.
- GALE, A. S. 1996. Turonian correlation and sequence stratigraphy of the Chalk in southern England. In *Sequence Stratigraphy in British Geology* (eds S. P. Hesselbo and D. N. Parkinson), pp. 177–95. Geological Society of London, Special Publication no. 103.
- GALE, A. S., HANCOCK, J. M., BRISTOW, R., MORTIMORE, R. N. & WOOD, C. J. 1999a. 'Lithostratigraphy for mapping the Chalk of southern England' by Bristow *et al.* (1997): discussion. *Proceedings of the Geologists' Association* **110**, 65–72.
- GALE, A. S., HANCOCK, J. M. & KENNEDY, W. J. 1999. Biostratigraphical and sequence correlation of the Cenomanian successions in Mangyshlak (W. Kazakhstan) and Crimea (Ukraine) with those in southern England. *Bulletin de l'Institut Royal des Sciences Naturelles de Belgique. Sciences de la Terre* **69 Supp. A**, 67–86.
- GALE, A. S., HARDENBOL, J., HATHWAY, B., KENNEDY, W. J., YOUNG, J. R. & PHANSALKAR, V. 2002. Global correlation of Cenomanian (Upper Cretaceous) sequences: evidence for Milankovitch control on sea level. *Geology* **30**, 291–4.
- GALE, A. S., JENKYN, H. C., KENNEDY, W. J. & CORFIELD, R. M. 1993. Chemostratigraphy versus biostratigraphy: data from around the Cenomanian–Turonian boundary. *Journal of the Geological Society, London* **150**, 29–32.
- GALE, A. S., KENNEDY, W. J., BURNETT, J. A., CARON, M. & KIDD, B. E. 1996. The late Albian to early Cenomanian succession at Mont Risou near Rosans (Drôme, SE France): An integrated study (ammonites, inoceramids, planktonic foraminifera, nannofossils, oxygen and carbon isotopes). *Cretaceous Research* **17**, 515–606.
- GALE, A. S., KENNEDY, W. J., VOIGT, S. & WALASZCZYK, I. 2005. Stratigraphy of the Upper Cenomanian–Lower Turonian Chalk succession at Eastbourne, Sussex, UK: ammonites, inoceramid bivalves and stable carbon isotopes. *Cretaceous Research* **26**, 460–87.
- GALE, A. S., MONTGOMERY, P., KENNEDY, W. J., HANCOCK, J. M., BURNETT, J. A. & MCARTHUR, J. M. 1995. Definition and global correlation of the Santonian–Campanian boundary. *Terra Nova* **7**, 611–22.
- GALE, A. S., SMITH, A. B., MONKS, N. E. A., YOUNG, J. A., HOWARD, A., WRAY, D. S. & HUGGETT, J. M. 2000. Marine biodiversity through the Late Cenomanian–Early Turonian: palaeoceanographic controls and sequence stratigraphic biases. *Journal of the Geological Society, London* **157**, 745–57.
- GALE, A. S., WOOD, C. J. & BROMLEY, R. G. 1987. The lithostratigraphy and marker bed correlation of the White Chalk (Late Cenomanian–Campanian) in southern England. *Mesozoic Research* **1**, 107–18.
- GALE, A. S. & WOODROOF, P. B. 1981. A Coniacian ammonite from the “Top Rock” in the Chalk of Kent. *Geological Magazine* **118**, 557–60.
- GALE, A. S., YOUNG, J. R., SHACKLETON, N. J., CROWHURST, S. J. & WRAY, D. S. 1999b. Orbital tuning of Cenomanian marly chalk successions: towards a Milankovitch time-scale for the Late Cretaceous. *Philosophical Transactions of the Royal Society Series A – Mathematical Physical and Engineering Sciences* **357**, 1815–29.
- GALLOIS, R. W. & MORTER, A. A. 1976. Trunch Borehole, Mundesley (132) Sheet. In *IGS Boreholes 1975*, pp. 8–10. Institute of Geological Sciences Report no. 76/10. London: Institute of Geological Sciences.
- GRANT, S. F., COE, A. L. & ARMSTRONG, H. A. 1999. Sequence stratigraphy of the Coniacian succession of the Anglo-Paris Basin. *Geological Magazine* **136**, 17–38.
- GROSSOUVRE, A. DE. 1901. Recherches sur la Craie Supérieure. Première Partie, Stratigraphie Générale. *Mémoires pour Servir à l'Explication de la Carte Géologique Détaillée de la France*. Paris: Imprimerie Nationale, 1013 pp.
- HANCOCK, J. M. 1989. Sea-level changes in the British region during the Late Cretaceous. *Proceedings of the Geologists' Association* **100**, 565–94.
- HANCOCK, J. M. 2000. Late Cretaceous eustatic highs. *Memoir Geological Society of India* **46**, 1–14.
- HANCOCK, J. M. & GALE, A. S. 1996. The Campanian Stage. In *Proceedings 'Second International Symposium on*

- Cretaceous Stage Boundaries*' Brussels 8–16 September 1995 (eds P. F. Rawson, A. V. Dhondt, J. M. Hancock and W. J. Kennedy), pp. 103–9. Bulletin de l'Institut Royal des Sciences Naturelles de Belgique Sciences de la Terre no. 66, supplement.
- HANCOCK, J. M. & KAUFFMAN, E. G. 1979. The great transgressions of the Late Cretaceous. *Journal of the Geological Society, London* **136**, 175–86.
- HAQ, B. U., HARDENBOL, J. & VAIL, P. R. 1987. Chronology of fluctuating sea levels since the Triassic. *Science* **235**, 1156–67.
- HAQ, B. U., HARDENBOL, J. & VAIL, P. 1988. Mesozoic and Cenozoic chronostratigraphy and cycles of sea-level change. In *Sea-Level Changes – An Integrated Approach* (eds C. K. Wilgus, B. S. Hastings, C. A. Ross, H. Posamentier, J. Van Wagoner and C. G. S. C. Kendall), pp. 71–108. SEPM Special Publication no. 42. Tulsa: The Society of Economic Paleontologists and Mineralogists.
- HARDENBOL, J., THIERRY, J., FARLEY, M. B., JACQUIN, T., GRACIANSKY, P.-C. D. & VAIL, P. R. 1998. Mesozoic and Cenozoic sequence chronostratigraphic framework in European basins. In *Mesozoic and Cenozoic Sequence Stratigraphy of European Basins* (eds P.-C. d. Graciansky, J. Hardenbol, T. Jacquin and P. R. Vail), pp. 3–13. SEPM Special Publication no. 60. Tulsa: SEPM (Society for Sedimentary Geology).
- HART, M. B. & LEARY, P. N. 1991. Stepwise mass extinctions – the case for the Late Cenomanian event. *Terra Nova* **3**, 142–7.
- HASEGAWA, T. 1997. Cenomanian–Turonian carbon isotope events recorded in terrestrial organic matter from northern Japan. *Palaeogeography, Palaeoclimatology, Palaeoecology* **130**, 251–73.
- HASEGAWA, T. 2003. A global carbon-isotope event in the Middle Turonian (Cretaceous) sequences in Japan and Russian Far East. *Proceedings of the Japan Academy Series B – Physical and Biological Sciences* **79**, 141–4.
- HASEGAWA, T. & HATSUGAI, T. 2000. Carbon-isotope stratigraphy and its chronostratigraphic significance for the Cretaceous Yezo Group, Kotanbetsu area, Hokkaido, Japan. *Paleontological Research (Japan)* **4**, 95–106.
- HERBIN, J.-P., MONTADERT, L., MULLER, C., GOMEZ, R., THUROW, J. & WIEDMANN, J. 1986. Organic-rich sedimentation at the Cenomanian–Turonian boundary in oceanic and coastal basins in the North Atlantic and Tethys. In *North Atlantic Palaeoceanography* (eds C. P. Summerhayes and N. J. Shackleton), pp. 389–422. Geological Society of London, Special Publication no. 21.
- HILBRECHT, H., FRIEG, C., TRÖGER, K.-A., VOIGT, S. & VOIGT, T. 1996. Shallow water facies during the Cenomanian–Turonian anoxic event: Bio-events, isotopes, and sea level in southern Germany. *Cretaceous Research* **17**, 229–53.
- HILL, W. 1888. On the lower beds of the Upper Cretaceous Series in Lincolnshire and Yorkshire. *Quarterly Journal of the Geological Society of London* **44**, 320–67.
- JARVIS, I., CARSON, G. A., COOPER, M. K. E., HART, M. B., LEARY, P. N., TOCHER, B. A., HORNE, D. & ROSENFELD, A. 1988a. Microfossil assemblages and the Cenomanian–Turonian (late Cretaceous) oceanic anoxic event. *Cretaceous Research* **9**, 3–103.
- JARVIS, I., CARSON, G. A., HART, M. B., LEARY, P. N. & TOCHER, B. A. 1988b. The Cenomanian–Turonian (late Cretaceous) anoxic event in SW England: evidence from Hooken Cliffs near Beer, SE Devon. *Newsletters on Stratigraphy* **18**, 147–64.
- JARVIS, I., MABROUK, A., MOODY, R. T. J. & DE CABRERA, S. C. 2002. Late Cretaceous (Campanian) carbon isotope events, sea-level change and correlation of the Tethyan and Boreal realms. *Palaeogeography, Palaeoclimatology, Palaeoecology* **188**, 215–48.
- JARVIS, I., MURPHY, A. M. & GALE, A. S. 2001. Geochemistry of pelagic and hemipelagic carbonates: criteria for identifying systems tracts and sea-level change. *Journal of the Geological Society, London* **158**, 685–96.
- JEANS, C. V. 1973. The Market Weighton Structure: tectonics, sedimentation and diagenesis during the Cretaceous. *Proceedings of the Yorkshire Geological Society* **39**, 409–44.
- JEANS, C. V. 1980. Early submarine lithification in the Red Chalk and Lower Chalk of east England: a bacterial control model and its implications. *Proceedings of the Yorkshire Geological Society* **43**, 81–157.
- JEANS, C. V., LONG, D., HALL, M. A., BLAND, D. J. & CORNFORD, C. 1991. The geochemistry of the Plenus Marls at Dover, England: evidence of fluctuating oceanographic conditions and of glacial control during the development of the Cenomanian–Turonian  $\delta^{13}\text{C}$  anomaly. *Geological Magazine* **128**, 603–32.
- JEFFERIES, R. P. S. 1962. The palaeoecology of the *Actinocamax plenus* subzone (lowest Turonian) in the Anglo-Paris Basin. *Palaeontology* **4**, 609–47.
- JEFFERIES, R. P. S. 1963. The stratigraphy of the *Actinocamax plenus* subzone (Turonian) in the Anglo-Paris Basin. *Proceedings of the Geologists' Association* **74**, 1–34.
- JENKYN, H. C. 1980. Cretaceous anoxic events: from continents to oceans. *Journal of the Geological Society, London* **137**, 171–88.
- JENKYN, H. C. 1985. The early Toarcian and Cenomanian–Turonian anoxic events in Europe – comparisons and contrasts. *Geologische Rundschau* **74**, 505–18.
- JENKYN, H. C. 2003. Evidence for rapid climate change in the Mesozoic–Palaeogene greenhouse world. *Philosophical Transactions of the Royal Society Series A – Mathematical Physical and Engineering Sciences* **361**, 1885–1916.
- JENKYN, H. C., GALE, A. S. & CORFIELD, R. M. 1994. Carbon- and oxygen-isotope stratigraphy of the English Chalk and Italian Scaglia and its palaeoclimatic significance. *Geological Magazine* **131**, 1–34.
- JENKYN, H. C., FORSTER, A., SCHOUTEN, S. & DAMSTÉ, J. S. S. 2004. High temperatures in the Late Cretaceous Arctic Ocean. *Nature* **432**, 888–92.
- JENKYN, H. C., MUTTERLOSE, J. & SLITER, W. V. 1995. Upper Cretaceous carbon- and oxygen-isotope stratigraphy of deep-water sediments from the north-central Pacific (Site 869, flank of Pikinni-Wodejebato, Marshall Islands). In *Northwest Pacific Atolls and Guyots: Proceedings of the Ocean Drilling Program, Scientific Results vol. 143* (eds E. L. Winterer, W. W. Sager, J. V. Firth and J. M. Sinton), pp. 105–8. College Station, Texas.
- JUKES-BROWNE, A. J. & HILL, W. 1903. *The Cretaceous Rocks of Britain. Vol. II – The Lower and Middle Chalk of England*. Memoir of the Geological Survey of the United Kingdom. London: HMSO, 568 pp.
- JUKES-BROWNE, A. J. & HILL, W. 1904. *The Cretaceous Rocks of Britain. Vol. III – The Upper Chalk of England*. Memoir of the Geological Survey of the United Kingdom. London: HMSO, 566 pp.

- KAUFFMAN, E. G., KENNEDY, W. J. & WOOD, C. J. 1996. The Coniacian stage and substage boundaries. In *Proceedings "Second International Symposium on Cretaceous Stage Boundaries" Brussels 8–16 September 1995* (eds P. F. Rawson, A. V. Dhondt, J. M. Hancock and W. J. Kennedy), pp. 81–94. Bulletin de l'Institut Royal des Sciences Naturelles de Belgique Sciences de la Terre no. 66, supplement.
- KELLER, G., HAN, Q., ADATTE, T. & BURNS, S. J. 2001. Palaeoenvironment of the Cenomanian–Turonian transition at Eastbourne, England. *Cretaceous Research* **22**, 391–422.
- KELLER, G., STÜBEN, D., BERNER, Z. & ADATTE, T. 2004. Cenomanian–Turonian and  $\delta^{13}\text{C}$ , and  $\delta^{18}\text{O}$ , sea level and salinity variations at Pueblo, Colorado. *Palaeogeography, Palaeoclimatology, Palaeoecology* **211**, 19–43.
- KENNEDY, W. J. 1969. The correlation of the Lower Chalk in South-East England. *Proceedings of the Geologists' Association* **80**, 459–560.
- KENNEDY, W. J. 1984a. Ammonite faunas and the 'standard zones' of the Cenomanian to Maastrichtian stages in their type areas, with some proposals for the definition of the stage boundaries by ammonites. *Bulletin of the Geological Society of Denmark* **33**, 147–61.
- KENNEDY, W. J. 1984b. Systematic palaeontology and stratigraphic distribution of the ammonite faunas of the French Coniacian. *Special Papers in Palaeontology* **31**, 1–160.
- KENNEDY, W. J., WALASZCZYK, I. & COBBAN, W. A. 2000. Pueblo, Colorado, USA, candidate Global Boundary Stratotype Section and Point for the base of the Turonian Stage of the Cretaceous, and for the base of the Middle Turonian Substage, with a revision of the Inoceramidae (Bivalvia). *Acta Geologica Polonica* **50**, 295–334.
- KOLONIC, S., WAGNER, T., FORSTER, A., SINNINGHE DAMSTÉ, J. S. S., WALSWORTH-BELL, B., ERBA, E., TURGEON, S., BRUMSACK, H.-J., CHELLAI, E. H., TSIKOS, H., KUHN, W. & KUYPERS, M. M. M. 2005. Black shale deposition on the northwest African Shelf during the Cenomanian/Turonian oceanic anoxic event: climate coupling and global organic carbon burial. *Paleoceanography* **20**, PA1006, doi: 10.1029/2003PA000950.
- KUHN, W., LUDERER, F., NEDERBRAGT, S., THUROW, J. & WAGNER, T. 2005. Orbital-scale record of the late Cenomanian–Turonian oceanic anoxic event (OAE-2) in the Tarfaya Basin (Morocco). *International Journal of Earth Sciences (Geologische Rundschau)* **94**, 147–59.
- KUYPERS, M. M. M., LOURENS, L. J., RIJSTRA, W. R. C., PANCOST, R. D., NIJENHUIS, I. A. & DAMSTÉ, J. S. S. 2004. Orbital forcing of organic carbon burial in the proto-North Atlantic during oceanic anoxic event 2. *Earth and Planetary Science Letters* **228**, 465–82.
- KUYPERS, M. M. M., PANCOST, R. D., NIJENHUIS, I. A. & SINNINGHE DAMSTÉ, J. S. 2002. Enhanced productivity led to increased organic carbon burial in the euxinic North Atlantic basin during the late Cenomanian oceanic anoxic event. *Paleoceanography* **17**, Article 1051, 3–13.
- KVENVOLDEN, K. A. 1998. A primer on the geological occurrence of gas hydrate. In *Gas Hydrates: Relevance to World Margin Stability and Climate Change* (eds J.-P. Henriet and J. Mienert), pp. 9–30. Geological Society of London, Special Publication no. 137.
- LAMOLDA, M. A., GOROSTIDI, A. & PAUL, C. R. C. 1994. Quantitative estimates of calcareous nannofossil changes across the Plenus Marls (latest Cenomanian), Dover, England – implications for the generation of the Cenomanian–Turonian boundary event. *Cretaceous Research* **15**, 143–64.
- LAMOLDA, M. A. & HANCOCK, J. M. 1996. The Santonian Stage and substages. In *Proceedings "Second International Symposium on Cretaceous Stage Boundaries" Brussels 8–16 September 1995* (eds P. F. Rawson, A. V. Dhondt, J. M. Hancock and W. J. Kennedy), pp. 95–102. Bulletin de l'Institut Royal des Sciences Naturelles de Belgique Sciences de la Terre no. 66, supplement.
- LEARY, P. N. & PERYT, D. 1991. The late Cenomanian oceanic anoxic event in the western Anglo-Paris Basin and southeast Danish–Polish Trough: survival strategies of and recolonisation by benthonic foraminifera. *Historical Biology* **5**, 321–38.
- LEHMANN, J. 1999. Integrated stratigraphy and palaeoenvironment of the Cenomanian–Lower Turonian (Upper Cretaceous) of northern Westphalia, North Germany. *Facies* **40**, 25–69.
- LI, X., JENKINS, H. C., WANG, C., HU, X., CHEN, X., WEI, Y., HUANG, Y. & CUI, J. 2006. Upper Cretaceous carbon- and oxygen-isotope stratigraphy of hemipelagic carbonate facies from southern Tibet, China. *Journal of the Geological Society, London* **163**, 375–82.
- LOWRIE, W. & ALVAREZ, W. 1977. A review of magnetic stratigraphy investigations in Cretaceous pelagic carbonate rocks. *Journal of Geophysical Research* **85B**, 3597–605.
- MARCINOWSKI, R. 1980. Cenomanian ammonites from the German Democratic Republic, Poland and the Soviet Union. *Acta Geologica Polonica* **30**, 215–325.
- MATSUMOTO, T. 1980. Inter-regional correlation of transgressions and regressions in the Cretaceous Period. *Cretaceous Research* **1**.
- MCCARTHER, J. M., THIRLWALL, M. F., GALE, A. S., KENNEDY, W. J., BURNETT, J. A., MATTEY, D. & LORD, A. R. 1993. Strontium isotope stratigraphy for the Late Cretaceous: a new curve, based on the English Chalk. In *High Resolution Stratigraphy* (eds E. A. Hailwood and R. B. Kidd), pp. 195–209. Geological Society of London, Special Publication no. 70.
- MEYER, T. 1990. Biostratigraphische und Sedimentologische Untersuchungen in der Plänerfazies des Cenoman von Nordwestdeutschland. *Mitteilungen aus dem Geologischen Institut der Universität Hannover* **30**, 1–114.
- MIALL, A. D. 1992. The Exxon global cycle chart: an event for every occasion? *Geology* **20**, 787–90.
- MILLER, K. G., SUGARMAN, P. J., BROWNING, J. V., KOMINZ, M. A., HERNANDEZ, J. C., OLSSON, R. K., WRIGHT, J. D., FEIGENSON, M. D. & VAN SICKEL, W. 2003. Late Cretaceous chronology of large, rapid sea-level changes: Glacioeustasy during the greenhouse world. *Geology* **31**, 585–8.
- MILLER, K. G., SUGARMAN, P. J., BROWNING, J. V., KOMINZ, M. A., OLSSON, R. K., FEIGENSON, M. D. & HERNANDEZ, J. C. 2004. Upper Cretaceous sequences and sea-level history, New Jersey Coastal Plain. *Geological Society of America Bulletin* **116**, 368–93.
- MITCHELL, S. F. 1995. Lithostratigraphy and biostratigraphy of the Hunstanton Formation (Red Chalk, Cretaceous) succession at Speeton, North Yorkshire, England. *Proceedings of the Yorkshire Geological Society* **50**, 285–303.
- MITCHELL, S. F. 1996. Foraminiferal assemblages from the late Lower and Middle Cenomanian of Speeton

- (North Yorkshire, UK): Relationships with sea-level fluctuations and watermass distribution. *Journal of Micropalaeontology* **15**, 37–54.
- MITCHELL, S. F. & CARR, I. T. 1998. Foraminiferal response to mid-Cenomanian (Upper Cretaceous) palaeoceanographic events in the Anglo-Paris Basin (North-west Europe). *Palaeogeography, Palaeoclimatology, Palaeoecology* **137**, 103–25.
- MITCHELL, S. F., PAUL, C. R. C. & GALE, A. S. 1996. Carbon isotopes and sequence stratigraphy. In *High Resolution Sequence Stratigraphy: Innovations and Applications* (eds J. A. Howell and J. F. Aitken), pp. 11–24. Geological Society of London, Special Publication no. 104.
- MONTGOMERY, P., HAILWOOD, E. A., GALE, A. S. & BURNETT, J. A. 1998. The magnetostratigraphy of Coniacian–Late Campanian chalk sequences in southern England. *Earth and Planetary Science Letters* **156**, 209–24.
- MORTER, A. A. & WOOD, C. J. 1983. The biostratigraphy of Upper Albian–Lower Cenomanian *Aucellina* in Europe. *Zitteliana* **10**, 515–29.
- MORTIMORE, R. N. 1983. The stratigraphy and sedimentation of the Turonian–Campanian in the Southern Province of England. *Zitteliana* **10**, 27–41.
- MORTIMORE, R. N. 1986. Stratigraphy of the Upper Cretaceous White Chalk of Sussex. *Proceedings of the Geologists' Association* **97**, 97–139.
- MORTIMORE, R. N. 1988. Upper Cretaceous White Chalk in the Anglo-Paris Basin: a discussion of lithostratigraphical units. *Proceedings of the Geologists' Association* **99**, 67–70.
- MORTIMORE, R. N. 1997. *The Chalk of Sussex and Kent*. Geologists' Association Guide no. 57. London: Geologists' Association, 139 pp.
- MORTIMORE, R. N. & POMEROL, B. 1987. Correlation of the Upper Cretaceous White Chalk (Turonian to Campanian) in the Anglo-Paris Basin. *Proceedings of the Geologists' Association* **98**, 97–143.
- MORTIMORE, R. N., WOOD, C. J. & GALLOIS, R. W. 2001. *British Upper Cretaceous Stratigraphy*. Geological Conservation Review Series no. 23. Peterborough, Joint Nature Conservation Committee, 558 pp.
- MURPHY, A. M., JARVIS, I. & EDMUNDS, W. M. 1997. *Geochemistry of the Banterwick Barn Chalk Borehole*. Hydrogeology Series, Report WD/97/37. Keyworth, British Geological Survey, 37 pp.
- NIEBUHR, B. 1995. Fazies-Differenzierungen und ihre Steuerungsfaktoren in der höheren Oberkreide von S-Niedersachsen/Sachsen-Anhalt (N-Deutschland). *Berliner Geowissenschaftliche Abhandlungen Reihe A* **174**, 1–131.
- NIEBUHR, B., WOOD, C. J. & ERNST, G. 2000. Isolierte Oberkreide – vorkommen zwischen Wiehengebirge und Harz. In *Stratigraphie von Deutschland III. Die Kreide der Bundesrepublik Deutschland* (eds M. Hiss, J. Schönfeld and A. Thiermann), pp. 101–9. Courier Forschungsinstitut Senckenberg no. 226. Frankfurt am Main: Senckenbergische Naturforschende Gesellschaft.
- OGG, J. G., AGTERBERG, F. P. & GRADSTEIN, F. M. 2004. The Cretaceous Period. In *A Geologic Time Scale 2004* (eds F. M. Gradstein, J. G. Ogg and A. G. Smith), pp. 344–83. Cambridge: Cambridge University Press.
- OWEN, D. 1996. Interbasinal correlation of the Cenomanian stage; testing the lateral continuity of sequence boundaries. In *High Resolution Sequence Stratigraphy: Innovations and Applications* (eds J. A. Howell and J. F. Aitken), pp. 269–93. Geological Society of London, Special Publication no. 104.
- PAUL, C. R. C. 1992. Milankovitch cycles and microfossils: principles and practise of palaeoecological analysis illustrated by Cenomanian chalk-marl rhythms. *Journal of Micropalaeontology* **11**, 95–105.
- PAUL, C. R. C., LAMOLDA, M. A., MITCHELL, S. F., VAZIRI, M. R., GOROSTIDI, A. & MARSHALL, J. D. 1999. The Cenomanian–Turonian boundary at Eastbourne (Sussex, UK): a proposed European reference section. *Palaeogeography, Palaeoclimatology, Palaeoecology* **150**, 83–121.
- PAUL, C. R. C., MITCHELL, S. F., LAMOLDA, M. & GOROSTIDI, A. 1994a. The Cenomanian–Turonian Boundary Event in northern Spain. *Geological Magazine* **131**, 801–17.
- PAUL, C. R. C., MITCHELL, S. F., MARSHALL, J. D., LEARY, P. N., GALE, A. S., DUANE, A. M. & DITCHFIELD, P. W. 1994b. Palaeoceanographic events in the Middle Cenomanian of Northwest Europe. *Cretaceous Research* **15**, 707–38.
- PEAKE, N. B. 2002. A plea to subdivide the Chalk on future maps in a manner applicable to the whole of Britain. *Proceedings of the Geologists' Association* **113**, 345–7.
- PEARCE, M. A., JARVIS, I., SWAN, A. R. H., MURPHY, A. M., TOCHER, B. A. & EDMUNDS, W. M. 2003. Integrating palynological and geochemical data in a new approach to palaeoecological studies: Upper Cretaceous of the Banterwick Barn Chalk borehole, Berkshire, UK. *Marine Micropaleontology* **47**, 271–306.
- PECHERSKY, D. M., NAIDIN, D. P. & MOLOTOVSKY, E. A. 1983. The Santonian–Campanian reversed polarity magnetozone and the Late Cretaceous magnetostratigraphical timescale. *Cretaceous Research* **4**, 251–7.
- PENNING, W. H. & JUKES-BROWNE, A. J. 1881. *Geology of the Neighbourhood of Cambridge*. Memoir of the Geological Survey of England and Wales. London: HMSO.
- PHILLIPS, W. 1821. Remarks on the Chalk cliffs in the neighbourhood of Dover, and on the Blue Marle covering the Green Sand, near Folkestone. *Transactions of the Geological Society of London* **5**, 16–51.
- PRATT, L. M., ARTHUR, M. A., DEAN, W. E. & SCHOLLE, P. A. 1993. Paleooceanographic cycles and events during the Late Cretaceous in the Western Interior Seaway of North America. In *Cretaceous Evolution of the Western Interior Basin of North America* (eds W. G. E. Caldwell and E. G. Kauffman), pp. 333–53. Geological Association of Canada, Special Paper no. 39.
- PRATT, L. M. & THRELKELD, C. N. 1984. Stratigraphic significance of  $^{13}\text{C}/^{12}\text{C}$  ratios in mid-Cretaceous rocks of the Western Interior, USA. In *The Mesozoic of Middle North America* (eds D. F. Stott and D. J. Glass), pp. 305–12. Canadian Society of Petroleum Geologists, Memoir no. 9.
- PREMOLI SILVA, I. & SLITER, W. V. 1995. Cretaceous planktonic foraminiferal biostratigraphy and evolutionary trends from the Bottaccione section, Gubbio, Italy. *Palaeontographia Italica* **82**, 1–89.
- PRICE, F. G. H. 1877. On the beds between the Gault and Upper Chalk near Folkestone. *Quarterly Journal of the Geological Society of London* **33**, 431–48.
- PRINCE, I. M., JARVIS, I. & TOCHER, B. A. 1999. High-resolution dinoflagellate cyst biostratigraphy of the

- Santonian–basal Campanian (Upper Cretaceous): new data from Whitecliff, Isle of Wight, England. *Review of Palaeobotany and Palynology* **105**, 143–69.
- RASMUSSEN, K. W. 1961. A monograph on the Cretaceous Crinoidea. *Det Kongelige Danske Videnskabernes Selskab Biologiske Skrifter* **12**, 1–248.
- RAWSON, P. F., ALLEN, P. & GALE, A. S. 2001. The Chalk Group – a revised lithostratigraphy. *Geoscientist* **11**, 21.
- RAWSON, P. F., CURRY, D., DILLEY, F. C., HANCOCK, J. M., KENNEDY, W. J., NEALE, J. W., WOOD, C. J. & WORSSAM, B. C. 1978. *A correlation of Cretaceous rocks in the British Isles*. Geological Society Special Report no. 9. Edinburgh: Scottish Academic Press, 70 pp.
- RIPPERDAN, R. L. 2001. Stratigraphic variation in marine carbonate carbon isotope ratios. In *Stable Isotope Geochemistry* (eds J. W. Valley and D. R. Cole), pp. 637–62. Reviews in Mineralogy and Geochemistry no. 43. Mineralogical Society of America and Geochemical Society.
- ROBASZYNSKI, F. & CARON, M. 1979a. Atlas de Foraminifères planctoniques de Crétacé moyen (Mer Boréal et Téthys). Deuxième partie. *Cahiers de Micropaléontologie* **2**.
- ROBASZYNSKI, F. & CARON, M. 1979b. Atlas de Foraminifères planctoniques de Crétacé moyen (Mer Boréal et Téthys). Première partie. *Cahiers de Micropaléontologie* **1**.
- ROBASZYNSKI, F., GALE, A. S., JUIGNET, P., AMÉDRO, F. & HARDENBOL, J. 1998. Sequence stratigraphy in the Upper Cretaceous series of the Anglo-Paris Basin: exemplified by the Cenomanian stage. In *Mesozoic and Cenozoic Sequence Stratigraphy of European Basins* (eds P.-C. d. Graciansky, J. Hardenbol, T. Jacquin and P. R. Vail), pp. 363–86. SEPM Special Publication no. 60. Tulsa: SEPM (Society for Sedimentary Geology).
- ROBINSON, N. D. 1986. Lithostratigraphy of the Chalk Group of the North Downs, southeast England. *Proceedings of the Geologists' Association* **97**, 141–70.
- ROBINSON, N. D. 1987. Upper Cretaceous Chalk in the North and South Downs, England: a reply. *Proceedings of the Geologists' Association* **98**, 87–93.
- ROWE, A. W. 1899. An analysis of the genus *Micraster*, as determined by rigid zonal collecting from the zones of *Rhynchonella cuvieri* to that of *Micraster cor-anguinum*. *Quarterly Journal of the Geological Society, London* **55**, 494–547.
- ROWE, A. W. 1900. The zones of the White Chalk of the English coast I. Kent and Sussex. *Proceedings of the Geologists' Association* **16**, 289–368.
- ROWE, A. W. 1908. The zones of the White Chalk of the English coast V. The Isle of Wight. *Proceedings of the Geologists' Association* **20**, 209–352.
- SAGEMAN, B. B., MYERS, S. R. & ARTHUR, M. A. 2006. Orbital time scale and new C-isotope record for Cenomanian–Turonian boundary stratotype. *Geology* **34**, 125–8.
- SAHAGIAN, D., PINOUS, O., OLFERIEV, A. & ZAKHAROV, V. 1996. Eustatic curve for the Middle Jurassic–Cretaceous based on Russian Platform and Siberian stratigraphy: zonal resolution. *AAPG Bulletin* **80**, 1433–58.
- SCHLANGER, S. O., ARTHUR, M. A., JENKYN, H. C. & SCHOLLE, P. A. 1987. The Cenomanian–Turonian Oceanic Anoxic event, I. Stratigraphy and distribution of organic carbon-rich beds and the marine  $\delta^{13}\text{C}$  excursion. In *Marine Petroleum Source Rocks* (eds J. Brooks and A. J. Fleet), pp. 371–99. Geological Society of London, Special Publication no. 26.
- SCHOLLE, P. A. & ARTHUR, M. A. 1980. Carbon isotope fluctuation in Cretaceous pelagic limestones: potential stratigraphic and petroleum exploration tool. *AAPG Bulletin* **64**, 67–87.
- SCHÖNFELD, J. & BURNETT, J. A. 1991. Biostratigraphical correlation of the Campanian–Maastrichtian boundary: Lägerdorf-Hemmor (northwestern Germany), DSDP Sites 548A, 549 and 551 (eastern North Atlantic) with palaeobiogeographical and palaeoceanographical implications. *Geological Magazine* **128**, 479–503.
- SCHULZ, M.-G., ERNST, G., ERNST, H. & SCHMID, F. 1984. Coniacian to Maastrichtian stage boundaries in the standard sections for the Upper Cretaceous white chalk of N.W. Germany (Lägerdorf–Kronsmoor–Hemmor): Definitions and proposals. *Bulletin of the Geological Society of Denmark* **33**, 203–15.
- SKELTON, P. W. 2003. *The Cretaceous World*. Cambridge: Cambridge University Press, 360 pp.
- STOKES, R. B. 1975. *Royaumes et provinces faunistiques du Crétacé établis sur la base d'une étude systématique du genre Micraster*. Mémoires du Museum National d'Histoire Naturelle Série C, **31**, 94 pp.
- STOKES, R. B. 1977. The echinoids *Micraster* and *Epiaster* from the Turonian and Senonian Chalk of England. *Palaeontology* **20**, 805–27.
- STOLL, H. M. & SCHRAG, D. P. 2000. High-resolution stable isotope records from the Upper Cretaceous rocks of Italy and Spain: Glacial episodes in a greenhouse planet? *Geological Society of America Bulletin* **112**, 308–19.
- SUGARMAN, P. J., MILLER, K. G., OLSSON, R. K., BROWNING, J. V., WRIGHT, J. D., DEROMERO, L. M., WHITE, T. S., MULLER, F. L. & UPTEGROVE, J. 1999. The Cenomanian/Turonian carbon burial event, Bass River, NJ, USA: Geochemical, paleoecological, and sea-level changes. *Journal of Foraminiferal Research* **29**, 438–52.
- TRÖGER, K.-A. 1995. Die subherzyne Oberkreide-Beziehungen zum variscischen Grundgebirge und Stellung innerhalb Europas. *Nova Acta Leopoldina: Abhandlungen der Deutschen Akademie der Naturforscher Leopoldina* **71**, 217–31.
- TRÖGER, K.-A. & KENNEDY, W. J. 1996. The Cenomanian Stage. In *Proceedings "Second International Symposium on Cretaceous Stage Boundaries" Brussels 8–16 September 1995* (eds P. F. Rawson, A. V. Dhondt, J. M. Hancock and W. J. Kennedy), pp. 57–68. Bulletin de l'Institut Royal des Sciences Naturelles de Belgique Sciences de la Terre no. 66, supplement.
- TSIKOS, H., JENKYN, H. C., WALSWORTH-BELL, B., PETRIZZO, M. R., FORSTER, A., KOLONIC, S., ERBA, E., PREMOLI-SILVA, I. P., BAAS, M., WAGNER, T. & SINNINGHE DAMSTÉ, J. S. 2004. Carbon-isotope stratigraphy recorded by the Cenomanian–Turonian Oceanic Anoxic Event: correlation and implications based on three key localities. *Journal of the Geological Society, London* **161**, 711–19.
- VAIL, P. R., MITCHUM, R. M. J. & THOMPSON, S. I. 1977. Seismic stratigraphy and global changes of sea-level, part 4: global cycles of relative changes of sea level. In *Seismic Stratigraphy – Applications to Hydrocarbon Exploration* (ed. C. E. Payton), pp. 83–97. AAPG Memoir no. 26.
- VOIGT, E., HAY, W. W., HÖFLING, R. & DECONTO, R. M. 1999. Biogeographic distribution of late Early to Late

- Cretaceous rudist-reefs in the Mediterranean as climate indicators. In *Evolution of the Cretaceous Ocean-Climate System* (eds E. Barrera and C. C. Johnson), pp. 91–103. Special Papers (Geological Society of America) no. 332. Boulder: Geological Society of America.
- VOIGT, S. 2000. Cenomanian–Turonian composite  $\delta^{13}\text{C}$  curve for Western and Central Europe: the role of organic and inorganic carbon fluxes. *Palaeogeography, Palaeoclimatology, Palaeoecology* **160**, 91–104.
- VOIGT, S. & HILBRECHT, H. 1997. Late Cretaceous carbon isotope stratigraphy in Europe: correlation and relations with sea level and sediment stability. *Palaeogeography, Palaeoclimatology, Palaeoecology* **134**, 39–59.
- WALASZCZYK, I. & COBBAN, W. A. 2000. Inoceramid faunas and biostratigraphy of the Upper Turonian–Lower Coniacian of the Western Interior of the United States. *Special Papers in Palaeontology* **64**, 1–118.
- WALASZCZYK, I. & WOOD, C. J. 1998. Inoceramids and biostratigraphy at the Turonian/Coniacian boundary; based on the Salzgitter-Salder Quarry, Lower Saxony, Germany, and the Slupia Nadbrzezna section, Central Poland. *Acta Geologica Polonica* **48**, 395–434.
- WANG, C. S., HU, X. M., JANSÁ, L., WAN, X. Q. & TAO, R. 2001. The Cenomanian–Turonian anoxic event in southern Tibet. *Cretaceous Research* **22**, 481–90.
- WEISSERT, H. 1989. Carbon-isotope stratigraphy, a monitor of paleoenvironmental change: a case study from the Early Cretaceous. *Surveys in Geophysics* **10**, 1–61.
- WEISSERT, H., LINI, A., FÖLLMI, K. B. & KUHN, O. 1998. Correlation of Early Cretaceous carbon isotope stratigraphy and platform drowning events: a possible link? *Palaeogeography, Palaeoclimatology, Palaeoecology* **137**, 189–203.
- WHITAKER, W. 1865a. On the Chalk of the Isle of Thanet. *Quarterly Journal of the Geological Society of London* **21**, 395–8.
- WHITAKER, W. 1865b. On the Chalk of Buckinghamshire and on the Totternhoe Stone. *Quarterly Journal of the Geological Society, London* **21**, 398–400.
- WHITAKER, W., BRISTOW, H. W. & HUGHES, T. M. 1872. *The Geology of the London Basin Part I. The Chalk and the Eocene beds of the Southern and Western Tracts*. Memoir of the Geological Survey of England and Wales. London: HMSO, 619 pp.
- WHITE, H. J. O. 1921. *A Short Account of the Geology of the Isle of Wight*. Memoirs of the Geological Survey of Great Britain (England and Wales). London: HMSO, 201 pp.
- WIESE, F. 1997. Das Turon und Unter-Coniac im nordkantabrischen becken (Provinz Kantabrien, Nordspanien): Faziesentwicklung, Bio-, Event- und Sequenzstratigraphie. *Berliner Geowissenschaftliche Abhandlungen Reihe E* **24**, 1–131.
- WIESE, F. 1999. Stable isotope data ( $\delta^{13}\text{C}$ ,  $\delta^{18}\text{O}$ ) from the Middle and Upper Turonian (Upper Cretaceous) of Liencres (Cantabria, northern Spain) with a comparison to northern Germany (Söhlde & Salzgitter-Salder). *Newsletters on Stratigraphy* **37**, 37–62.
- WIESE, F. & KAPLAN, U. 2001. The potential of the Lengerich section (Münster Basin, northern Germany) as a possible candidate Global boundary Stratotype Section and Point (GSSP) for the Middle/Upper Turonian boundary. *Cretaceous Research* **22**, 549–63.
- WIESE, F. & KRÖGER, B. 1998. Evidence for a shallowing event in the Upper Turonian (Cretaceous) *Mytiloides scupini* Zone of northern Germany. *Acta Geologica Polonica* **48**, 265–84.
- WIESE, F., WOOD, C. J. & WRAY, D. S. 2004. New advances in the stratigraphy and geochemistry of the German Turonian (Late Cretaceous) tephro-stratigraphic framework. *Acta Geologica Polonica* **54**, 657–71.
- WILMSEN, M. 2003. Sequence stratigraphy and palaeoceanography of the Cenomanian Stage in northern Germany. *Cretaceous Research* **24**, 525–68.
- WILMSEN, M. & NIEBUHR, B. 2002. Stratigraphic revision of the upper Lower and Middle Cenomanian in the Lower Saxony Basin (northern Germany) with special reference to the Salzgitter area. *Cretaceous Research* **23**, 445–60.
- WOOD, C. J. 1992. Upper Cretaceous (Chalk). In *Geology of the Country around Kingston upon Hull and Brigg. Memoir for 1:50,000 Geological Sheets 80 and 89 (England and Wales)* (eds G. D. Gaunt, T. P. Fletcher and C. J. Wood), pp. 77–101. Memoir of the British Geological Survey. London: HMSO.
- WOOD, C. J. & ERNST, G. 1998. Cenomanian–Turonian of Wunstorf. In *Key Localities of the Northwest European Cretaceous* (eds J. Mutterlose, A. Bornemann, S. Rauer, C. Spaeth and C. J. Wood), pp. 62–73. Bochumer Geologische und Geotechnische Arbeiten no. 48.
- WOOD, C. J., ERNST, G. & RASEMANN, G. 1984. The Turonian–Coniacian stage boundary in Lower Saxony (Germany) and adjacent areas: the Salzgitter–Salder Quarry as a proposed international standard section. *Bulletin of the Geological Society of Denmark* **33**, 225–38.
- WOOD, C. J., MORTER, A. A. & GALLOIS, R. W. 1994. Appendix 1. Upper Cretaceous stratigraphy of the Trunch borehole. TG23SE8. In *Geology of the Country around Great Yarmouth. Memoir for 1:50,000 Sheet 162 (England and Wales) with an Appendix on the Trunch Borehole by Wood and Morter* (eds R. S. Arthurton, S. J. Booth, A. N. Morigi, M. A. W. Abbott and C. J. Wood), pp. 105–10. London: HMSO.
- WOOD, C. J. & MORTIMORE, R. N. 1995. An anomalous Black Band succession (Cenomanian–Turonian boundary interval) at Melton Ross, Lincolnshire, eastern England and its international significance. *Berliner Geowissenschaftliche Abhandlungen Reihe E* **16** (Gundolf Ernst Festschrift), 277–87.
- WOOD, C. J. & SMITH, E. G. 1978. Lithostratigraphical classification of the Chalk in North Yorkshire, Humberside and Lincolnshire. *Proceedings of the Yorkshire Geological Society* **42**, 263–87.
- WOOD, C. J., WALASZCZYK, I., MORTIMORE, R. N. & WOODS, M. A. 2004. New observations on the inoceramid biostratigraphy of the higher part of the Upper Turonian and the Turonian–Coniacian boundary transition in Poland, Germany and the UK. *Acta Geologica Polonica* **54**, 541–9.
- WOODS, M. A. & ALDISS, D. T. 2004. The stratigraphy of the Chalk Group of the Berkshire Downs. *Proceedings of the Geologists' Association* **115**, 249–65.
- WOODS, M. A., ALDISS, D. T., HOPSON, P. M., MORTIMORE, R. N., BRISTOW, R., BROMLEY, R. G., GALE, A. S. & HANCOCK, J. M. 2002. Invited comments on Peake's 'Plea to subdivide the Chalk'. *Proceedings of the Geologists' Association* **113**, 348–62.
- WRAY, D. S. 1999. Identification and long-range correlation of bentonites in Turonian–Coniacian (Upper

- Cretaceous) chalks of northwest Europe. *Geological Magazine* **136**, 361–71.
- WRAY, D. S. & GALE, A. S. 1993. Geochemical correlation of marl bands in Turonian chalks of the Anglo-Paris Basin. In *High Resolution Stratigraphy* (eds E. A. Hailwood and R. B. Kidd), pp. 211–26. Geological Society of London, Special Publication no. 70.
- WRAY, D. S. & WOOD, C. J. 1998. Distinction between detrital and volcanogenic clay-rich beds in Turonian–Coniacian chalks of eastern England. *Proceedings of the Yorkshire Geological Society* **52**, 95–105.
- WRAY, D. S., WOOD, C. J., ERNST, G. & KAPLAN, U. 1996. Geochemical subdivision and correlation of clay-rich beds in Turonian sediments of northern Germany. *Terra Nova* **8**, 603–10.
- WRIGHT, C. W. & KENNEDY, W. J. 1981. *The Ammonoidea of the Plenus Marls and the Middle Chalk*. Monograph of the Palaeontographical Society no. 134. London: Palaeontographical Society, 148 pp.
- WRIGHT, C. W. & KENNEDY, W. J. 1984. The Ammonoidea of the Lower Chalk, Part 1. *Monograph of the Palaeontographical Society* **137**, 1–126.